University of Alberta

Identification of Asymmetrically Expressed Transcripts in the Developing Chick Retina

by

Rhonda L. Witte ©

A thesis submitted to the Faculty of Graduate Studies and Research in partial fulfillment of the requirements for the degree of Master of Science

in

Medical Sciences – Oncology

Edmonton, Alberta

Fall, 2000

National Library of Canada
Acquisitions and Bibliographic Services
395 Wellington Street
Ottawa ON K1A 0N4
Canada

Bibliothèque nationale du Canada
Acquisitions et services bibliographiques
395, rue Wellington
Ottawa ON K1A 0N4
Canada

Your file Votre référence

Our file Notre référence

The author has granted a non-exclusive licence allowing the National Library of Canada to reproduce, loan, distribute or sell copies of this thesis in microform, paper or electronic formats.

The author retains ownership of the copyright in this thesis. Neither the thesis nor substantial extracts from it may be printed or otherwise reproduced without the author's permission.

L'auteur a accordé une licence non exclusive permettant à la Bibliothèque nationale du Canada de reproduire, prêter, distribuer ou vendre des copies de cette thèse sous la forme de microfiche/film, de reproduction sur papier ou sur format électronique.

L'auteur conserve la propriété du droit d'auteur qui protège cette thèse. Ni la thèse ni des extraits substantiels de celle-ci ne doivent être imprimés ou autrement reproduits sans son autorisation.

0-612-59901-9

Canada

University of Alberta

Library Release Form

Name of Author: Rhonda L. Witte

Title of Thesis: Identification of Asymmetrically Expressed Transcripts in the Developing Chick Retina

Degree: Master of Science

Year this Degree Granted: 2000

Permission is hereby granted to the University of Alberta Library to reproduce single copies of this thesis and to lend or sell such copies for private, scholarly or scientific research purposes only.

The author reserves all other publication and other rights in association with the copyright in the thesis, and except as herein before provided, neither the thesis nor any substantial portion thereof may be printed or otherwise reproduced in any material form whatever without the author's prior written permission.

Rhonda L Witte

Rhonda L. Witte
2112-11135 83 Avenue
Edmonton, Alberta
Canada, T6G 2C6

July 20, 2000

ABSTRACT

Asymmetrical expression gradients in the retina and the subsequent distribution of factors produced by these proteins are thought to play a role in targeting retinal ganglion axons from the retina to the brain. The main objective of this project was to identify asymmetrically expressed genes of the developing chick retina in order to increase our understanding of retinal patterning. Specifically, we compared gene expression in dorsal (D) and ventral (V) chick retina. Embryonic day 7 (E7) chicken retinae were dissected along the D-V plane and poly A+ RNA extracted for differential display - polymerase chain reaction (DD-PCR) analysis. A total of 42 bands preferentially expressed in either dorsal or ventral retina were excised from the DD-PCR gels. Seven of these bands showed patterns consistent with the original pattern on the DD-PCR gel when used to probe Northern blots, indicating D-V expression in the retina. Fetal tissue Northern blots, which included retinal tissue from different stages of development and tissues other than retina, were also probed. Of particular interest was a spermidine/spermine N^1-acetyltransferase (*SSAT*) cDNA clone predominantly expressed in the retina. This clone showed ventrodorsal expression on the Northern blot but *in situ* hybridization revealed a temporal-nasal gradient of expression at E7. Since the temporal-nasal gradient of *SSAT* mRNA coincides with ganglion axon innervation of the optic tectum, we postulate that this clone plays a role guiding the axons to their target area in the brain. SSAT is known to be a rate-limiting enzyme in the degradation of the intracellular polyamines spermidine and spermine to putrescine, all of which are thought to have a pivotal role in cell growth and differentiation.

University of Alberta

Faculty of Graduate Studies and Research

The undersigned certify that they have read, and recommend to the Faculty of Graduate Studies and Research for acceptance, a thesis entitled *Identification of Asymmetrically Expressed Transcripts in the Developing Chick Retina* submitted by Rhonda L. Witte in partial fulfillment of the requirements for the degree of Masters of Science in Medical Sciences - Oncology.

Dr. Roseline Godbout

Dr. Paul Grundy

Dr. Charlotte Spencer

Dr. Paul Wong

Date: June 23, 2000

DEDICATION

To my little Wemily-emily.
"I am woman, hear me roar!"

ACKNOWLEDGEMENT

For all of those individuals who have made me into the person I am today, I thank you. To my parents, Daryl and Diane, I owe you both much gratitude for many things, including your support and encouragement at times when I needed it the most. To my sister Cheryl, I say the same. You're my bestest buddy. And to Steve, for staying by my side and for simply being you.

Of course, many thanks are given to the Godbout lab, largely to Dr. Roseline Godbout. RG, thanks for the many talks and for helping me decide what is best regarding both lab and career "stuff." You have been a tremendous help over the years and your lab expertise was invaluable (the chocolate also helped). To Stacey Hume, Mary Packer, Randy Andison, Elizabeth Monckton, Dwayne Bisgrove, Sachin Katyal and John Rowe: thanks for being the finest bunch of bench-mates anyone could ask for in a group. Thanks also to Laith Dabbagh for all the tissue sectioning. I would also like to thank my supervisory committee members, Drs. Charlotte Spencer and Paul Wong for their guidance, as well as Dr. Paul Grundy, for taking the time to read my thesis.

TABLE OF CONTENTS

CHAPTER 1. INTRODUCTION 1

1.1 Development of the Eye 1
1.1.1 Eye Morphogenesis 1

1.2 The Retina 5
1.2.1 Structure 5
1.2.2 Generation of Cellular Diversity 8

1.3 The Retinotectal System 13
1.3.1 The Path to the Brain 13
1.3.2 Specificity of Synaptic Connections 15
1.3.3 Axonal Guidance 16
1.3.4 Molecular Gradients in the Developing Retina 17

1.4 Polyamines 24
1.4.1 Structure and Proposed Functions of Polyamines 24
1.4.2 Polyamines and Cancer 26
1.4.3 The Polyamine Metabolic Pathway and SSAT Involvement 27
1.4.4 Polyamine Transport 31
1.4.5 Müller Glial Cells – Possible Polyamine Storage Centers? 33
1.4.6 Other Role of Polyamines in the Central Nervous System 35

1.5 DD-PCR 36
1.5.1 The DD-PCR Protocol 36
1.5.2 Disadvantages Associated with DD-PCR 39
1.5.3 Advantages Associated with DD-PCR 41

1.6 Objective of Thesis 43

CHAPTER 2. METHODS AND MATERIALS 44

2.1 Differential Display Polymerase Chain Reaction (DD-PCR) 44
2.1.1 Poly A+ RNA Extraction and First Strand cDNA Synthesis 44
2.1.2 cDNA Amplification 45
2.1.3 Reamplification of Eluted DNA 47
2.1.4 Cloning of Isolated DD-PCR cDNAs 48

2.2 Library Screening 48

2.3 Mini-Phage Preparation 50

2.4 Plasmid Purification 51

2.5 DNA Insert Purification 51

2.6 Southern Blotting 51

2.7 DNA Sequencing 52
2.7.1 Primers used for DNA Sequencing 52
2.7.2 Automated and Manual Sequencing Procedures 52

2.8 Eye Dissections 53

2.9 Northern Blotting 54

2.10 *In Situ* Hybridization 55
2.10.1 Probe Construction: Linearization of Plasmid DNA 55
2.10.2 DNA → RNA: DIG Incorporation 55

2.10.3 Detection of mRNA in Tissue Sections 56
2.10.4 Detection of mRNA in Whole Mounts 58

CHAPTER 3. RESULTS 61

3.1 DD-PCR 61
3.1.1 Isolation of RNA from Day 7 Retina and cDNA Synthesis 61
3.1.2 Initial Band Selection and Primer Efficiency 61
3.1.3 Reamplification and Subcloning into pBluescript 64

3.2 Northern Blot Analysis of Isolated DD-PCR cDNAs 68
3.2.1 Confirmation of Differential Expression 68
3.2.2 Comparison of Expression Patterns on the Original DD-PCR Gels and Northern Blots 70

3.3 Sequencing Results of Isolated DD-PCR cDNAs 72

3.4 Fetal Tissue Distribution Northern Blots 75

3.5 Characterization of the Chicken *SSAT* cDNA 79
3.5.1 Isolating and Sequencing the Full-Length Clone 79
3.5.2 Northern Blot Analysis of *SSAT* Expression throughout Retinal Development 81
3.5.3 Northern Blot Analysis of E11 and E15 Dorsal and Ventral Retina 85
3.5.4 Differential Expression of *SSAT* – *In Situ* Hybridization 86

CHAPTER 4. DISCUSSION 102

CHAPTER 5. FUTURE OBJECTIVES 118

Objective 1. To Further Characterize the Remaining Differentially Expressed DD-PCR clones 118

Objective 2. To Further Characterize SSAT Expression in the Developing CNS 119

CHAPTER 6. BIBLIOGRAPHY 121

LIST OF TABLES

Table	Title	Page
Table 2-1	Primers used for DD-PCR and sequencing	46
Table 3-1	Summary of all DD-PCR reactions performed indicating the bands selected and the primers used	65-66
Table 3-2	Sequence similarities of DD-PCR clones to known sequences entered in Genbank	74

LIST OF FIGURES

Figure	Title	Page
Figure 1-1	Early embryonic development of the eye	3
Figure 1-2	The major cell types and layers of the retina	6
Figure 1-3	Order of birth of retinal cells in the mouse retina	11
Figure 1-4	The retinotectal projection map in birds and lower vertebrates	14
Figure 1-5	Sperry's proposed molecular gradients of the retina	18
Figure 1-6	Mechanisms by which axons are guided towards their targets	19
Figure 1-7	The structural formulas of the naturally occurring polyamines putrescine, spermidine, and spermine, protonated at physiological pH	25
Figure 1-8	The polyamine biosynthetic and degradative pathways	29
Figure 1-9	DD-PCR	37
Figure 3-1	*ALDH1* is expressed in the dorsal chick retina	62
Figure 3-2	A typical autoradiograph of a DD-PCR gel	63
Figure 3-3	DD-PCR analysis of E7 chick retina and confirmation of differential expression by Northern blot analysis	69
Figure 3-4	A schematic representation of the relative distances migrated by each of the mRNA species, hybridized to each of the differentially expressed DD-PCR cDNA clones, as indicated by Northern blots	71
Figure 3-5	Fetal tissue distribution of differentially expressed DD-PCR bands	76-77

Figure 3-6	(A) Nucleotide and predicted amino acid sequence of the chick *SSAT* cDNA (B) Amino acid sequences of mammalian SSATs and chick SSAT	82-83
Figure 3-7	*SSAT* mRNA levels at different stages of chick retinal development	84
Figure 3-8	*SSAT* mRNA is differentially expressed in the developing chick retina	87
Figure 3-9	The axes of the retina	88
Figure 3-10	*In situ* hybridization of E7 chick retina using *ALDH1*	89
Figure 3-11	*In situ* hybridization of E7 chick retina showing *SSAT* expression: sections 7-1, 11-1, 13-1	90
Figure 3-12	*In situ* hybridization of E7 chick retina showing *SSAT* mRNA expression: section 17-1	91
Figure 3-13	*In situ* hybridization of E7 chick retina showing *SSAT* mRNA expression: section 20-2	92
Figure 3-14	*In situ* hybridization of E7 chick retina showing *SSAT* mRNA expression: section 24-1	93
Figure 3-15	*In situ* hybridization of E7 chick retina showing *SSAT* mRNA expression: section 24-3	94
Figure 3-16	*In situ* hybridization of E7 chick retina showing SSAT mRNA expression: section 25-2	95

Figure 3-17 *In situ* hybridization of E7 chick retina showing *SSAT* mRNA expression: section 28-3 96

Figure 3-18 *In situ* hybridization of E7 chick retina showing *SSAT* mRNA expression: section 29-2 97

Figure 3-19 *In situ* hybridization of E11 chick retina using *ALDH1*, *CAII* and *SSAT* 99

Figure 3-20 Magnified view of *in situ* hybridization of E7 and E11 chick retina showing *SSAT* expression in Müller glial cells 100

LIST OF ABBREVIATIONS

A	anterior
AcCoA	acetyl-CoenzymeA
ALDH1	aldehyde dehydrogenase type 1
AMPA	α-amino-3-hydroxy-5-methyl-4-isoxazolepropionic acid
Arg	arginine
ATP	adenosine 5'-triphosphate
B	band
BCIP	bromo-4-chloro-3-indolyl-phosphate
BSA	bovine serum albumin
C	central
CAII	carbonic anhydrase II
cDNA	complementary deoxyribonucleic acid
CHAPS	3-[(3-cholamidopropyl)-dimethyl-ammonio]-1-propane sulfonate
Ci	curie
CNS	central nervous system
CNTF	ciliary neurotrophic factor
CsCl	cesium chloride
CSPG	chondroitin sulfate proteoglycan
D	dorsal

dATP (dA)	deoxyadenosine triphosphate
dCTP (dC)	deoxycytidine triphosphate
DD-PCR	differential display-polymerase chain reaction
DFMO	2-difluromethylornithine
dGTP (dG)	deoxyguanosine triphosphate
DIG	digoxigenin
DNA	deoxyribonucleic acid
dNTP	deoxynucleoside triphosphate
DTT	dithiothreitol
dTTP (dT)	deoxythymidine triphosphate
E	embryonic day
E. coli	*Eshericia coli*
EDTA	[ethylenedinitrilo]tetraacetic acid
ELF-1	ephrin ligand family 1
Eph	ephrin
FAD	flavin adenine dinucleotide
GABA	γ-aminobutyric acid
GAD	glutamic acid decarboxylase
GCL	ganglion cell layer
INCENP	inner centromere protein
INL	inner nuclear layer
K^+	potassium
kb	kilobases

K_{ir}	inward rectifying K^+ channel
L	left
LiCl	lithium chloride
LIF	leukemia inhibitory factor
M	molar
Met	methionine
Mg^{2+}	magnesium
$MgCl_2$	magnesium chloride
mM	millimolar
ml	millilitre
MOPS	3-(N-morpholino)propanesulfonic acid
mRNA	messenger ribonucleic acid
N	nasal
N^1AcSpd	N^1-acetylspermidine
N^1AcSpm	N^1-acetylspermine
$Na_4P_2O_7$	sodium pyrophosphate
NaCl	sodium chloride
NaH_2PO_4	monobasic sodium phosphate
NaN_3	sodium azide
NaOAc	sodium acetate
NBT	nitro-blue tetrazolium salt
NH_4OAc	ammonium acetate
NMDA	N-methyl-D-aspartate

NO	nitric oxide
O.N.	optic nerve
OD_{260}	optical density at 260 nm
ODC	ornithine decarboxylase
oligo(dT)	oligodeoxythymidylic acid
Orn	ornithine
P	peripheral
PAO	polyamine oxidase
PCR	polymerase chain reaction
PEG	polyethylene glycol
pfu	plaque forming units
Po	posterior
poly A+	polyadenylated messenger ribonucleic acid
PUT	putrescine
PVA	polyvinyl alcohol
R	right
RA	retinoic acid
RAGS	repulsive axon guidance signal
RNA	ribonucleic acid
RNase	ribonuclease
RPE	retinal pigmented epithelium
RPTP	receptor protein tyrosine phosphatase
rRNA	ribosomal ribonucleic acid

RT-PCR	reverse transcriptase-polymerase chain reaction
SAM-DC	S-adenosylmethionine decarboxylase
SPD	spermidine
Spd syn	spermidine synthase
SPM	spermine
Spm syn	spermine synthase
SSAT	spermidine/spermine N^1-acetyltransferase
T	total
Taq	*Thermus aquaticus*
TATA	thymine/adenine repeat promoter element
Te	temporal
TOP	toponymic
tRNA	transfer ribonucleic acid
TYRP2/DCT	tyrosine-related protein-2/DOPAchrome tautomerase
µl	microlitre
µM	micromolar
V	ventral
xNopp180	*Xenopus* Nopp 180

CHAPTER 1. INTRODUCTION

1.1 Development of the Eye

The eye is a remarkable structure. Its detailed organization and connection with the brain demands recognition as one of the most intricate of the human systems. The retina is the neural tissue of the eye. Examination of the retina yields information about the visual system itself. As well, much can be learned about central nervous system (CNS) development through molecular analysis of the retina.

Hundreds of millions of cells exist in the retina itself, with many more millions of related cell types existing in the brain and the rest of the CNS (Dowling, 1987). What is extremely intriguing, however, is the diversity of cell types within the nervous system. Just how many neuronal cell types exist, in addition to glial cells, is not known. Estimates of a few hundred mammalian neuronal subtypes in the nervous system appear to be overly conservative (Stevens, 1998; Edlund and Jessell, 1999). How are these cell types formed? How are their respective fates determined and at what stage of development? What intrinsic or extrinsic cues exist to help generate such cellular diversity? These questions are the subject of intense investigation and many are using the retina as a model to help reveal the answers.

1.1.1 Eye Morphogenesis

Eye development can be subdivided into three phases: 1. The formation of major ocular structures through induction and regional specification; 2. The maturation of the major structures into a functional eye; and 3. The formation of neuronal connections between

the retina (via the optic nerve) and the optic tectum (Jean *et al.*, 1998). Eye development is a complex process involving many genes, the expression of which are regionalized in certain areas within the developing eye. The expression patterns of these genes is not constant throughout retinal development, suggesting that expression at particular stages of development is crucial for proper eye formation. For example, many homeobox containing genes which encode transcription factors are known to be involved in eye morphogenesis and in the formation of retinal axes important in targeting retinal ganglion axes to the brain. Among these genes are the vertebrate homeobox genes *Pax6*, *Chx10*, *Tbx5*, *cVax2*, *mVax* and *Otx2* (Liu *et al.*, 1994; Davis and Reed, 1996; Belecky-Adams *et al.*, 1997; Bovolenta *et al.*, 1997; Barbieri *et al.*, 1999; Schulte *et al.*, 1999; Koshiba-Takeuchi *et al.*, 2000). *Pax6* has been shown to be essential for eye morphogenesis, as homozygous *Pax6* mutations resulted in the absence of eyes in mouse embryos and were lethal (reviewed in Gehring and Ikeo, 1999).

Formation of Major Ocular Structures

During the first stage of eye development, the optic vesicle is formed and the lens placode is induced, followed by the formation of the optic cup and lens vesicle (Jean *et al.*, 1998). A regionalized area of the neuroectoderm, termed the eye field, evaginates from the forebrain during neural folding to form a primitive optic pit, which subsequently becomes the optic vesicle (Figure 1-1). Contact of the optic vesicle with the overlying ectoderm induces the ectoderm to become primitive lens tissue. The primitive lens tissue then thickens, forming the lens placode, followed by invagination and formation of the

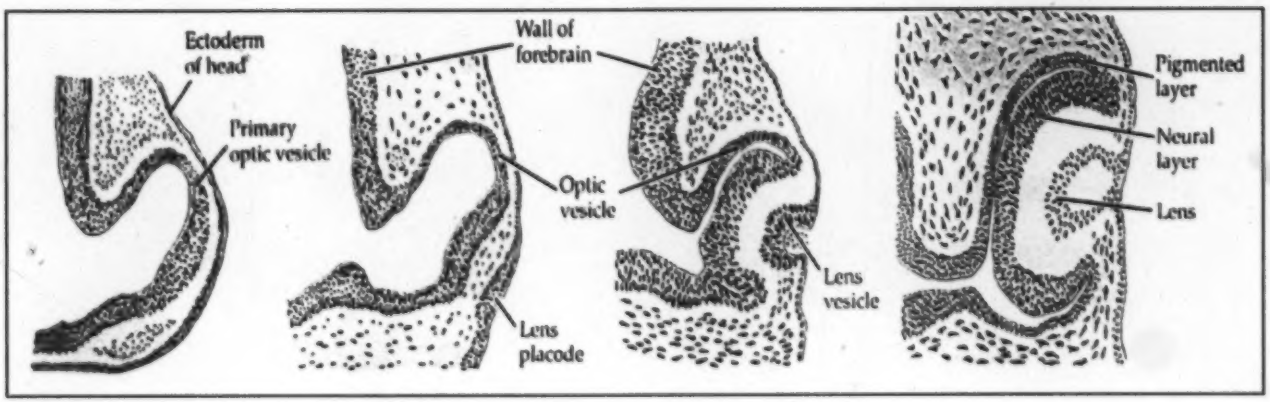

Figure 1-1. Early embryonic development of the eye (Mann, 1964).

lens vesicle. Also during this time, the optic stalk and optic cup (inner and outer layers) are formed. In the chick retina, cell proliferation is most extensive at embryonic day 3 (E3) and is greatly reduced by E9; cell migration occurs between E8 and E10; and differentiation between E11 and E21 (hatching). At E5, the retinal axons that connect the retina and brain have reached the surface of the optic tectum, and by E7 they have started to cover the tectal surface (Bellairs and Osmond, 1998).

Maturation of Major Ocular Structures

During the maturation phase of eye development, the primary structures differentiate to acquire their specific traits. The lens vesicle becomes the lens, the optic stalk later differentiates into the optic nerve, while the inner and outer layers of the optic cup form the neural retina and the retinal pigmented epithelium, respectively. The cornea is formed from ectoderm overlying the lens while the iris, sclera, ciliary body and lachrymal gland are all formed from differentiated mesenchymal cells of neural crest origin (Jean *et al.*, 1998). Each of these specialized structures of the eye undergoes specific events resulting in the emergence of the functional tissue.

Formation of Neuronal Connections

Finally, during the last phase of eye development, the connection between the eye and brain is formed by the retinal ganglion cells. As previously mentioned, the axons of the ganglion cells form the optic nerve and leave the back of the eye to connect with specified areas within the brain. Specifically, the ganglion axons form a topographic map of the retina onto the optic tectum, such that any one axon from the retina can be traced to

a definite area within the tectum. In no way are the connections between the retina and the brain random.

1.2 The Retina

1.2.1 Structure

The retina is a relatively simple structure in terms of its arrangement and composition. The layers are well-defined and molecular markers are known for the different cell types comprising each layer. Because of this, it is possible to study the cells located in a specific layer of the retina. Furthermore, the retina can be easily isolated from other ocular tissues, making it an ideal system for biological and biochemical analysis. For example, we chose the chick as our model system because chick embryos can be easily obtained at different stages of development. Also, chicken eyes are large, allowing the isolation of comparatively large amount of tissue.

The retina is composed of three cellular layers, the outer and inner nuclear layers and the ganglion cell layer, all of which primarily contain cell bodies (Figure 1-2). Two synaptic layers, the outer and inner plexiform layers, separate the cellular layers and contain neuronal processes. A third synaptic layer, the optic nerve fiber layer, consists of ganglion cell axons. There are seven main cell types found in these different layers, six neuronal and one glial. These are the ganglion cells, photoreceptor cells (rods and cones), amacrine cells, bipolar cells, horizontal cells, interplexiform cells and the Müller glial cells. Thus, despite being composed of millions of cells, only seven major cell types are responsible for the correct functioning of the retina.

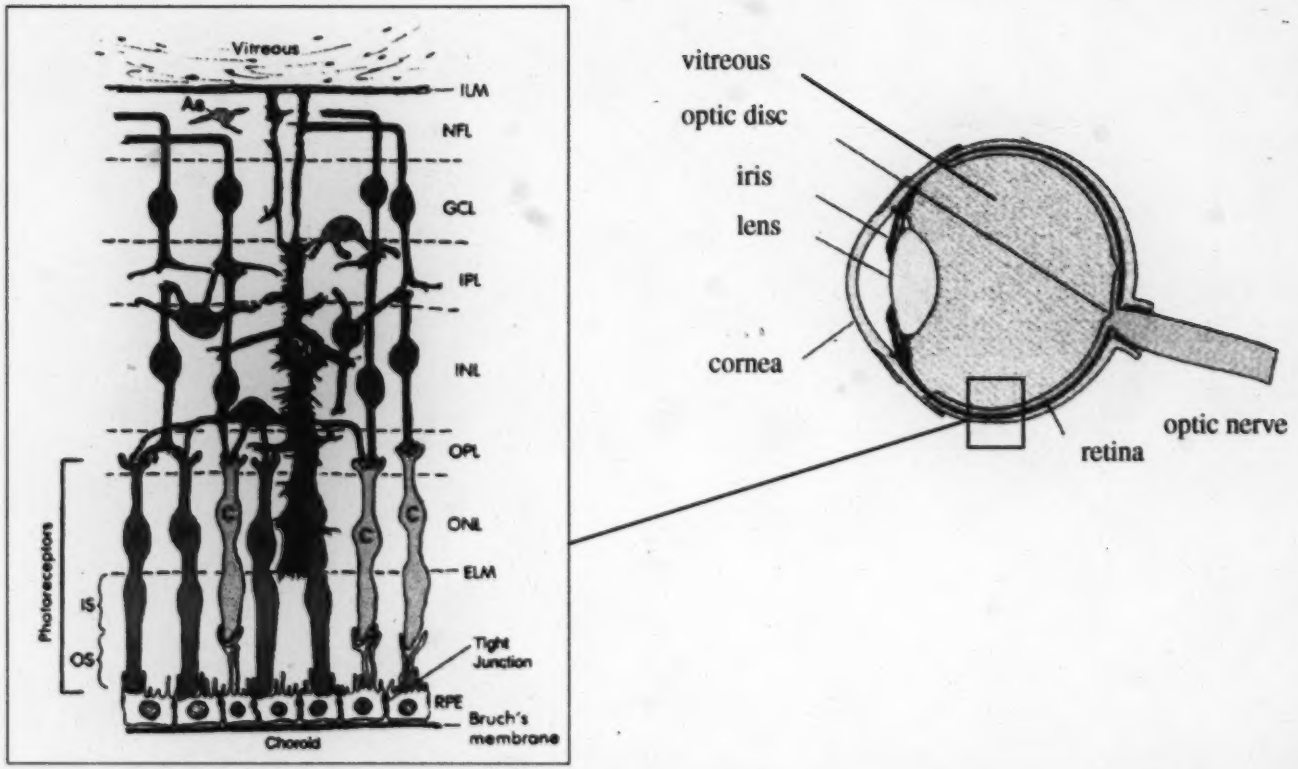

Figure 1-2. The major cell types and layers of the retina. The diagram of the eye on the right is for orientation. Cell types: G: ganglion cells; DA: displaced amacrine cells; Am: amacrine cells; I: interplexiform cells; M: müller glial cells; B: bipolar cells; H: horizontal cells; R: rod photoreceptors; C: cone photoreceptors. Retinal layers: ILM: inner limiting membrane; NFL: nerve fiber layer; GCL: ganglion cell layer; IPL: inner plexiform layer; INL: inner nuclear layer; OPL: outer plexiform layer; ONL: outer nuclear layer; ELM: external limiting membrane; IS: inner segments of rods and cones; OS: outer segments of rods and cones (adapted from Ogden, 1987).

The cell bodies of the photoreceptor cells are found in the outer nuclear layer, and the cell bodies of the bipolar, horizontal, amacrine and interplexiform cells are found in the inner nuclear layer (Figure 1-2). From the outer margin to the inner margin of the inner nuclear layer, the order is as follows: horizontal cells, bipolar cells (middle), and amacrine and interplexiform cells.

The ganglion cells comprise the most proximal (innermost) layer of the retina, the ganglion cell layer, which is separated from the inner nuclear layer by the inner plexiform layer. The axons of ganglion cells relay information from the retina to the brain by extending their processes through the optic nerve at the back of the eye. Amacrine cells can also be found in the ganglion cell layer and are then termed "displaced" amacrine cells. Müller glial cells extend vertically throughout the retina, from the distally located outer limiting membrane to the proximally located inner limiting membrane of the retina. Cell bodies of Müller glial cells are located primarily in the inner nuclear layer (Dowling, 1987).

When light enters the eye through the pupil, it passes through the different layers of the retina and is first received by the photoreceptor cells, the light-sensitive cells of the retina (Dowling, 1987). Photoreceptor cells synapse with bipolar and horizontal cells and when stimulated, information is relayed to these cells via synapses located in the outer plexiform layer. Processes of the horizontal cells are confined to the outer plexiform layer and extend laterally, interconnecting photoreceptor cells, bipolar cells and horizontal cells. Bipolar cells act as output neurons, transmitting information to the next synaptic

zone, the inner plexiform layer, where they connect to ganglion cells and amacrine cells. Here, the ganglion cells act as the output neurons for the entire retina, with their axons leaving the eye through the optic nerve and relaying information to the brain to be processed.

Amacrine cells act similarly to horizontal cells, interconnecting bipolar cells, ganglion cells and amacrine cells within the inner plexiform layer. As their name suggests, interplexiform cells extend their processes into both the outer and inner plexiform layers. The Müller glial cells are radial glial cells and function to support the retina, possibly aiding the orientation, displacement and positioning of neuronal cells as the retina develops (Ogden, 1988).

1.2.2 Generation of Cellular Diversity

Evidence is beginning to surface which shows that cells in the developing retina respond to both extrinsic and intrinsic cues for cell-fate determination. Extrinsic cues refer to secreted or transmembrane signals present in a cell's environment while intrinsic cues refer to the "gene complement" of a cell (Cepko *et al.*, 1996; Edlund and Jessell, 1999). A retinal cell is subject to both extrinsic and intrinsic cues and the delicate balance between the two types of signals is thought to play a role in cell-fate decisions. Once committed to a particular cell type, environmental factors can no longer alter the cell-fate and the intrinsic factors of the cell are said to be stabilized.

Retinal Progenitor Cells are Multipotent

It has been shown that retinal progenitor cells (neuroepithelial cells) are multipotent, meaning they are able to give rise to virtually all cell types in the retina as long as they are dividing (Turner and Cepko, 1987; Holt *et al.*, 1988; Wetts and Fraser, 1988; Turner *et al.*, 1990; Fekete *et al.*, 1994). Evidence strongly supports the hypothesis that cell-fate determination in the retina is not lineage dependent. In early studies, individual retinal progenitors in the frog retina were injected with lineage tracer dyes (fluorescent dextran or horseradish peroxidase) which labelled the clones of each retinal precursor cell (Holt *et al.*, 1988; Wetts and Fraser, 1988; Wetts *et al.*, 1989). Tracer dyes revealed various cell types among the retinal clones derived from an individual retinal progenitor cell, suggesting that cell type determination in the frog was lineage-independent.

Turner and Cepko (1987) and Turner and colleagues (1990) used a retroviral marker to show similar findings in the mouse and rat retina. The gene encoding the *E. coli* β-galactosidase enzyme was introduced into retinal precursor cells via infection with a replication-incompetent retroviral vector (BAG). Cells containing the integrated virus expressed the β-galactosidase enzyme and were identified by histochemical detection of enzyme activity (blue color). Both the number of cells and the cell type varied with each clone. For example, one retinal progenitor cell gave rise to four cell types (34 rod photoreceptor cells, five bipolar cells, a Müller glial cell and two amacrine cells), while another progenitor cell gave rise to five cell types (54 rod photoreceptor cells, 11 bipolar cells, four amacrine cells, one Müller glial cell and a ganglion cell) (Turner *et al.*, 1990).

The same findings were also obtained using the chick retina as a model, indicating common mechanisms of cell type determination in all vertebrates (Cepko, 1990).

Cell Fate is Determined by Intrinsic and Extrinsic Factors

A model based on recent findings suggests that both multipotential progenitor cells and the environment change over time and that changes in each are intertwined (reviewed in Cepko, 1996; Edlund and Jessell, 1999). Not only does the environment change with the response properties of a cell, but also the gene complement of a cell dictates its response to the environment. Thus, environmental cues are interpreted differently by cells depending on their intrinsic environment and immediate external environment (Cepko, 1996). This leads to a progressive restriction in the cell-fates available to the cell, reflected in both extrinsic and intrinsic changes.

The first post-mitotic cell is generated after the formation of the optic cup, with the birth of a particular cell type defined by its final S-phase (Cepko, 1996). This is followed by its migration out of an area termed the ventricular zone where the progenitor cells lie, to its appropriate layer within the developing retina where it differentiates into its determined cell type (Cepko, 1996). Different species have been examined to determine and compare the order that the different cell types are generated. In the various species examined, retinal cell types were generated in a consistent order, as shown by [^{3}H]thymidine labelling (Altshuler *et al.*, 1991; Prada *et al.*, 1991) (Figure 1-3). Consistent throughout, the ganglion cells appear to be the first cell type born, followed by the birth of the remaining cell types whose birth dates may overlap with each other

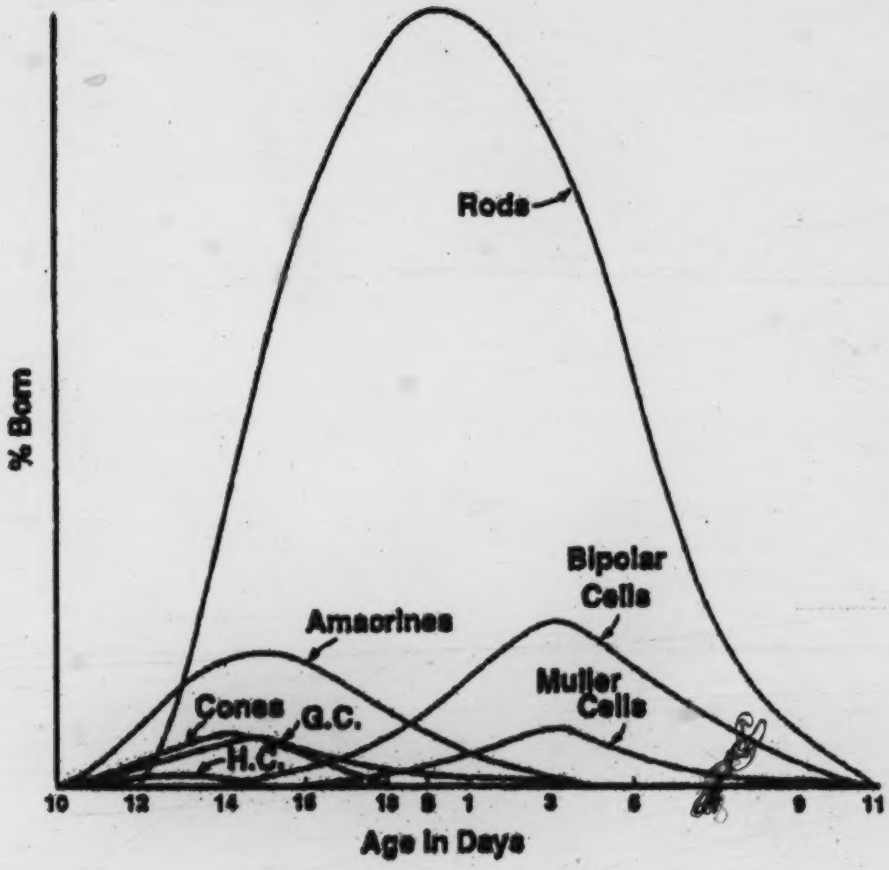

Figure 1-3. Order of birth of retinal cells in the mouse retina. The percentage of cells born on a given day is given shown on the Y-axis. [^{3}H]thymidine was used to label the cells (Cepko et al., 1996).

(Figure 1-3). This presents another interesting question: How are the appropriate cell types generated in the proper sequence and in the proper ratios in order to set-up the appropriate environment? Obviously, intrinsic factors are key for they must enable the cell to respond to extrinsic cues, and by doing so, determine the environmental surroundings of other cells.

Rod development is an example of cell-fate determination which is thought to be largely governed by intrinsic factors. Opsin expression is a marker of differentiating rods. When treated with either CNTF (ciliary neurotrophic factor) or LIF (leukemia inhibitory factor), non-opsin expressing rod-fated cells can be blocked from expressing opsin and instead become bipolar neurons (see Cepko, 1996). Retinal and brain extracts have also been found to block opsin expression, resulting in the differentiation of bipolar neurons, and indicate the existence of an inhibitor to rod development (Altshuler *et al.*, 1993). When opsin-expressing rods are treated with the above factors, they are resistant and still become rods. Thus, rods serve as an example of a post-mitotic commitment step that is likely governed by intrinsic factors which dictate a cell's response to inhibitory or stimulatory factors. Failure to commit in response to various environmental factors results in bipolar cell formation. This shows how critical it is to have the correct balance between extrinsic and intrinsic factors at the appropriate time.

1.3 The Retinotectal System

1.3.1 The Path to the Brain

As previously mentioned, retinal ganglion cells are the neurons which connect the retina to the brain. Ganglion cells leave the posterior portion of the eye at optic disk. Because of this arrangement, ganglion axons must turn posteriorly and migrate through the layers of the retina before they can exit the eye. Once they meet at the optic disk, the ganglion axons travel through the sclera and fasciculate to form the optic nerve. Up until this point, the axons are unmyelinated but because the optic nerve is part of the CNS, they become myelinated upon exit from the eye (Nolte, 1988).

Ganglion axons travel through the optic nerve to the optic chiasm where the optic nerves from each eye meet. In mammals, the optic nerves partially decussate. Fibers originating in the nasal half of each retina cross to the contralateral (opposite) optic tract while fibers originating in the temporal half of each retina do not cross and enter the ipsilateral (same) optic tract. In birds and lower vertebrates, such as fish and amphibia, the optic nerves completely cross over at the optic chiasm and enter the contralateral tract (Figure 1-4) (Bellairs and Osmond, 1993; Goodman and Shatz, 1993).

In all vertebrates, the retinal ganglion axons project onto their target area in the brain in a topographically precise manner. Neighbouring retinal ganglion axons project to neighbouring target cells in the brain. In mammals, the most important visual pathway involves projections to the lateral geniculate nucleus, while in nonmammalian vertebrates, it is the optic tectum (Nolte, 1988). The end result is the formation of a

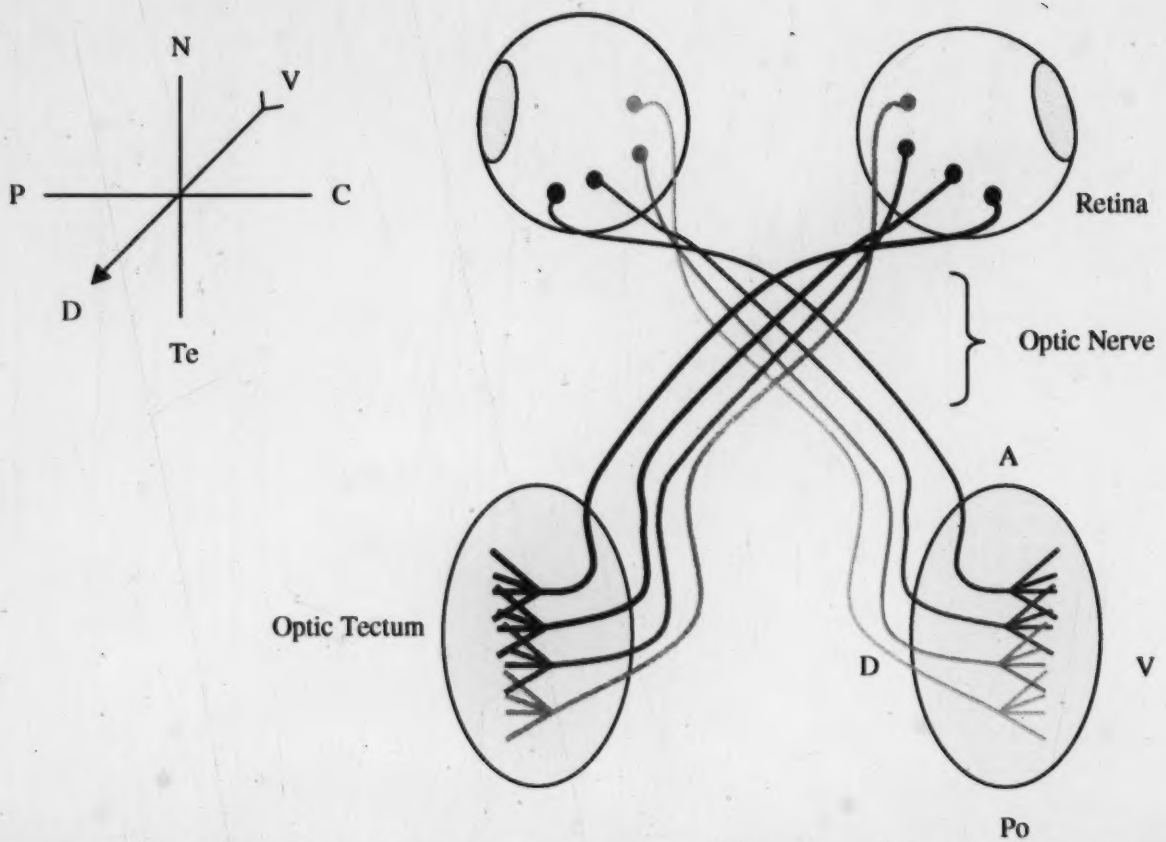

Figure 1-4. The retinotectal projection map in birds and lower vertebrates. The retina projects onto specific areas of the optic tectum. Neighboring ganglion cells in the retina have neighboring ganglion axons in the tectum. Nasal (N) retina projects to posterior (Po) tectum; temporal (Te) retina projects to anterior (A) tectum; dorsal (D) retina projects to ventral (V) tectum; and ventral retina projects to dorsal tectum. C: central; P: peripheral. The axes are shown for the retina (left) and optic tectum (right). The tail of the arrow is towards the back of the eye (adapted from Goodman and Shatz, 1993).

topographic map: a projection of the retina's map of visual space across the target area in the brain (Goodman and Shatz, 1993). Nasal retinal axons project to the posterior tectum, and temporal retinal axons project to the anterior tectum (Figure 1-4). In the perpendicular axis, dorsal retinal axons project to the ventral tectum and ventral retinal axons to the dorsal tectum (Figure 1-4). What guides the ganglion axons to their precise locations within the optic tectum? The answer is thought to lie in positional guidance cues.

1.3.2 Specificity of Synaptic Connections

The axons of retinal ganglion cells travel a considerable distance before reaching the appropriate target area in the optic tectum. Goodman and Shatz (1993) outline three events that happen *en route* to the brain. The first of these is pathway selection. As they leave the retina, ganglion axons do not bundle together in a random fashion. They choose their neighbors carefully since they reflect a specific position in the retina. They then find their way to the optic chiasm where they must choose whether to cross over to the other eye. In the second major event, ganglion axons select their target area and migrate to the optic tectum, forming the initial scaffolding of neurons. Once there, they make a very specific choice regarding the exact point of innervation. This last event is termed address selection and involves the generation of spontaneous activity by neurons themselves (Goodman and Shatz, 1993; Zhang *et al.*, 1998).

Waves of action potentials are present in the developing vertebrate retina, spontaneously generated by ganglion cells even before visual stimulation (Meister *et al.*,

1991; Wong *et al.*, 1993; Wong *et al.*, 1998). Specifically, in the developing chick, spontaneous activity is first detected at E7 and becomes most prominent through E13-E18, which is the same time period when retinotectal connections are being reorganized to form a precise map (Nakamura and O'Leary, 1989; Wong *et al.*, 1998; Ichijo, 1999). This activity is thought to be a "refinement" process involving the retraction and expansion of axonal terminals to ensure precise connectivity. However, this spontaneous activity is not thought to have a direct role in *targeting* axons to their specific place in the optic tectum (Wong *et al.*, 1998). The migration and targeting of ganglion axons to their appropriate areas in the brain is thought to be mediated by cell surface cues.

1.3.3 Axonal Guidance

Sperry's Experiments

Much of the work that has been done regarding the retinotectal system can be attributed to the previous findings and hypotheses of Roger Sperry in the 1950's and 1960's. Sperry conducted a number of convincing experiments in which he revealed topographic connections between the retina and the brain. Most notable was his proposal of the chemoaffinity hypothesis (Sperry, 1963; reviewed in Goodman and Shatz, 1993 and Meyer, 1998).

The chemoaffinity hypothesis proposed that the retina and tectum have complementary gradients of molecular markers or what he called "identification tags." Sperry proposed that retinal axons possess markers that correspond to markers on tectal target cells and that these molecular markers are the products of cellular differentiation.

Ganglion and tectal cells possess at least two types of markers that label them according to cell type (ganglion or tectal) and position (Meyer, 1998). These markers act as "affinity forces" which actively direct a retinal axon to a corresponding area on the tectum (Sperry, 1963). The end result is a map of the retina across the surface of the tectum such that a retinal ganglion axon projects to a predictable location in the tectum.

Furthermore, Sperry believed that these molecular markers exist in concentration gradients throughout the retina, tectum and the pathway itself leading from the retina to the tectum. Sperry proposed three positional concentration gradients that exist in complementary fashions between the retina and tectum: 1. Dorsal -Ventral; 2. Anterior-Posterior; and 3. Central-Peripheral (Figure 1-5). Much work has been done in this area of developmental biology and evidence exists to support Sperry's early hypotheses.

1.3.4 Molecular Gradients in the Developing Retina

Examples of molecular gradients of the type that Sperry proposed have been shown to exist and their functional roles are being examined. Studies examining the spatial limits on axon guidance, that is the distance over which an axon can detect a molecular target factor, are also being performed and are providing some interesting insights into this area (reviewed in Goodhill, 1998). Axons could possibly be guided towards their targets by several mechanisms, which include chemorepulsion, chemoattraction, contact-dependent repulsion, and contact-dependent attraction (reviewed in Mueller, 1999) (Figure 1-6). Although some molecules have been shown to exist in gradients in either the retina or the

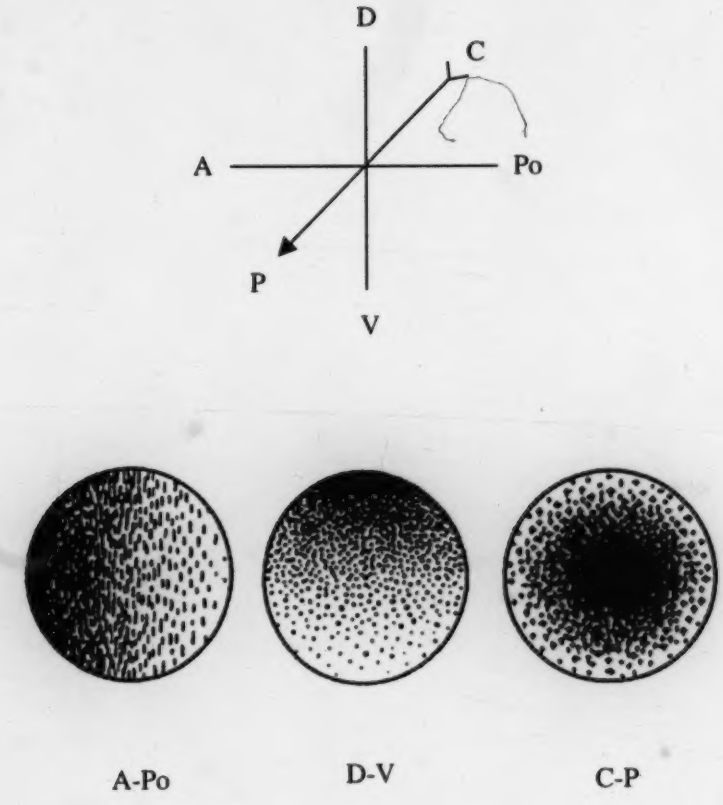

Figure 1-5. Sperry's proposed molecular gradients of the retina. A-Po: anterior (nasal) to posterior (temporal); D-V: dorsal to ventral; C-P: central to peripheral. Axes are indicated for the retina (adapted from Meyer, 1998).

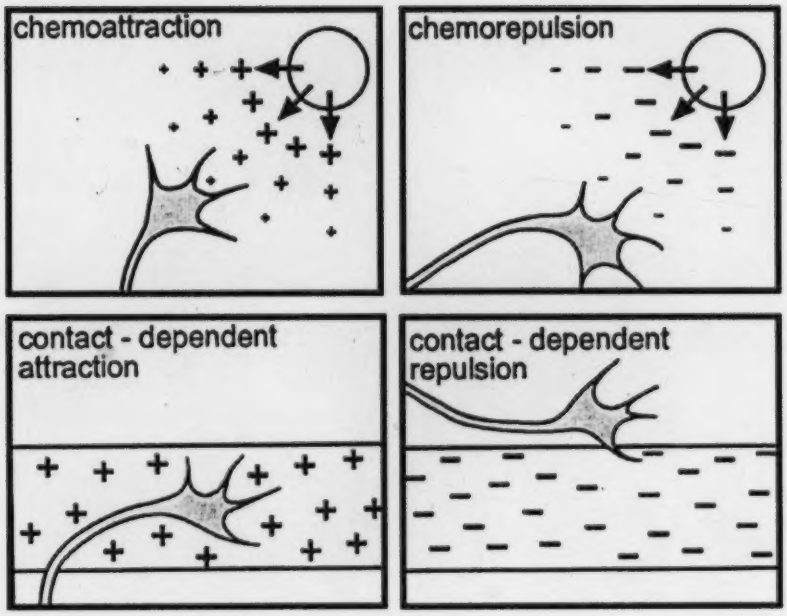

Figure 1-6. Mechanisms by which axons are guided towards their targets. Guidance mechanisms are classified as attractive or repulsive. Chemoattraction and chemorepulsion act over long-range distances, versus contact-dependent attraction or repulsion which act over short-range distances (adapted from Mueller, 1999).

brain, their complementary gradients may not yet be known. Convincing hypotheses are being presented regarding the purpose of such gradients.

Aldehyde Dehydrogenase type 1 (ALDH1): ALDH1 is a cytosolic enzyme responsible for the enzymatic conversion of retinaldehyde to retinoic acid (RA), a known transcriptional regulator with important roles in neuronal differentiation and patterning in the developing embryo (reviewed in Dräger *et al.*, 1998). The synthesis of RA via ALDH1 has been shown as fundamental to the differentiation and development of certain embryonic structures, including the retina. Specifically, ALDH1 is expressed in the dorsal retina of embryonic vertebrate species (Dräger *et al.*, 1998), appearing early in development and decreasing to low levels in the differentiated embryonic and adult retina of mouse and chick (McCaffery *et al.*, 1991; Godbout *et al.*, 1996). Furthermore, activity of an unidentified ALDH isoform, which is more effective in the conversion of retinaldehyde to RA than ALDH1, has also been detected in the ventral retina (McCaffery *et al.*, 1992; McCaffery *et al.*, 1993). The result is in an asymmetric gradient of RA throughout the retina, with higher levels in the ventral retina as compared to dorsal retina. Inhibition of the unidentified ventral ALDH at early developmental stages, resulting in the inhibition of RA synthesis in the ventral retina, generated half-eyes lacking a ventral retina (Marsh-Armstrong *et al.*, 1994). Conversely, uniform levels of RA throughout the eye enhanced the expression of ventral markers (*pax2*) in the dorsal retina and suppressed the expression of dorsal markers (*msh[c]*) (Hyatt *et al.*, 1996).

Since RA is known to exert dose-dependent effects on the formation of embryonic structures, possibly through altered gene expression, (Durston *et al.*, 1989; Ruiz I Altaba and Jessell, 1991), it is possible that RA may be involved in generating asymmetric gene expression in a dorsoventral gradient. This could result in a gradient of molecular markers like Sperry postulated, which could be responsible for guiding ganglion axons to the optic tectum.

Toponymic (TOP) molecules: TOP molecules were the first molecules found to be expressed in asymmetric gradients in both the retina and the tectum (Trisler *et al.*, 1981; Trisler, 1990). Two TOP molecules have been identified, TOP_{AP} and TOP_{DV}, which are cell surface molecules expressed in the retina in anteroposterior and dorsoventral gradients, respectively. Inverted expression gradients corresponding to each molecule are found in the tectum, making it plausible that they are involved in axon guidance to the tectum (Trisler, 1990). The functions of either TOP molecule are not yet known. However, TOP_{AP} has been cloned and was found to be an integral membrane protein possibly involved in protein-protein interactions due to the presence of a coiled-coil motif and leucine-zipper-like sequences (Savitt *et al.*, 1995).

Chondroitin Sulfate Proteoglycan (CSPG): CSPG has been implicated in axon guidance in the developing retina (Brittis, 1992). CSPG was detected in the retina as early as E11 and was shown to move peripherally with development in the murine retina, remaining ahead of developing ganglion axons (Snow *et al.*, 1991; Chung *et al.*, 2000). CSPG was also detected at the optic chiasm, where dorsal and ventral retinal axons are sorted

(Chung *et al.*, 2000). Previous observations demonstrated a concentration-dependent inhibitory effect of CSPG on neurite outgrowth (Snow *et al.*, 1990). Depending on the concentration of CSPG present, neurites either stopped or turned to grow along the boundary of CSPG and even showed varying degrees of crossing over. Enzymatic degradation of CSPG in the retina resulted in random axonal outgrowth (Brittis *et al.*, 1992). More recent studies have also shown an inhibitory effect of CSPG on neurite outgrowth in different neuronal tissues (Erskine and McCaig, 1997; Zuo *et al.*, 1998; Anderson *et al.*, 1998). These observations support a role for CSPG in the initial elongation and guidance of axons through the retina.

Ephrin (Eph) family: The Eph-related receptors and their ligands (ephrins) are also thought to be involved in axon guidance based on their distribution patterns in the developing retina and brain. The Eph family is the largest known family of receptor tyrosine kinases and most are solely expressed in the nervous system, making them attractive subjects of developmental neurobiology (Cheng *et al.*, 1995). Also, it has recently been found that certain members of the receptor protein tyrosine phosphatase (RPTP) family are expressed in gradients within the retina and tectum, which would indicate a possible role in axon growth and formation of the retinotectal projection (Ledig *et al.*, 1999).

It was only a few years ago that the first ligands for the Eph-related receptors were identified. Close examination has revealed complementary expression gradients for some of the receptor-ligand pairs along the anteroposterior axis of the retina and tectum.

For example, two ligands, RAGS (repulsive axon guidance signal; ephrin-A5) and ELF-1 (Eph ligand family 1; ephrin-A2), are both expressed in an increasing anterior to posterior gradient in the developing tectum (Cheng *et al.*, 1995; Monschau *et al.*, 1997). However, expression of RAGS is restricted to the very posterior pole of the tectum (Monschau *et al.*, 1997), whereas ELF-1 is present in a more graded distribution across the entire tectum (Cheng *et al.*, 1995).

Both the RAGS and ELF-1 ligands have been shown to behave as repulsive guidance molecules towards temporal, but not nasal, retinal ganglion axons, with RAGS having the strongest effect on repulsion (Drescher *et al.*, 1995; Nakamoto *et al.*, 1996; Monschau *et al.*, 1997; O'Leary *et al.*, 1999). The receptor for both ligands, Cek4 (EphA3) is expressed in an increasing nasal to temporal gradient in the retina (Cheng *et al.*, 1995) and RAGS has been shown to have a higher binding affinity for Cek4 than ELF-1. Exactly how this arrangement of gradients works is not known but it is thought to work based on guidance repulsion and receptor-ligand binding affinities (Pasquale, 1997; O'Leary *et al.*, 1999).

In retinotopic mapping, temporal retinal axons target the anterior tectum and nasal axons target the posterior tectum. Ingrowing retinal ganglion axons pass from the anterior to posterior tectum. Thus, retinal ganglion axons are first sorted in the anterior tectum. Here, temporal retinal ganglion axons with high Cek4 expression are repelled from entering the posterior tectum and are guided to the anterior tectum where they bind ELF-1 (expressed at low levels in the anterior tectum). Axons with low Cek4 expression

(nasal axons) are not repelled from the posterior tectum, causing them to enter the posterior tectum towards high levels of ELF-1 and RAGS. It is thought that RAGS and ELF-1 act as repulsive guidance molecules for temporal retinal ganglion axons, which, in addition to their differential binding affinities for the Cek4 receptor, helps target ganglion axons.

1.4 Polyamines

1.4.1 Structure and Proposed Functions of Polyamines

Despite extensive characterization of the biosynthetic and degradative pathways of polyamines, their exact functions remain largely unknown. The polyamines putrescine, spermidine and spermine are ubiquitously expressed organic polycations necessary for cell growth and differentiation (Pegg, 1988; reviewed in Seiler, 1990 and Casero and Pegg, 1993). They are simple aliphatic amines that are protonated at physiological pH (Figure 1-7). Putrescine, spermidine and spermine possess two, three and four positive charges, respectively, which are important for interactions with DNA and protein. Both eukaryotes and prokaryotes require polyamines and their intracellular concentrations are tightly regulated by biosynthesis, degradation, excretion and uptake.

The specific functions of polyamines are still under investigation but their roles are thought to be widespread and of great physiologic importance. Studies have shown that polyamines can interact with DNA (Makita and Yoshikawa, 1999; Antony *et al.*, 1999) and that polyamine levels fluctuate with cell cycle progression (Bettuzi *et al.*,

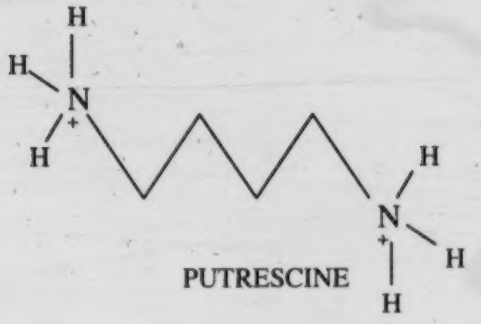

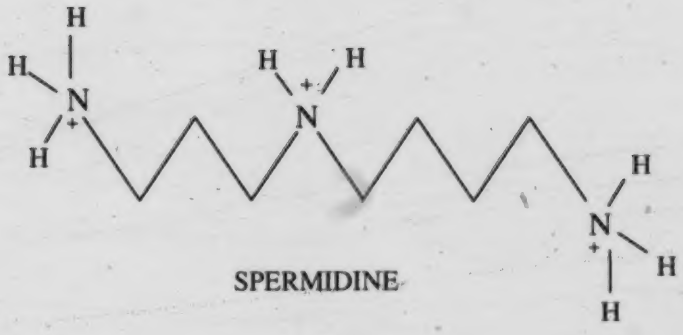

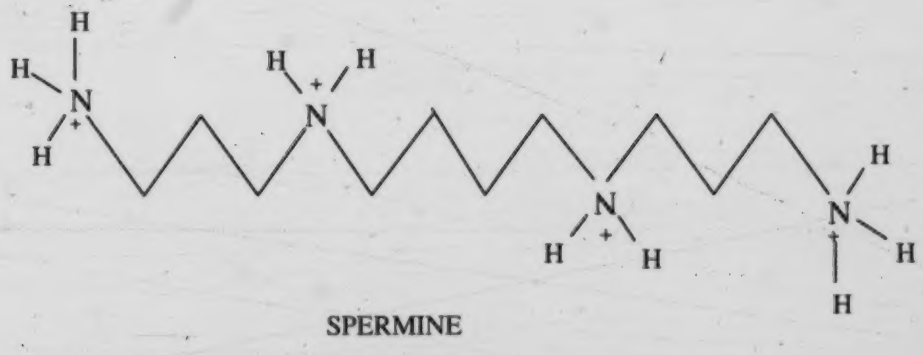

Figure 1-7. The structural formulas of the naturally occurring polyamines putrescine, spermidine, and spermine, protonated at physiological pH (adapted from Morgan, 1999).

1999). These findings suggest that polyamines affect cell growth and differentiation through close association with DNA structure.

Because they are positively charged, polyamines are able to bind to the negative phosphate groups of the DNA double helix, neutralizing the negative charge of the DNA backbone and stabilizing its structure (reviewed in Heby and Persson, 1990). Polyamines, in particular spermidine and spermine, have also been shown to stabilize other structures, including DNA-RNA hybrids (Antony *et al.*, 1999), stems and loops in rRNA and mRNA, and tRNA conformation (Heby and Persson, 1990). However, the mechanisms that govern polyamine interactions with nucleic acids are sketchy and largely speculative.

1.4.2 Polyamines and Cancer

Polyamines are also of interest to cancer researchers. Rapidly dividing tissues, including tumors, have higher levels of polyamines than non-dividing tissues and exhibit increased uptake of polyamines. Enhanced activity of the polyamine biosynthetic enzyme ornithine decarboxylase (ODC) increases intracellular polyamine levels and is associated with tumor growth (reviewed in Seiler *et al.*, 1998). Therefore, the degradation of polyamines has become the focus of many investigators interested in anti-tumor therapy.

Polyamine analogs which result in the superinduction of spermidine/spermine N^1-acetyltransferase (SSAT), the rate limiting enzyme in polyamine degradation (see below), have been developed (Casero *et al.*, 1994; Xiao and Casero, 1996; Fogel-Petrovic *et al.*,

1997). When superinduced, *SSAT* is cytotoxic to certain tumor cells. Induced SSAT enzyme activity occurs through a variety of mechanisms which include increased transcription (Wang *et al.*, 1998) and stabilization of *SSAT* mRNA and protein (Fogel-Petrovic *et al.*, 1996; Fogel-Petrovic *et al.*, 1997).

The exact mechanisms by which superinduced *SSAT* exerts its cytotoxic effects remain unknown. It has been suggested that superinduction of *SSAT* may be cytotoxic through a possible role in programmed cell death (Ha *et al.*, 1997). However, other studies have not found any correlation between *SSAT* superinduction and programmed cell death (reviewed in Seiler *et al.*, 1998). Clinical trials using polyamine analogues have been initiated, providing hope for an effective anti-tumor therapy. Trials are also underway with 2-difluoromethylornithine (DFMO), a selective inhibitor of the polyamine biosynthetic enzyme ODC.

1.4.3 The Polyamine Metabolic Pathway and SSAT Involvement

Intracellular concentrations of polyamines are controlled at the levels of synthesis, degradation and transport. ODC, S-adenosylmethionine decarboxylase (SAM-DC) and SSAT are the primary metabolic regulators of the polyamines putrescine, spermidine and spermine. Each of these enzymes has a short life-span and the activities of each vary depending on the physiological situation (reviewed in Seiler, 1990 and Heby and Persson, 1990). For example, ODC and SAM-DC are both down-regulated with increasing polyamine levels (Holm *et al.*, 1989; Heby and Persson, 1990), while *SSAT* is up-regulated, making it one of only a few genes known to be induced by naturally occurring

polyamines (Fogel-Petrovic *et al.*, 1996; Wang *et al.*, 1998). Recently, a cis-polyamine-responsive element was found in the 5' regulatory region of the human *SSAT* gene (Wang *et al.*, 1998). *SSAT* is also induced by various hormones and growth factors and its regulation appears to mainly occur via post-transcriptional mechanisms at the level of mRNA translation (Fogel-Petrovic *et al.*, 1996; Wang *et al.*, 1998). ODC and SAM-DC are also induced by various growth stimuli, resulting in rapid regulation of polyamine levels (reviewed in Heby and Persson, 1990).

Polyamine Biosynthesis

Putrescine serves as the diamine precursor for spermidine and spermine in the *de novo* synthesis of polyamines. In eukaryotic cells, the first step of the polyamine biosynthetic pathway is the formation of putrescine by the decarboxylation of ornithine by ODC, a rate-limiting enzyme in polyamine biosynthesis (Figure 1-8). It is not clear what serves as the source of ornithine for this step (Morgan, 1999). It is thought that ornithine present in the blood plasma or from the urea cycle may be recruited as the source. Also, some cells that lack a complete urea cycle possess the enzyme arginase, which cleaves the guanidino group of arginine to form ornithine, which may serve as the source for ornithine in these cells.

In the next step of the biosynthetic pathway, S-adenosylmethionine, formed by the reaction of ATP with methionine, is decarboxylated via S-adenosylmethionine decarboxylase (SAM-DC) to form decarboxy-S-adenosylmethionine. Aminopropyl groups are then transferred from decarboxy-S-adenosylmethionine by spermidine

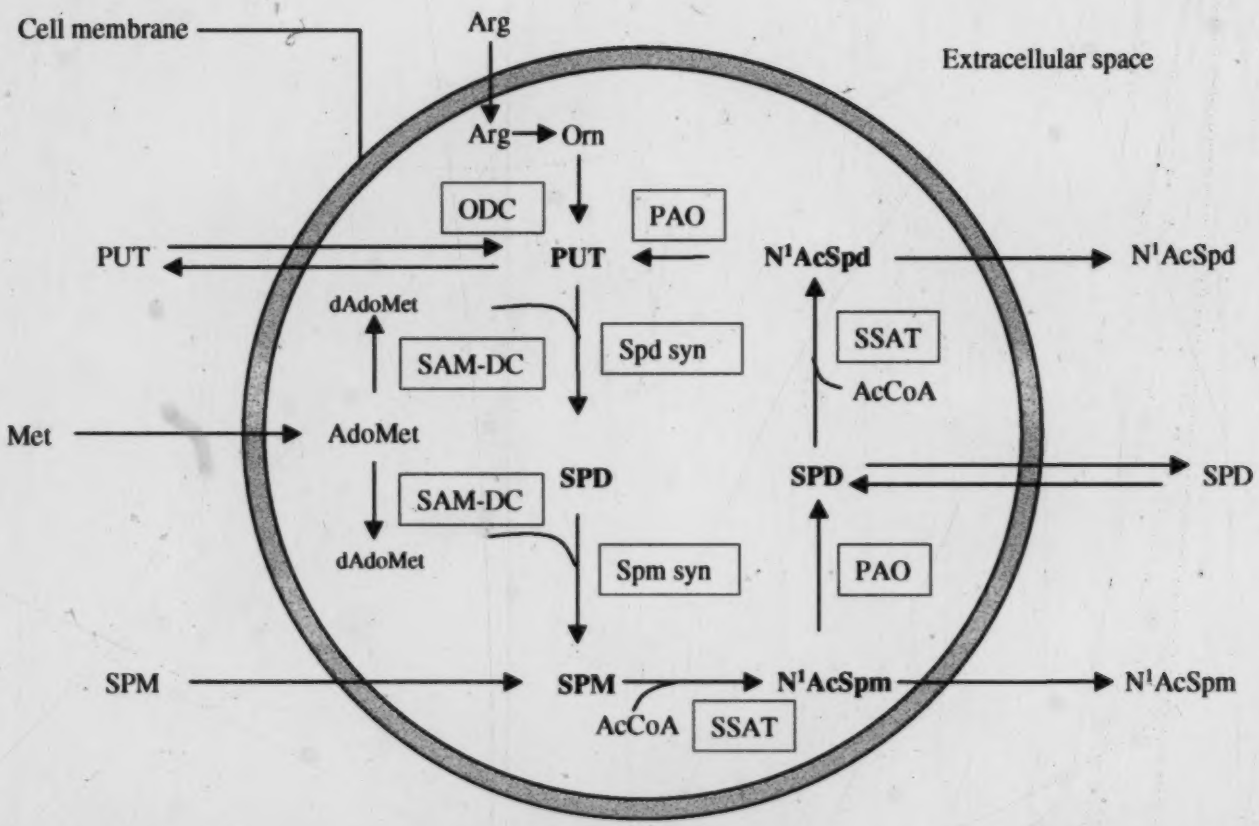

Figure 1-8. The polyamine biosynthetic and degradative pathways. Transport pathways are also shown for the polyamines and their derivatives. Arg, Arginine; Met, Methionine; Orn, Ornithine; PUT, putrescine; SPD, spermidine; SPM, spermine; N^1AcSpd, N^1-acetylspermidine; N^1AcSpm, N^1-acetylspermine; AdoMet, S-Adenosylmethionine; dAdoMet, decarboxylation product of SAM-DC; AcCoA, acetylCoA; ODC, Ornithine decarboxylase; PAO, Polyamine oxidase (FAD dependent); Spd syn, Spermidine synthase; Spm syn, Spermine synthase; SAM-DC, S-adenosylmethionine decarboxylase; SSAT, Spermidine/spermine N^1-acetyltransferase (adapted from Seiler, 1998).

synthase and spermine synthase to form spermidine and spermine, respectively. Transfer of an aminopropyl group to putrescine forms spermidine, while transfer of another aminopropyl group to spermidine forms spermine. Since the synthesis of spermidine and spermine is dependent upon the availability of the amino-propyl donor decarboxy-S-adenosylmethionine, SAM-DC is also a rate-limiting enzyme in the biosynthetic pathway for polyamines. Spermidine synthase and spermine synthase are not rate limiting since they are constitutively expressed and regulated by substrate availability.

Polyamine Degradation

There are two routes for the degradation of intracellular polyamines, both of which are regulated by the rate-limiting action of SSAT (reviewed in Morgan, 1999). The first route is an interconversion, or recycling pathway, whereby spermine and spermidine are converted back to putrescine (Figure 1-8). In the first step of the interconversion pathway, SSAT catalyzes the acetylation of spermine at the N^1-position, producing N^1-acetylspermine. Acetylation is the rate-limiting step in polyamine catabolism in eukaryotes and reduces the positive charges in polyamines, thus changing their physical properties. Next, flavin adenine dinucleotide (FAD)-dependent polyamine oxidase (PAO) cleaves the polyamine at a secondary amino nitrogen to release spermidine and an aldehyde, 3-acetamidopropanal.

SSAT can also acetylate the single aminopropyl group of spermidine, resulting in the formation of N^1-acetylspermidine which is cleaved by PAO, forming putrescine and 3-acetamidopropanal. Putrescine can then be recycled through the pathway to form

spermidine and spermine or excreted from the cell. The acetylated derivatives can also be excreted from the cell. If PAO activity is blocked, high levels of N^1-acetylspermidine are excreted from the cell and putrescine cannot be recycled. In rapidly dividing cells, the amount of putrescine formed by the degradation of spermidine is said to be minor in comparison to the amount formed *de novo* by the decarboxylation of ornithine (Seiler *et al.*, 1998). Conversely, in non-proliferating cells, degradation of spermidine is a major contributor to putrescine content.

The second pathway in polyamine degradation is terminal since the end products cannot be recycled back to polyamines. It involves copper-containing polyamine oxidases which oxidize the *primary* (terminal) amino group of the polyamines or their monoacetyl derivatives. This results in the formation of aminoaldehydes which cannot be recycled to polyamines and are instead targeted for terminal degradation (reviewed in Morgan *et al.*, 1999). The contribution of the latter pathway to polyamine homeostasis is not well known.

1.4.4 Polyamine Transport

Polyamine uptake and release are important mechanisms in the regulation of polyamine homeostasis and function in addition to the regulation of biosynthesis and degradation (reviewed in Seiler, 1990). However, little is known about the polyamine transport pathways which are thought to be highly complex. Transport of spermidine, spermine and putrescine appears to be sodium-sensitive in most cells and uptake and release are generally thought to occur via different transporters. However, a recent study suggests

that the same transporter may be capable of both uptake and release (Sakata *et al.*, 2000). Both polyamines and their acetylated derivatives are excreted from cells and the same transporter is thought to be responsible for their excretion (Sakata *et al.*, 2000).

Polyamine uptake is increased with a decrease in the intracellular concentrations of polyamines and can substitute for *de novo* synthesis of polyamines in certain conditions, such as inhibition of ODC by DFMO (Cullis *et al.*, 1999). It appears that the affinity of the transport systems for the polyamines is not altered, but instead that transport activity is increased under such conditions. The amount of polyamines that enter the cell, versus the amount synthesized *de novo*, is characteristic of specific cell types (Seiler *et al.*, 1998).

A mammalian family of antizyme proteins exists and to date, two members have been identified as important regulators of polyamine levels. Antizyme1 and antizyme2 have been shown to both inhibit the biosynthetic enzyme ODC and polyamine transport (Murakami *et al.*, 1994; Zhu *et al.*, 1999; Sakata *et al.*, 2000). Both enzymes bind to and inhibit ODC by forming an antizyme-ODC complex, and also inhibit polyamine uptake. Antizyme1, however, appears to have a more prominent role in targeting ODC for degradation and also stimulates polyamine excretion (Sakata *et al.*, 2000). These effects of antizyme appear to occur via a polyamine-induced negative-feedback mechanism, whereby polyamines up-regulate antizyme gene expression. Nitric oxide (NO) has also been found to inhibit both polyamine biosynthesis, via inhibition of ODC, and polyamine transport independent of antizyme (Satriano *et al.*, 1999).

1.4.5 Müller Glial Cells – Possible Polyamine Storage Centers?

As described later, my study found *SSAT* mRNA to be localized to the Müller glial cells of the developing chick retina. A recent study has provided evidence that supports Müller glial cells as being the polyamine storage cells of the retina (Biedermann *et al.*, 1998). Almost all spermine and spermidine immunoreactivity was confined to the vitread stem processes and endfeet of mammalian Müller glial cells, with no reactivity found in any neuronal cells. In addition, ODC immunoreactivity was confined to the inner segments of the photoreceptors (weak labelling) and also to the vitread stem processes and endfeet of Müller glial cells. The pattern of ODC immunoreactivity was high in the central retina and weaker towards the periphery. These findings would suggest that Müller glial cells are the primary center for polyamine biosynthesis and storage.

Polyamines and their Effects on Müller Glial Cell Function

In all vertebrate retinae, the Müller glial cells have an important homeostatic role. They "clean up" the extracellular space, controlling the levels of neuroactive substances, such as γ-aminobutyric acid (GABA), glutamate and potassium (K^+), as well as metabolites, which are released by active neurons (reviewed in Reichenback *et al.*, 1993 and Newman and Reichenback, 1996). A reduction in the uptake of neuroactive substances by Müller glial cells may alter neuronal excitability and enhance synaptic transmission.

The specific molecular targets for polyamines are not well known but polyamines have been shown to interact with cation channels (Ficker *et al.*, 1994; Lopatin *et al.*,

1994). A great deal of attention has been given to their involvement with inward rectifying K^+ channels (K_{ir}), defined as channels that conduct inward current more readily than outward current (for reviews, see Johnson, 1996; Nichols and Lopatin, 1997; Williams, 1997a and b). These channels are present in the Müller glial cells of all vertebrate species studied to date (Newman, 1993; Newman and Reichenback, 1996) and serve to regulate K^+ uptake from the extracellular space, moving K^+ from regions of high to low concentration.

The process by which K^+ is cleared from the extracellular space is often referred to as "spatial buffering," but more descriptive of the process is the term "K^+ siphoning" (reviewed in Newman, 1986 and Newman and Reichenback, 1996). The latter term best describes the process because K^+ is siphoned through the Müller glial cell and deposited out through the endfoot instead of being distributed uniformly across the glial cell (Newman *et al.*, 1984). K_{ir} channels are non-uniformly distributed over the surface of Müller glial cells, with the greatest density being at the proximal endfeet of the glial cells to aid in the siphoning process (Newman, 1986; Newman, 1993).

Intracellular polyamines are largely responsible for the inward rectification property of K_{ir} channels (Lopatin *et al.*, 1984; Ficker *et al.*, 1994). In a voltage-dependent process, intracellular polyamines, together with magnesium (Mg^{2+}), move into the inner mouth of the channel pore, blocking the outward, but not the inward, current of K^+ ions in regions of high extracellular K^+ (Skatchkov *et al.*, 1995; Amédée *et al.*, 1997; Aschroft, 2000). Only in these regions is K^+ influx increased through the K_{ir} channels

and "siphoned" primarily to the endfeet of the Müller glial cells which are adjacent to the vitreous humor (Newman *et al.*, 1984).

K^+ is siphoned to the endfeet for efflux from the cells. The endfeet are in areas of low extracellular K^+, away from active neurons and K_{ir} channels at the endfeet conduct outward currents when in areas of low extracellular K^+ (Newman, 1993; Skatchkov *et al.*, 1995; Solessio *et al.*, 2000). K^+ is effluxed into the vitreous humor, which acts as a K^+ sink. Thus, polyamines play a role in K^+ homeostasis in the retina by being necessary for the rectification property of K_{ir} channels. Through their involvement with K_{ir} channels, polyamines may indirectly modulate neuronal activity since a major role of the mature Müller glial cells of the retina is K^+ clearance.

1.4.6 Other Role of Polyamines in the Central Nervous System

Evidence collected so far is suggestive of extensive functions for polyamines in the CNS, primarily due to their interactions with cation channels. Despite evidence for such involvement, concrete answers have not yet surfaced and the consequences of their actions remain hypothetical. The best known interactions between polyamines and cation channels is with the K_{ir} channels described above, and with glutamate receptor channels (for reviews, see Williams, 1997a; Williams, 1997b; Rock and Macdonald, 1999; Yamakura and Shimoji, 1999). The N-methyl-D-aspartate (NMDA), α-amino-3-hydroxy-5-methyl-4-isoxazolepropionic acid (AMPA) and kainate glutamate receptor channels have all been shown to interact with polyamines. All three of these channel receptors are activated by glutamate, the major excitatory neurotransmitter in the CNS.

They are involved in mediating synaptic transmission and NMDA receptors have important roles in developing synaptic plasticity. Interaction of polyamines with these three receptors indicates important functions in neurotransmission in the CNS.

1.5 DD-PCR

Differential display – polymerase chain reaction (DD-PCR) is a technique developed by Liang and Pardee (1992). DD-PCR has revolutionized many areas of molecular biology, including developmental biology and cancer research. It provides a way of comparing the levels of gene expression between separate cell populations. Since the levels of gene expression determine a cell's properties, and ultimately control the fate of an organism, DD-PCR helps us gain an understanding of both normal physiological and disease states by allowing the comparison of separate cell populations (Zhang *et al.*, 1998). DD-PCR compares the levels of mRNA in separate cell populations, providing an "RNA fingerprint" of each cell. It utilizes both PCR and standard DNA techniques, making it a very convenient and efficient procedure.

1.5.1 The DD-PCR Protocol

Two or more cell types or tissues can be directly compared by the DD-PCR technique. Total or poly A+ RNA is isolated from the cell populations and must be of high quality and free of DNA for the DD-PCR technique to work efficiently. The first step of the protocol is the separation of the isolated RNA into specific subpopulations of cDNA by reverse transcription. This is accomplished using 3' oligo(dT) primers, also called "anchor" primers, which anneal to the 3' poly A tail of the mRNA (Figure 1-9). After

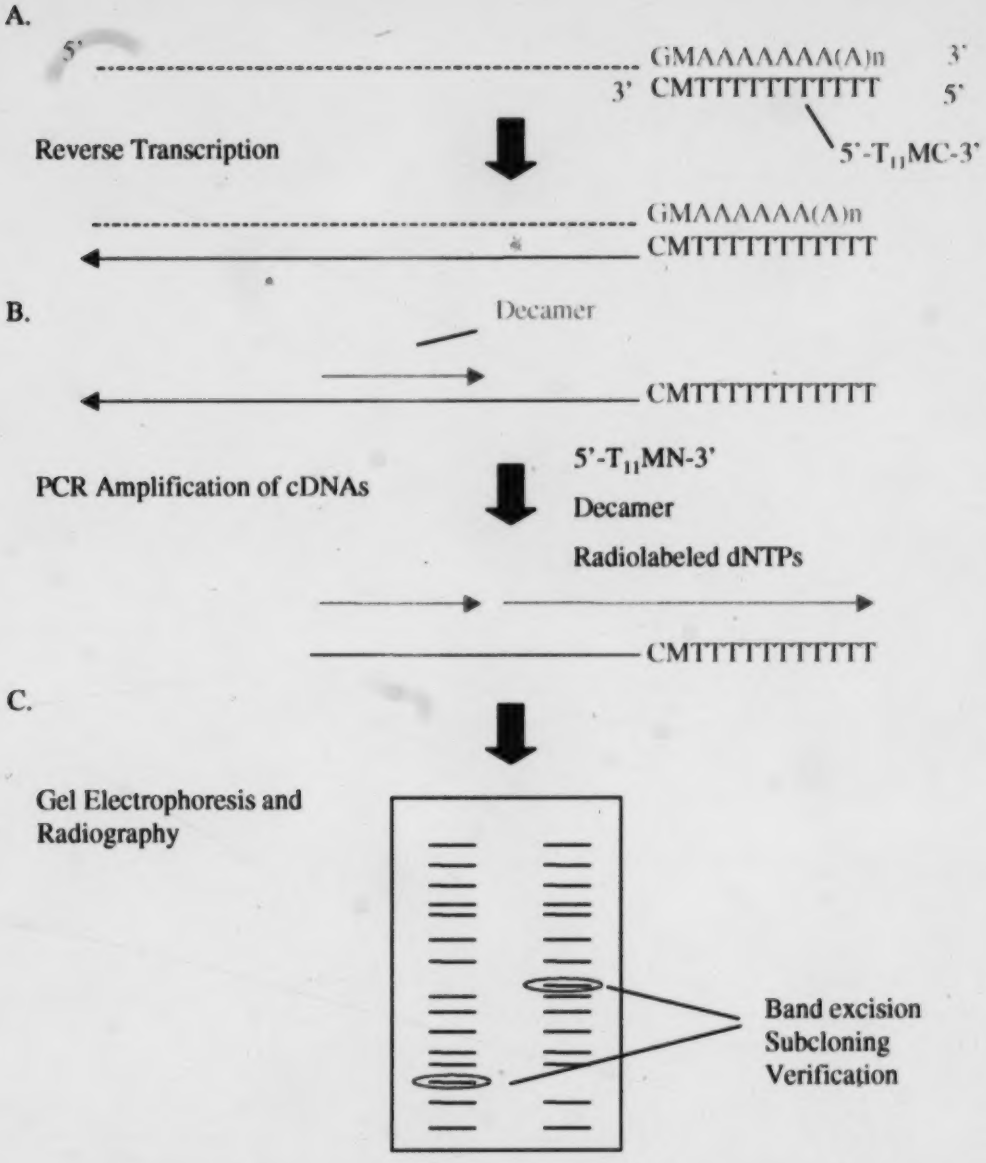

Figure 1- 9. DD-PCR. (A). Reverse transcription is initiated using the "anchor" primer 5'-T_{11}MN-3' (M = dG, dA or dC; N = dG, dA, dT or dC). The string of T's anchor the primer to the poly A tail of the mRNA species, while the last two bases provide specificity. (B). cDNAs are PCR-amplified using the same anchor primer as used for cDNA synthesis, plus an additional decamer of arbitrary, yet defined, sequence and radiolabeled dNTPs. This step amplifies the 5' region of the cDNAs which corresponds to the 3' ends of the mRNAs. (C). The cDNAs are then electrophoresed on polyacrylaminde sequencing gels. Bands are selected and excised based on the differential expression between different mRNA populations. The cDNA is eluted, subcloned and the differential expression is then verified using Northern blotting, etc. (adapted from Zhu and Liang, 1997).

reverse transcription, the cDNAs are used as templates for PCR. The same anchor primer is used in combination with an arbitrary 5' primer of defined sequence, which must be short enough to anneal frequently, yet long enough to provide specificity. Arbitrary 5' primers are typically ten nucleotides in length and are 50% GC. Each primer set generates approximately 50-100 bands per lane. Theoretically, each band on the gel represents a different cDNA and comparisons can be made between the bands of different cell populations side-by-side on the gel (Figure 1-9). Isolated cDNA bands are then reamplified and subcloned using T-A overhang vectors. The inserts are isolated and used to confirm differential expression by a variety of techniques which include Northern blot analysis, ribonuclease protection assay, *in situ* hybridization, reverse Northern analysis and multiplex relative reverse transcriptase-PCR (RT-PCR) (Spencer and Christensen, 1999).

Primer Specifics

Theoretically, each anchor primer, eg. $T_{11}GC$, will be specific for one twelfth of the mRNAs in a population. Since there are an estimated minimum 10,000 mRNAs in a given cell, at least 20-25 different arbitrary primers should be used in combination with each anchor primer to provide a complete representation of the total mRNAs (Liang *et al.*, 1993; Zhang *et al.*, 1998).

The efficiency of primer pairing has been shown to be heavily dependent upon the last two 3' bases of the T_{11} anchor primer (Mou *et al.*, 1994; Linskens *et al.*, 1995). An example of an anchor primer is 5'-(dT_{11})MN-3', where M is a degenerate base of dATP,

dCTP or dGTP and N is any one of dATP, dCTP, dGTP or dTTP, where d = deoxy. These nucleotides will be abbreviated as dA, dC, dG and dT. It has been noted that primers with dG or dC in the last two bases tend to anneal and extend more efficiently than those with dA or dT (Mou *et al.*, 1994; Malhotra *et al.*, 1998). Furthermore, the penultimate (second to last) base from the 3' end of the anchor primer appears to possess some degree of degeneracy (Liang *et al.*, 1993). This would suggest that the last 3' base of the anchor primer provides the greatest specificity, and that four degenerate primers, which differ only at the last 3' base, are all that is necessary to represent the majority of mRNAs in a population (Liang *et al.*, 1993).

Decamers that are approximately 50% GC are often used in combination with the anchor primers. Because of degeneracy, decamers tend to behave as 6-7mers, which is seen as advantageous since it allows the amplification and revealing of more mRNAs (Ledakis *et al.*, 1998).

1.5.2 Disadvantages Associated with DD-PCR

The major problems and concerns associated with DD-PCR involve band recovery, verification of differential expression and false positives, and a bias for high copy mRNAs (Liang *et al.*, 1993; Ledakis *et al.*, 1998; Zhang *et al.*, 1998; Jo *et al.*, 1998). It is not unusual to get multiple cDNAs from a single band as a result of different cDNAs of the same length co-migrating along the length of the gel. When the cDNA is isolated, different cDNAs are present, only one of which might be differentially expressed. Problems arise when verifying the differential expression of this band. For example, if

the cDNA is not subcloned but used directly as a probe for Northern analysis, multiple bands will appear on the autoradiograph. Furthermore, even if the cDNAs are subcloned and then used to probe a Northern blot, there is still a risk that the differential expression will not be verified if the correct clone was not chosen for the verification analysis. It is highly recommended that multiple clones be chosen to reduce the risk of missing the differentially expressed clone. This can increase both the cost and time involved in the DD-PCR procedure.

False positives are also a common occurrence. Often a band will appear differentially expressed on the original DD-PCR gel but verification of its expression fails. Reasons for false positives include the contamination of neighboring bands and multiple cDNAs of the same size generated by a given primer set, as mentioned above (Rohde *et al.*, 1997). The percentage of false positives can be as high as 90% (Sompayrac *et al.*, 1995) and it has also been demonstrated that approximately 40% of DD-PCR bands are not reproducible (Kociok *et al.*, 1998).

There have been many suggestions made to increase reproducibility and the elimination of false positives. Suggestions include changing primer design and concentration (Liang *et al.*, 1994; Guimaraes *et al.*, 1995; Ikonomov and Jacob, 1996; Zhu and Liang, 1997; Martin *et al.*, 1998), improving cloning techniques (Callard *et al.*, 1994; Poirier and Erlander, 1998), and improving verification analysis (Zhang *et al.*, 1996; Smith *et al.*, 1997; Miele *et al.*, 1998; Kociok *et al.*, 1998; Denovan-Wright *et al.*,

1999). However, if one is able to afford the time necessary to analyze all possible differentially expressed clones, a true positive is likely to be found.

Theoretically, all mRNA species represented in a population should be identified using DD-PCR, provided that enough primer combinations have been used (Rohde *et al.*, 1997). However, there are concerns that the nature of DD-PCR is biased towards more abundantly expressed transcripts. Because PCR is competitive, meaning that primers compete to bind transcripts, more abundant transcripts have a greater chance of being amplified. The argument behind DD-PCR is that all primer combinations will be exhausted so that eventually the correct primer set will amplify the less abundant transcripts. One study has shown that DD-PCR was unable to detect target genes which represented less than 1.2% of the total mRNA using 23 different primer combinations. (Bertioli *et al.*, 1995). Others have succeeded in modifying the protocol and have identified low abundance mRNAs (Guimaraes *et al.*, 1995). Despite such concerns, DD-PCR appears to be an efficient way of detecting rare transcripts that are differentially expressed.

1.5.3 Advantages Associated with DD-PCR

Rapid output, requirement for small amounts of RNA, the ability to detect rare transcripts, the identification of both up-regulated and down-regulated mRNAs, and the conversion of mRNA to cDNA, thereby allowing the use of DNA technologies, are the many advantages of DD-PCR as a tool to identify differentially expressed transcripts (Liang and Pardee, 1992; Zhang *et al.*, 1998). It has been used in many instances to

identify differentially expressed genes involved in developmental biology, tumor biology and the study of inducible genes (McClelland *et al.*, 1995; Linskens *et al.*, 1995; van Groningen *et al.*, 1995; Jo *et al.*, 1998; Leimeister *et al.*, 1999; Carter *et al.*, 1999).

Compared to other methods for isolating differentially expressed genes, such as differential screening, subtractive hybridization and microarrays, DD-PCR is a cost effective, fast and relatively sensitive technique that allows the comparison of multiple cell populations. Differential screening is labor intensive and mostly detects highly abundant transcripts, while subtractive hybridization only allows the comparison of two different samples at one time and may not detect subtle changes in gene regulation, e.g. up or down-regulation. Microarrays, although a very attractive concept, are expensive and limited to certain model systems. For the intent of this project, analysis of microchip arrays or arrays of cDNAs was not feasible since there are currently no cDNA arrays available of the chick retina. We chose DD-PCR as our strategy as it was the most convenient and efficient protocol and had already been shown to work in our lab for a separate study.

1.6 Objective of Thesis

Asymmetrically expressed gradients in the retina, and the subsequent distribution of factors produced by these proteins, are thought to play a role in targeting axons from the retina to the brain. The main objective of this project was to identify asymmetrically expressed genes, specifically those with dorsoventral asymmetry, in the developing chick retina in order to increase our understanding of retinal patterning. E7 chick retinae were dissected along the dorsoventral plane and poly A+ RNA extracted for DD-PCR analysis. A total of 42 bands preferentially expressed in either dorsal or ventral retina were excised from the DD-PCR gels. Seven of these bands showed patterns consistent with the original pattern on the DD-PCR gel when used to probe Northern blots of dorsoventral poly A+ RNA, indicating asymmetrical expression in the retina. Fetal tissue Northern blots, which included retinal tissue from different stages of development, as well as tissues other than retina, were also probed. Isolated DD-PCR clones were sequenced and searched against known sequences in the Genbank database.

Of particular interest was a spermidine/spermine N^1-acetyltransferase (*SSAT*) cDNA clone predominantly expressed in the retina, shown by Northern blot analysis to be expressed in a ventrodorsal gradient. SSAT is known to be a rate-limiting enzyme in the degradation of intracellular polyamines, which play a pivotal role in cell growth and differentiation. *In situ* hybridization analysis revealed that expression of *SSAT* mRNA was confined to the Müller glial cells. *In situ* hybridization also showed a temporal-nasal gradient of expression for this clone in the developing chick retina, different from the ventrodorsal gradient suggested by Northern blot analysis.

CHAPTER 2. METHODS AND MATERIALS

2.1 Differential Display Polymerase Chain Reaction (DD-PCR)

2.1.1 Poly A+ RNA Extraction and First Strand cDNA Synthesis

Day 7 chick retinae were dissected along the dorsal-ventral plane and poly A+ RNA extracted from dorsal and ventral halves of the retina, as well as from whole (total), chick retinae. Poly A+ RNA was extracted using a protocol modified from Sambrook *et al.*, 1989. Briefly, retinal tissue was homogenized in homogenization buffer [50 mM Tris-HCl (pH 7.5), 1 mM EDTA (ethylenediaminetetraacetic acid), 1% SDS] and RNA phenol (140 ml H_20, 35 ml m-cresol and 500 mg 8-hydroxyquinoline) and repeatedly extracted with RNA phenol until the interphase was clean. After ethanol precipitation, pellets (containing both DNA and RNA) were washed, resuspended in 2M LiCl, and placed at 4°C for 4-6 hours with mixing. DNA remained in the LiCl while RNA precipitated out after spinning. Pellets were resuspended in 10 mM Tris-HCl (pH 7.5) and polyA+ RNA was isolated using oligo(dT)-cellulose chromatography. Following ethanol precipitation, dried RNA pellets were resuspended in H_2O to a final concentration of 1 μg/μl and stored at –80°C.

Reverse transcriptase (Gibco BRL) was used to synthesise cDNA. Briefly, 0.1 μg/μl poly A+ RNA and 4.25 μM external primer (T_{11}MG, T_{11}MC, T_{11}MA, T_{11}MT, M = dA, dG, or dC) were combined and heat-shocked for 2 minutes at 65°C and put on ice. Single-strand cDNA was synthesized by incubating the RNA and primer with reverse transcriptase (10U) (Gibco BRL), 1X first strand buffer [50 mM Tris-HCl (pH 8.3), 75 mM KCl, 3 mM $MgCl_2$], 0.05 mM each dG, dA, dT, dC, 0.5U/μl RNase

inhibitor (Amersham Pharmacia Biotech), 10 mM DTT, and 0.5 mM spermidine at 45°C for 1 hour. The samples were then heat-shocked at 95°C for 5 minutes and put on ice. cDNA was stored at -80°C.

2.1.2 cDNA Amplification

cDNAs were amplified using PCR as follows, listed as final concentrations in 20 µl final volume: 1/10 of cDNA made from 0.1 µg poly A+ RNA, 1X *Taq* polymerase buffer, 1 unit *Taq* polymerase, 0.5 µM internal primer (OPA series kit, Operon Technologies, Table 2-1), 2.5 µM external primer (same primer used to synthesise cDNA), 2 µM dNTP's, 1.25 mM $MgCl_2$ and 1 µl α-[S^{35}]–dATP (1250 Ci/mmol). cDNAs were PCR-amplified in a thermal cycler (PE Applied Biosystems) as follows: 95°C for 5 minutes; 40 cycles of 94°C for 30 seconds, 41°C for 90 seconds; 72°C for 30 seconds; 72°C for 5 minutes followed by a hold at 4°C. PCR samples were mixed with loading dye (0.09% xylene cyanol FF + 0.09% bromophenol blue + 95% formamide) and electrophoresed in a denaturing 6% polyacrylamide gel (standard sequencing size) in 1X TBE (0.09 M Tris-borate, 0.001 M EDTA) buffer at 70W constant power for approximately 4 hours. Film (Kodak®) was exposed at room temperature for 24 hours or longer.

Bands showing differential expression between the total, dorsal and ventral lanes were excised using a sterile scalpel and DNA from the bands was eluted in sterile eppendorf tubes containing 100 µl H_20. To elute DNA, tubes were placed at room temperature for 15 minutes then boiled for 15 minutes. The water, which now contained eluted DNA, was transferred to fresh tubes and precipitated at -80°C using 1/10 volume

Table 2-1. Primers used for DD-PCR and sequencing. The OPA series of arbitrary primers was used for DD-PCR analysis, in combination with four anchor primers (T_{11}MG, T_{11}MC, T_{11}MA, T_{11}MT; M = dG, dA or dC). M13 universal and reverse primers were used to sequence inserts in pBluescript. pBR322 forward and reverse primers were used to sequence inserts in pBR322. SSAT primer was used to sequence internal regions of *SSAT* cDNA clones.

PRIMERS FOR DD-PCR	5' TO 3'	PRIMERS FOR SEQUENCING	5' TO 3'
OPA-01	CAGGCCCTTC	M13 Universal	GTAAAACGACGGCCAGT
OPA-02	TGCCGAGCTG	M13 Reverse	AACAGCTATGACCATG
OPA-03	AGTCAGCCAC	pBR322 Forward	GTGCCACCTGACGTCTAAGA
OPA-04	AATCGGGCTG	pBR322 Reverse	GTGCCTGACTGCGTTAGC
OPA-05	AGGGGTCTTG	SSAT	CGCACGACCACTGTTCTTT
OPA-06	GGTCCCTGAC		
OPA-07	GAAACGGGTG		
OPA-08	GTGACGTAGG		
OPA-09	GGGTAACGCC		
OPA-10	GTGATCGCAG		
OPA-11	CAATCGCCGT		
OPA-12	TCGGCGATAG		
OPA-13	CAGCACCCAC		
OPA-15	TTCCGAACCC		
OPA-16	AGCCAGCGAA		
OPA-17	GACCGCTTGT		
OPA-18	AGGTGACCGT		
OPA-19	CAAACGTCGG		
OPA-20	GTTGCGATCC		

3M NaOAc (pH 7.0) and 100% EtOH. Dried pellets were resuspended in 10 µl sterile H_20 and stored at -20°C.

2.1.3 Reamplification of Eluted DNA

In a second round of PCR, isolated cDNAs were reamplified with the same primer set used in the first amplification to generate sufficient DNA for subcloning. Eluted DNA (4 µl) was reamplified as follows, listed as final concentrations in 40 µl final volume: 1X *Taq* polymerase buffer, 1 unit *Taq* polymerase, 2.5 µM external primer, 0.5 µM internal primer, 20 µM dNTPs, and 1.25 mM $MgCl_2$. cDNAs were PCR-amplified in a DNA thermal cycler as described for the initial amplification. PCR samples were added to loading dye (50% sucrose + 0.3% bromophenol in TE buffer, filtered) and electrophoresed in 5% acrylamide gels. DNA was visualized with ethidium bromide. Bands were excised and placed in 100 µl elution buffer (0.5 M NH_4OAc + 1 mM EDTA). Tubes were covered in foil (to prevent DNA damage caused by ethidium bromide exposure to UV light) and DNA eluted overnight at 37°C. The elution buffer was then transferred to sterile tubes and DNA precipitated with 100% EtOH at -80°C. Dried pellets were resuspended in 100 µl TE buffer [10 mM Tris-HCl (pH 7.5) + 1 mM EDTA] and then reprecipitated with 1/10 volume 3M NaOAc. Dried pellets were resuspended in 10 µl sterile H_20 and stored at -20°C. cDNAs were then subcloned into T-A overhang vectors (see below).

2.1.4 Cloning of Isolated DD-PCR cDNAs

T-A overhang vectors were generated using the method from Current Protocols in Molecular Biology (Ausubel). Briefly, pBluescript vector was cut with *Eco*RI and the T overhang added by incubating in the presence of *Taq* DNA polymerase and dTTP. Because *Taq* polymerase is known to add a single nontemplated nucleotide (most often A) to the 3' ends of PCR products (Clark, 1988), T-A overhang vectors are suitable for cloning DD-PCR cDNAs generated by PCR.

cDNAs were ligated into T-A overhang pBluescript vector using a method adapted from Sambrook *et al.* (1989). Approximately 200 ng insert (~50 ng/ul) was used for every 200 ng vector in a final volume of 20 μl containing 0.1 μg/μl BSA, 1X ligase buffer [50 mM Tris-HCl (pH 7.8), 10 mM $MgCl_2$, 20 mM DTT (dithiothreitol)], 1 mM ATP and 1 unit T_4 DNA ligase. Reactions were incubated at 16°C overnight. Colour selection by transformation into *Escherichia coli* (*E. coli*) XL1-Blue bacteria cells was used to detect positive colonies. Positive (white) colonies were selected and plasmid DNA isolated as described below. Automated sequencing was performed to determine sequence similarity to any known cDNA clones. Northern blotting (described below) was also performed to confirm differential expression between dorsal and ventral retina.

2.2 Library Screening

Lambda ZAP (Stratagene) bacteriophage cDNA libraries of E7 and E16 chick retina were titered by serial dilution of the phage stocks. Host cells (*E. coli* BB4, 600 µl of 2 OD/ ml per 150 mm plate) were incubated with 3-5 X 10^4 pfu (plaque forming units)

for 20 minutes at 37°C with shaking. Top agar (0.8 %) in NZY amine was added to the infected BB4, poured onto plates and incubated at 37°C for 5-6 hours until plaques were approximately 1 mm in diameter. Plaques were lifted using Millipore HA (0.45 µm) nitrocellulose filters. Filters were placed for 5 minutes each in denaturing solution (1.5 M NaCl, 0.5 N NaOH) and neutralizing solution [1.5 M NaCl, 0.5 M Tris-HCl (pH 7.5)], respectively, and rinsed in 2X SSC + 0.2 M Tris-HCl (pH 7.5). Filters were air-dried at room temperature and baked at 80°C for 2½ hours in a vacuum oven.

After drying, filters were sealed in a bag with prehybridization solution [50% formamide (Fluka), 5X SSC, 5X Denhardt's, 50 mM NaH_2PO_4 (pH 6.5), 250 µg/ml salmon sperm DNA] and incubated for a minimum of 4 hours in a shaking H_2O bath at 42°C. Probe was labelled with $\alpha[^{32}P]$-dCTP (800 Ci/mmol) by nick translation, denatured, mixed with hybridization solution (50% formamide, 5X SSC, 1X Denhardt's solution, 20 mM NaH_2PO_4, 10% dextran sulfate), added to the filters and incubated overnight at 42°C with shaking. The following day, filters were washed in 2X SSC + 0.1% SDS at room temperature (3 X 5 minutes) and 0.1X SSC + 0.1% SDS (2 X 1 hour) at 60°C. Filters were air-dried and exposed overnight using X-ray film (Kodak®) at –80°C with intensifying screens.

After developing the film, plates were aligned with the film and positive clones were cored. Primary cores were placed in 500 µl SM buffer [0.1 M NaCl, 0.01 M $MgSO_4$, 0.05 M Tris-HCl (pH 7.5) and 0.01 % gelatin] and 35 µl chloroform (to kill contaminating bacteria), vortexed occasionally for 3 hours at room temperature and

placed at 4ºC to elute phage particles. Phage dilutions (1/10 or 1/100) were prepared in SM buffer and plated as described above, only this time using 200 µl BB4 and 3 ml 0.8% top agar with 100 mm plates. Once again, plaques were lifted and filters probed using the same DNA.

Secondary cores were obtained and treated as described above. Phage dilutions were plated and plaques were picked onto a grided NZY amine agar plate covered in a lawn of BB4. Following incubation at 37ºC, plaques were lifted and probed as before. Tertiary cores of positive plaques were obtained from grids and placed in 500 µl SM buffer and 35 µl chloroform for storage at 4°C. DNA was obtained from cores using *in vivo* excision to excise pBluescript plasmids containing the DNA insert of interest (protocol by Stratagene) or by mini-phage preparation (see below). After plasmid isolation and purification, inserts were isolated by restriction enzyme digestion using *Eco*RI (Gibco BRL). Southern blotting of the isolated clones using the probe used to screen the library ensured that the correct insert was isolated.

2.3 Mini-Phage Preparation

In some instances where it was not possible to recover pBluescript with inserts by *in vivo* excision, a protocol from Miller (1987) was used for isolating pBluescript plasmid from lambda ZAP bacteriophage. Briefly, *E. coli* LE392 were infected with bacteriophage isolated from tertiary cores and incubated for 6-12 hours at 37°C with shaking until lysis. Bacteriophage in the lysate were concentrated using polyethylene glycol (PEG) 6000 (Sigma) in high salt and DNA was purified using phenol/chloroform extraction, followed

by ethanol precipitation. Dried pellets were resuspended in TE buffer and stored at -20°C. Inserts were isolated by digesting the DNA with *Eco*RI and were ligated into pBR322 and transformed into HB101. Colonies were picked onto a grid and probed with the insert of interest to detect positive clones.

2.4 Plasmid Purification

Lysis by boiling using lysozyme (Sambrook *et al.*, 1989) was used to isolate small amounts of plasmid DNA, while the alkali lysis method using NaOH and CsCl purification (Sambrook *et al.*, 1989) was used to isolate larger amounts of more highly purified plasmid DNA.

2.5 DNA Insert Purification

DNA inserts were isolated from plasmid DNA by restriction enzyme digestion followed by electrophoresis in a 5% polyacrylamide gel in 1X TBE at 170 volts. Gel slices containing the inserts were electroeluted at 170 volts in 1X TBE. TE was added to a volume of 2 ml and the DNA was phenol/chloroform extracted and precipitated for at least one hour in 2 volumes 100% ethanol and 1/10 volume 5 M NaCl. Dried DNA pellets were resuspended in sterile H_20 and stored at –20°C.

2.6 Southern Blotting

Loading dye was added to DNA (1 µg) and electrophoresed in 1% agarose gels in 1X Howley [40 mM Tris, 33 mM NaoAc, 1 mM EDTA; pH 7.2]. Following denaturation in 0.5 N NaOH + 1.5 M NaCl and neutralization in 0.5 M Tris-HCl (pH 7.5) + 3 M NaCl,

DNA was transferred overnight to a nitrocellulose membrane (Amersham) by capillary action. The membrane was then baked at 80°C for 2 hours in a vacuum oven. After prehybridization, labelled probe (in hybridization solution) was added and hybridized overnight at 42°C. Membranes were washed in 2X SSC + 0.1% SDS (3 X 5 minutes) at room temperature and 0.1X SSC + 0.1% SDS (2 X 1 hour) at the appropriate temperature depending on probe size. (Generally, probes between 200-400 base pairs were washed at 45-50°C, while probes greater than 500 base pairs were washed at 60°C).

2.7 DNA Sequencing

2.7.1 Primers used for DNA Sequencing

M13 universal and reverse primers (Pharmacia) were used to sequence DNA inserts in pBluescript. All other primers were made on site by Dr. Brian Taylor, Department of Oncology, University of Alberta. Custom primers were designed for sequencing DNA inserts in pBR322 and for sequencing regions of DNA within the *SSAT* cDNA sequence that could not be sequenced by forward and reverse pBR322 primers because the insert was too large. All primers used for sequencing are listed in Table 2-1.

2.7.2 Automated and Manual Sequencing Procedures

1. Automated sequencing was used to sequence DD-PCR clones. Automated sequencing was performed according to the manufacturer's directions (Perkin Elmer Applied Biosystems). Half reactions were used for all automated sequencing. Briefly, 200-500 ng of double-stranded DNA template, 4 µl Terminator Ready Reaction Mix (Perkin Elmer), 1.5 µM primer and H_20 to a final volume of 10 µl,

were cycle-sequenced in a thermal cycler (PE Applied Biosystems) as follows: 25 cycles of 96°C for 10 seconds, 50°C for 5 seconds and 60°C for 4 minutes, followed by a hold at 4°C. Extension products were precipitated 15 minutes at room temperature with 25 µl 100% ethanol and 1 µl 3 M NaOAc (pH 5.2). Pellets were spun down, washed twice in 70% ethanol, dried in a vacuum centrifuge and resuspended in 12.5 µl fresh formamide (Fluka). After boiling for five minutes, products were immediately cooled on ice and loaded into the automated sequencer (ABI PRISM 310 Genetic Analyser).

2. Manual sequencing was used to sequence clones isolated with library screening. Manual sequencing was performed using the dideoxynucleotide chain-termination method, modified for double-stranded DNA templates (Sanger *et al.*, 1977; Mierendorf and Pfeffer, 1987), with T7 DNA polymerase (Pharmacia). Exonuclease III/mung bean nuclease (Pharmacia) were used to generate overlapping fragments for the sequencing of larger DNA templates (Henikoff, 1987).

Sequences were entered into the BLAST network service of the National Center for Biotechnology Information (NCBI, www.ncbi.nlm.nih.gov/BLAST/) to search for similarity with known sequences.

2.8 Eye Dissections

Eggs from White Leghorn chickens were purchased from the University of Alberta farm (Edmonton, AB) and incubated at 37°C (50% humidity) until sacrificed. Embryos were

staged according to Hamburger and Hamilton (1951). Total retinae were collected after 7, 9, 10, 12, 14, 15 and 16 days of incubation. Dorsal and ventral retinae were collected after 7, 11, 15 and 16 days of incubation. Neural retinae were dissected from the eyes, rinsed in 1X PBS and immediately frozen in liquid nitrogen. All retinal tissues were stored at -80°C until ready for RNA extraction.

2.9 Northern Blotting

Poly A+ RNA (2 µg per lane, unless stated otherwise) was electrophoresed in a denaturing 1.5% agarose gel containing 6% formaldehyde in 1X MOPS buffer [3-(*N*-morpholino) propanesulfonic acid: 0.2 M MOPS, 50 mM NaOAc, 10 mM EDTA; pH 7.3] for 60V for 5-6 hours. RNA samples were prepared in sample buffer containing both formamide and formaldehyde and heat-shocked at 65°C for 15 minutes prior to loading with dye (1X MOPS, 50% glycerol, 0.1% bromophenol blue). RNA was transferred to reinforced nitrocellulose membrane (Amersham) by capillary action overnight, rinsed in 2X SSC and baked for 2 hours at 80°C in a vacuum oven. Prehybridization, probe labelling, hybridization and washing were the same as for Southern blotting. Northern blots were stored at room temperature in plastic bags. Labelled probe was stripped from the blots using 5 ml of 10X Thomas buffer [0.5 M Tris-HCl (pH 8.0), 20 mM EDTA, 5% $Na_4P_2O_7$ (sodium pyrophosphate), 0.2% BSA (bovine serum albumin), 0.2% Ficoll, 0.2% PVA (polyvinyl alcohol)] per liter of solution. Blots were stripped at 60°C (2 X 1.5 hours).

2.10 *In Situ* Hybridization

2.10.1 Probe Construction: Linearization of Plasmid DNA

pBluescript plasmids with inserts were linearized using restriction enzymes generating a 5' overhang. Enzymes were chosen to cut on either side of the insert such that T7 and T3 promoter sites could be used to generate either sense or antisense probes. Linearized inserts were purified using phenol/chloroform extraction and ethanol precipitated. Dried pellets were resuspended in 10 mM Tris-HCl (pH 8.0) to a final concentration of 1 μg/μl.

2.10.2 DNA → RNA: DIG Incorporation

An *in situ* hybridization kit was purchased from Boehringer Mannheim and used to generate and label the RNA probes. The protocols for probe construction were taken from the Nonradioactive *In Situ* Hybridization Application Manual, Second Edition, provided by Boehringer Mannheim.

Briefly, linearized DNA (1 μg) was added to a mixture containing 2 μl 10X concentrated DIG (Digoxigenin) RNA labelling mix, 2 μl 10X concentrated transcription buffer, 2 μl RNA polymerase (T3 or T7) and water to a final volume of 20 μl. Tubes were incubated at 37°C for 2 hours. The polymerase reaction was stopped by the addition of 4 μl 0.1 M EDTA (pH 8.0) and DIG-labelled RNA was precipitated with 2 M LiCl and 100% ethanol. Dried pellets were resuspended in 100 μl H_2O and tubes were incubated at 37°C to allow the RNA to go into solution.

DIG-labelled RNA was quantitated using control DIG-labelled RNA provided in the Boehringer Mannheim kit. Labelled RNA was spotted onto a nitrocellulose membrane (Amersham) and UV-Crosslinked (UV Stratalinker®, Stratagene). After blocking in 5% milk in 1X TBS (Tris buffered saline), anti-DIG-alkaline phosphatase antibody (Boehringer Mannheim) was incubated with the membrane. Membranes were washed in TBS-Tween (0.1%) at room temperature and incubated in 10 ml alkaline phosphatase detection buffer [0.1 M Tris-HCl (pH 9.5), 0.5 mM $MgCl_2$] with 45 μl NBT (75 mg/ml nitro-blue tetrazolium salt in dimethylformamide, BioRad) and 35 μl BCIP (50 mg/ml 5-bromo-4-chloro-3-indolyl-phosphate in dimethyl formamide, Bio Rad). Labelled RNA was quantitated by comparing the intensity with that of the control RNA. Probes were stored at -80°C.

2.10.3 Detection of mRNA in Tissue Sections

Chicks were decapitated at different stages of development and heads were fixed overnight at 4°C in 4% paraformaldehyde in PBS. Tissues were cryoprotected by incubating in sucrose gradients (12%, 16% and 18% in PBS, respectively) for 2 hours each at room temperature, embedded in Tissue-Tek ® O.C.T. compound (Miles Inc.), snap-frozen in a dry ice-methanol bath and stored at -80°C until sectioned.

Frozen sections (6 microns thick) were prepared and stored at -80°C. Prior to use, sections were dried for one hour at room temperature and washed in 1X PBS, followed by washing in 1X PBS + 100 mM glycine, each for 2 X 5 minutes. Slides were washed in 1X PBS + 0.3% TritonX-100 for 15 minutes and washed in 1X PBS for 2 X 5 minutes.

Tissues were permeabilized for 30 minutes at 37°C in 1 μg/ml RNase-free proteinase K (Boehringer Mannheim) in TE buffer. Sections were post-fixed for 5 minutes in 4% paraformaldehyde in 1X PBS and washed in 1X PBS for 2 X 5 minutes, followed by acetylation with 0.25% acetic anhydride in 0.1 M triethanolamine, 2 X 5 minutes. Sections were washed again in 1X PBS for one minute, dehydrated for one minute each in 30%, 50%, 75%, 85%, 95% and 100% (X 2) ethanol and left at room temperature to dry for ½ hour.

Sections were prehybridized with a solution containing 40% formamide, 10% dextran sulfate, 1X Denhardt's, 4X SSC, 10 mM DTT, 1 mg/ml yeast tRNA and 1mg/ml salmon sperm DNA for 6 hours at 55°C. Probe was added to the prehybridization cocktail to a final concentration of 30 ng/100 μl, denatured for 10 minutes at 70°C, added to sections, coverslipped and left overnight at 55°C.

The following day, sections were washed in 50% formamide + 2 X SSC for 2 X 30 minutes at 60°C and 2 X SSC for 2 X 15 minutes at 37°C. Sections were treated with 20 μg/μl RNase A in NTE (0.5 M NaCl in TE buffer) for 30 minutes at 37°C, followed by washing in 50% formamide + 0.1% CHAPS (Sigma) + 2 X SSC for 15 minutes at 60°C and 0.1% Tween 20 + 0.2 X SSC for 15 minutes at 45°C. Sections were blocked for 4-6 hours in PBS + 2% blocking solution [from a stock of 10% blocking powder: 0.058 g maleic acid (pH 7.5) in 5 ml H_20, 0.5 g blocking powder (Boehringer Mannheim), 0.15 M NaCl] + 0.3% TritonX-100 at room temperature. Alkaline phosphatase-conjugated anti-DIG antibody (Boehringer Mannheim) was diluted to

1/1000 in the blocking mixture, added to the slides, coverslipped and left overnight at room temperature.

Post-blocking, sections were washed in PBS + 0.3% TritonX-100 for 2 X 5 minutes and PBS + 0.5% TritonX-100 for 3 X 20 minutes. After washing in a solution containing 100 mM Tris (pH 9.5) + 150 mM NaCl + 25 mM $MgCl_2$ + 0.3% TritonX-100 for 2 X 15 minutes, mRNA was detected using a solution of 10% polyvinyl alcohol (PVA) + 100 mM Tris (pH 9.5) + 150 mM NaCl + 25 mM $MgCl_2$. For every 1 ml of solution, 4.5 μl NBT and 3.5 μl BCIP were added. Enough detection solution was added to cover the tissue sections (approximately 100 μl). The purple colour substrate could be detected after 2-8 hours depending on the probe and the amount of RNA present. After detection, slides were rinsed in 1X PBS, counterstained with methyl green and mounted.

2.10.4 Detection of mRNA in Whole Mounts

Protocols for whole mount *in situ* hybridization were adapted from Henrique *et al.* (1995). All washes were for 5 minutes unless stated otherwise.

Eyes from day 7 and day 11 chick embryos were dissected and retinae separated from the pigment epithelium. Retinae were fixed overnight at 4°C in 4% paraformaldehyde (1X PBS). After washing with PBT (PBS + 0.1% Tween 20), retinae where dehydrated by washing for 10 minutes each in 25%, 50%, 75% and 100% methanol/PBT and stored at -20°C until ready to use.

Retinae were rehydrated by washing for 10 minutes each in 100%, 75%, 50% and 25% methanol/PBT, followed by washing with PBT at room temperature. To permeabilize the tissue, retinae were treated with 10 μg/ml RNase-free proteinase K (Boehringer Mannheim) in PBT for 10-15 minutes at room temperature, rinsed with PBT, and post-fixed in 4% paraformaldehyde + 0.1% glutaraldehyde in PBT for 20 minutes at room temperature. After washing in PBT, retinae were rinsed with 1:1 PBT / hybridization mix [50% formamide + 5 X SSC (pH 5) + 50 μg/ml yeast tRNA + 1% SDS + 50 μg/ml heparin], then hybridization mix only, followed by incubation at 70°C for 1 hr with fresh hybridization mix. DIG-labelled RNA probe was added to hybridization mix (approximately 1 μg/ml) and incubated overnight with retinal tissue at 70°C.

Following hybridization, retinae were washed 2 X 30 minutes at 70°C in post-hybridization solution [50% formamide + 5X SSC (pH 5) + 1% SDS]. After washing 20 minutes at 70°C with pre-warmed 1:1 post-hybridization solution and MABT [100 mM maleic acid + 150 mM NaCl (pH 7.5) + 0.5% Tween 20], retinae were rinsed and then washed 2 X 30 minutes with MABT at room temperature. For blocking, retinae were incubated 1 hour with MABT + 2% blocking powder (Boehringer Mannheim), followed by a 4 hour incubation with MABT + 2% blocking powder + 20% sheep serum (Sigma) (heat treated at 65°C). Retinae were incubated overnight at 4°C with MABT + 2% blocking powder + 20% sheep serum + 1/1000 dilution alkaline phosphatase-conjugated anti-DIG antibody (Boehringer Mannheim).

The following day, retinae were washed 3 X 1 hour in MABT and 3 X 10 minutes in NTMT [100 mM NaCl + 100 mM Tris-HCl (pH 9.5) + 50 mM $MgCl_2$ + 1% Tween 20]. For detection, retinae were incubated with 4.5 μl NBT + 3.5 μl BCIP per 1 ml NTMT at room temperature. When the purple colour had developed sufficiently, the reaction was stopped by washing in PBT and re-fixing for 2 hours in 4% paraformaldehyde + 0.1% glutaraldehyde in PBT at room temperature (or overnight at 4°C). Retinae were rinsed in PBT and stored at 4°C in PBT + 0.1% NaN_3.

CHAPTER 3. RESULTS

3.1 DD-PCR

3.1.1 Isolation of RNA from Day 7 Retina and cDNA Synthesis

Whole, dorsal and ventral chick retinae were isolated from day 7 chick embryos. Poly A+ RNA was extracted and Northern blotting was performed to test the quality of each RNA preparation. Separation of dorsal and ventral halves was confirmed with Northern blotting using *ALDH1* antisense RNA as a probe because *ALDH1* is expressed only in dorsal retina (Godbout *et al.*, 1996) (Figure 3-1).

After poly A+ RNA was extracted from whole (total), dorsal and ventral chick retina, cDNAs were made from the poly A+ RNA using four anchor (external) primers (T_{11}MG, T_{11}MA, T_{11}MC, T_{11}MT). The cDNAs were then used for DD-PCR analysis. In total, 19 internal primers (OPA series, GC rich) were used in combination with each of the four anchor primers used for cDNA synthesis. Overall, 76 DD-PCR reactions were performed, with each reaction comparing total, dorsal and ventral retina. Figure 3-2 shows a typical DD-PCR gel that was obtained with T_{11}MG and OPA1, 2, 3 and 4. Approximately 100-150 bands were generated per lane for T_{11}MG, T_{11}MA and T_{11}MC, with each band theoretically representing a different cDNA. T_{11}MT produced a significantly lower number of bands per lane, averaging approximately 40 bands.

3.1.2 Initial Band Selection and Primer Efficiency

From the DD-PCR reactions, 42 bands were selected based on their differential expression on the original DD-PCR gel. Varying degrees of expression differences

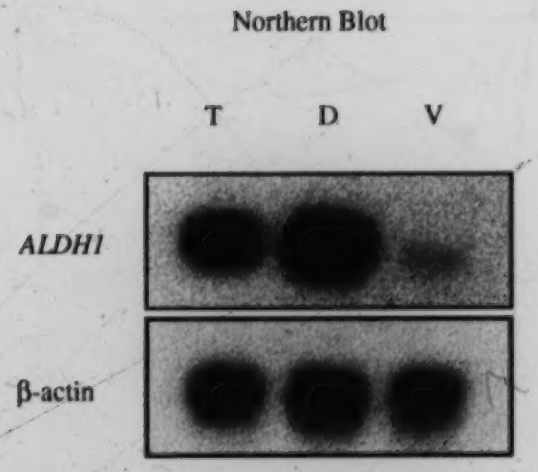

Figure 3-1. *ALDH1* is expressed in the dorsal chick retina. *ALDH1* was used as a control for the separation of dorsal (D) and ventral (V) retina. Poly A+ RNA was extracted from total (T), dorsal and ventral retina from E7 chick embryos. Two micrograms of poly A+ RNA were loaded per lane. β-actin was used as a loading control.

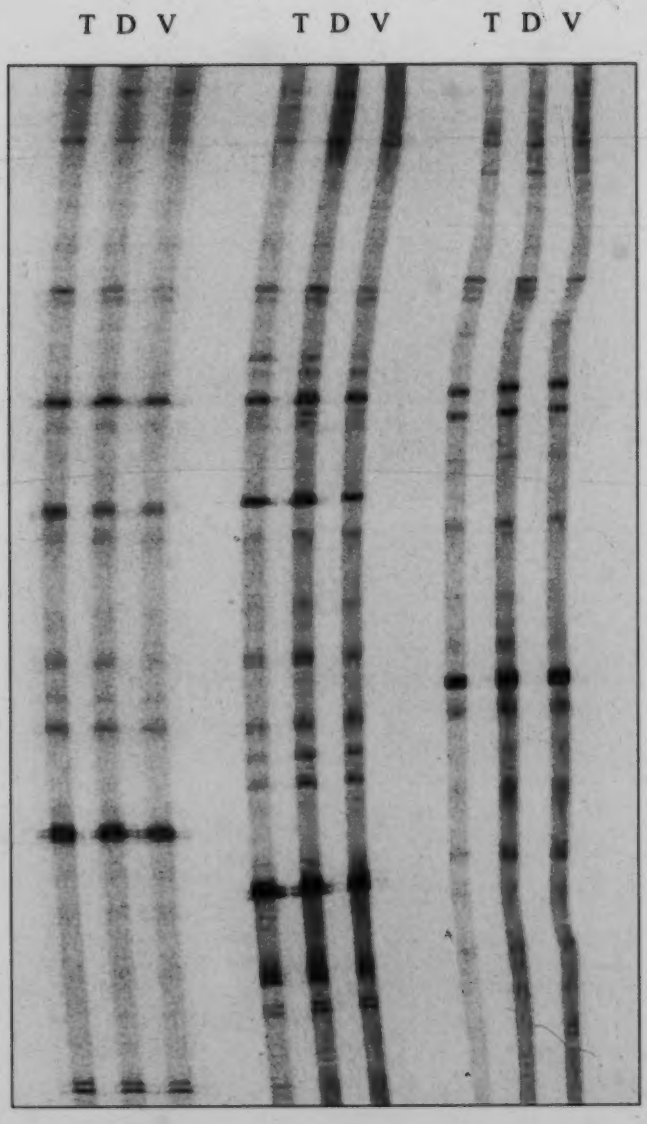

Figure 3-2. A typical autoradiograph of a DD-PCR gel. Each band theoretically represents a different cDNA. Lanes representing total (T), dorsal (D) and ventral (V) amplified cDNAs were loaded side-by-side for comparison.

between dorsal and ventral lanes, based on band intensity, were observed with the different bands. $T_{11}MG$ and $T_{11}MA$ produced the highest number of differentially expressed bands of all four anchor primers (see Table 3-1 for a summary of DD-PCR results). Nineteen, 3 and 20 bands were isolated using the $T_{11}MG$, $T_{11}MC$ and $T_{11}MA$ anchor primers, respectively. No differentially expressed bands were found with $T_{11}MT$ when used in combination with any of the 19 internal primers (OPA1-13, OPA15-20). For $T_{11}MG$, $T_{11}MC$ and $T_{11}MA$, an average of 120 bands were generated per lane. $T_{11}MT$ generated an average of only 40 bands per lane. Therefore, in combination with the 19 internal primers and four anchor primers used, approximately 7600 bands were generated in total, representing ~ 76% of the estimated minimum of 10, 000 transcripts in a cell (Liang *et al.*, 1993).

The internal primers OPA1, OPA2, OPA3, OPA4, OPA5, OPA6, OPA13, OPA17 and OPA19 yielded differentially expressed bands when used in combination with $T_{11}MG$ (Table 3-1). Only internal primers OPA2, OPA3 and OPA6 gave differentially expressed bands when used in combination with $T_{11}MC$, while OPA2, OPA5, OPA6, OPA7, OPA10, OPA13, OPA16, and OPA20 gave differentially expressed bands when used with $T_{11}MA$ (Table 3-1).

3.1.3 Reamplification and Subcloning into pBluescript

cDNA from each of the 42 bands selected was eluted, reamplifed and subcloned into pBluescript. Approximately, 4-10 colonies with inserts (white colonies) were selected for each reamplifed band. Of the 42 bands, three bands (B17, B20 and B34) could not be

Table 3-1. Summary of all DD-PCR reactions performed indicating the bands selected and the primers used. "Intensity of band" refers to the difference in intensity between the dorsal and ventral lanes, e.g. band 1 was 3 times higher in the ventral lane. Doublet: a double band was isolated from the reamplification step and was treated as two separate bands. No insert: either the band did not reamplify or could not be sequenced. Odd: the intensity of the "Total" band was greater than that of "Dorsal" or "Ventral." N/A: not applicable. N/D: the signal was not detectable.

Band	Anchor Primer	Internal Primer	Intensity of Band	Did the Band Reamplify?	Sequenced	Northern	Dorso-ventral Pattern
1	T_{11} MG	01	3X ↑ V	YES	YES	YES	N/D
2	T_{11} MG	01	5X ↑ D	YES	YES	YES	NO
3	T_{11} MG	02	2X ↑ V	YES/ DOUBLET	NO INSERT	N/A	N/A
4	T_{11} MG	02	2X ↑ V	YES/ DOUBLET	NO INSERT	N/A	N/A
5	T_{11} MG	02	2X ↑ V	YES/ DOUBLET	BOTTOM BAND	YES	N/D
6	T_{11} MG	03	2-3X ↑ D	YES	YES	NO	N/A
7	T_{11} MG	03	2X ↑ D	YES	YES	YES	YES
8	T_{11} MG	04	2X ↑ V	YES	NO INSERT	N/A	N/A
9	T_{11} MG	05	3-5X ↑ D	YES	YES	YES	YES
10	T_{11} MG	05	ODD	YES	NO	YES	N/D
11	T_{11} MG	05	2-3X ↑ D	YES	NO INSERT	N/A	N/A
12	T_{11} MG	05	2-3X ↑ D	YES	NO INSERT	N/A	N/A
13	T_{11} MG	06	>5X ↑ V	YES	NO	YES	N/D
14	T_{11} MG	06	>5X ↑ V	YES	NO	YES	N/D
15	T_{11} MG	13	ODD	YES	YES	YES	NO
16	T_{11} MG	13	ODD	YES	NO	YES	NO
17	T_{11} MG	17	>2X ↑ V	NO	N/A	N/A	N/A
18	T_{11} MG	19	2X ↑ D	YES/ DOUBLET	BOTTOM BAND	YES/YES	NO/NO
19	T_{11} MG	19	>2X ↑ V	YES	YES	YES	NO
20	T_{11}MC	02	5X ↑ D	NO	N/A	N/A	N/A
21	T_{11}MC	03	2X ↑ D	YES	YES	YES	YES
22	T_{11}MC	06	NOT SIG.	YES	NO	YES	NO
23	T_{11}MA	02	>5X ↑ V	YES/ DOUBLET	NO	YES	NO
24	T_{11}MA	05	2X ↑ V	YES	YES	YES	YES
25	T_{11}MA	06	2X ↑ V	YES/ DOUBLET	NO	YES	NO

Band	Anchor Primer	Internal Primer	Intensity of Band	Did the Band Reamplify?	Sequenced	Northern	Dorso-ventral Pattern
26	$T_{11}MA$	06	2X ↑ V	YES	NO	YES	N/D
27	$T_{11}MA$	07	>2X ↑ D	YES/ DOUBLET	YES	YES/YES	NO/NO
28	$T_{11}MA$	10	2X ↑ V	YES	NO	YES	NO
29	$T_{11}MA$	10	>3X ↑ V	YES	NO	YES	N/D
30	$T_{11}MA$	10	3X ↑ V	YES/ DOUBLET	NO	YES	NO
31	$T_{11}MA$	13	2-3X ↑ V	YES/ DOUBLET	NO	YES/YES	N/D N/D
32	$T_{11}MA$	13	2X ↑ D	YES	YES	YES	YES
33	$T_{11}MA$	13	2X ↑ D	YES	NO	YES	N/D
34	$T_{11}MA$	16	2X ↑ D	NO	N/A	N/A	N/A
35	$T_{11}MA$	16	3-5X ↑ D	YES	NO	YES	NO
36	$T_{11}MA$	16	2X ↑ V	YES	YES	YES	YES
37	$T_{11}MA$	16	2X ↑ V	YES	NO	YES	NO
38	$T_{11}MA$	16	2X ↑ D	YES	NO	YES	NO
39	$T_{11}MA$	20	3-5X ↑ D	YES/ DOUBLET	NO	YES	NO
40	$T_{11}MA$	20	5X ↑ D	YES	YES	YES	NO
41	$T_{11}MA$	20	2-3X ↑ V	YES	YES	YES	N/D
42	$T_{11}MA$	20	2X ↑ V	YES	YES	YES	YES
-	$T_{11}MT$	NO BANDS SELECTED					

reamplified during the reamplification PCR cycle and therefore could not be characterized further (Table 3-1). For some bands (B3, B4, B5, B18, B23, B25, B27, B31 and B39), doublets were obtained during the reamplification step. Generally, both bands from the doublet were isolated in these cases and treated separately. However, it was often the case that only one of the two bands could be subcloned into pBluescript and analyzed further. Other times, only the size of one of the reamplified bands corresponded to the size on the original DD-PCR gel, and only this band was excised and subcloned.

On occasion, colonies that appeared to be positive (white) by color selection were, in fact, negative and contained no insert. This was repeatedly the case for five bands (B3, B4, B8, B11 and B12). These bands were not characterized further since no insert could be isolated (Table 3-1).

It is interesting to note that the same internal primers can be linked to five of the eight problem bands that either did not reamplify or could not be subcloned. For example, internal primers OPA2 or OPA5 generated bands B3, B4, B11, B12 and B20, none of which could be reamplified or subcloned (Table 3-1). Because insert DNA could not be isolated from eight of the 42 isolated DD-PCR bands, only 34 bands could be analyzed further by Northern blot analysis and sequencing.

3.2 Northern Blot Analysis of Isolated DD-PCR cDNAs

3.2.1 Confirmation of Differential Expression

Northern blots containing total, dorsal and ventral polyA+ RNA were used to confirm differential expression of the selected bands at the RNA level. The 34 bands described above were used for Northern blot analysis. Only seven of these bands (B2, B7, B9, B21, B24, B36 and B42) were confirmed to be differentially expressed (Figure 3-3B). That is, either the dorsal or ventral lane was of greater intensity. The expression patterns observed for all seven bands corresponded to the expression patterns observed on the original DD-PCR gel (Figure 3-3A). Ten of the 42 bands (24%) did not produce a detectable signal with Northern blot analysis (B1, B5, B10, B13, B14, B26, B29, B31, B33 and B41) and therefore, the pattern of expression could not be attained for these bands. The control probe, β-actin, showed equal loading of all lanes. All other bands were considered to be false-positives since Northern blot analysis did not reveal a differential expression pattern.

Only one of the 34 bands, band 6, was not used as a probe for Northern blot analysis. Band 6 was discounted based on sequence analysis which revealed identity to a region of the chicken mitochondrial genome spanning nucleotides 2904 to 3209. The chicken mitochondrial genome consists of 16,775 base pairs. Previous Northern blots with various regions of the chicken mitochondrial genome failed to confirm differential expression and generated strong signal intensities, making it difficult to strip the Northern blot of residual signal.

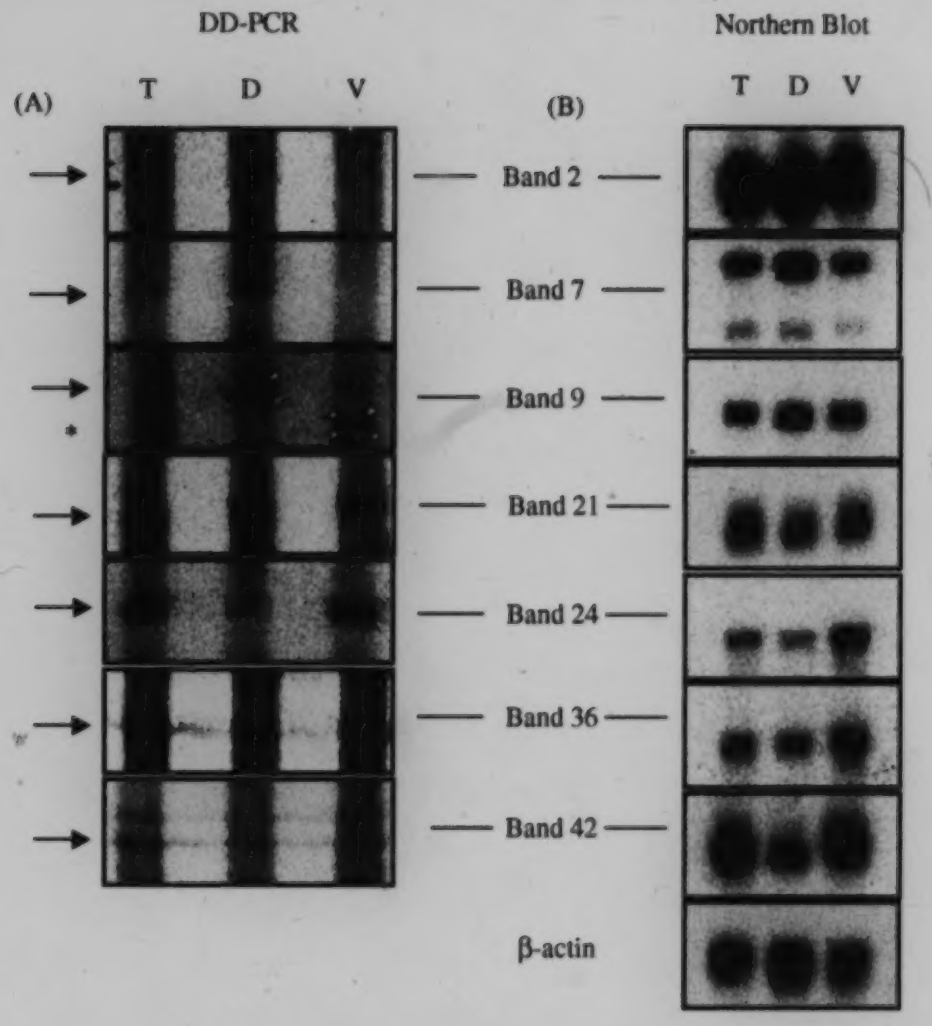

Figure 3-3. (A) DD-PCR analysis of E7 chick retina. In total, 42 bands appeared differentially expressed on DD-PCR gels. DNA was eluted from all 42 bands, cloned and used to probe a Northern blot. Only those DD-PCR bands which were confirmed to be differentially expressed are shown. The asterix (*) marks a "false positive" DD-PCR band, generating the "Odd" pattern described earlier. (B) Confirmation of differential expression by Northern blot analysis. Two micrograms of poly A+ RNA were loaded per lane, extracted from E7 total (T), dorsal (D) and ventral (V) retina. β-actin was used as a loading control.

3.2.2 Comparison of Expression Patterns on the Original DD-PCR Gels and Northern Blots

Figure 3-4 illustrates the relative differences in transcript size for all seven differentially expressed bands. Band 2 was more highly expressed in the dorsal versus ventral retina. The DD-PCR gel showed an estimated five-fold increase in intensity of the dorsal compared to the ventral lane, with hardly any transcript detected in the ventral retina (Figure 3-3A). The difference in intensity between the dorsal and ventral lanes was not as strong as the Northern blot, however, with only a two-fold increase in expression in the dorsal compared to the ventral retina (Figure 3-3B). Nonetheless, the difference in expression between dorsal and ventral retina was significant.

Band 7 was also expressed at higher levels in the dorsal retina on the original DD-PCR gel, with the difference in intensity being approximately two-fold greater than in the ventral retina (Figure 3-3A). This was similar to the pattern of expression detected with Northern blotting which also showed a two-fold increase in the dorsal versus ventral retina (Figure 3-3B). Also, the Northern blot of band 7 revealed two transcripts of different sizes (Figure 3-3B).

Band 9 showed a three to five-fold increase in expression in the dorsal versus ventral retina on the original DD-PCR gel (Figure 3-3A). The pattern on the Northern blot also showed an increase in expression in the dorsal retina, but it was less than two-fold (Figure 3-3B).

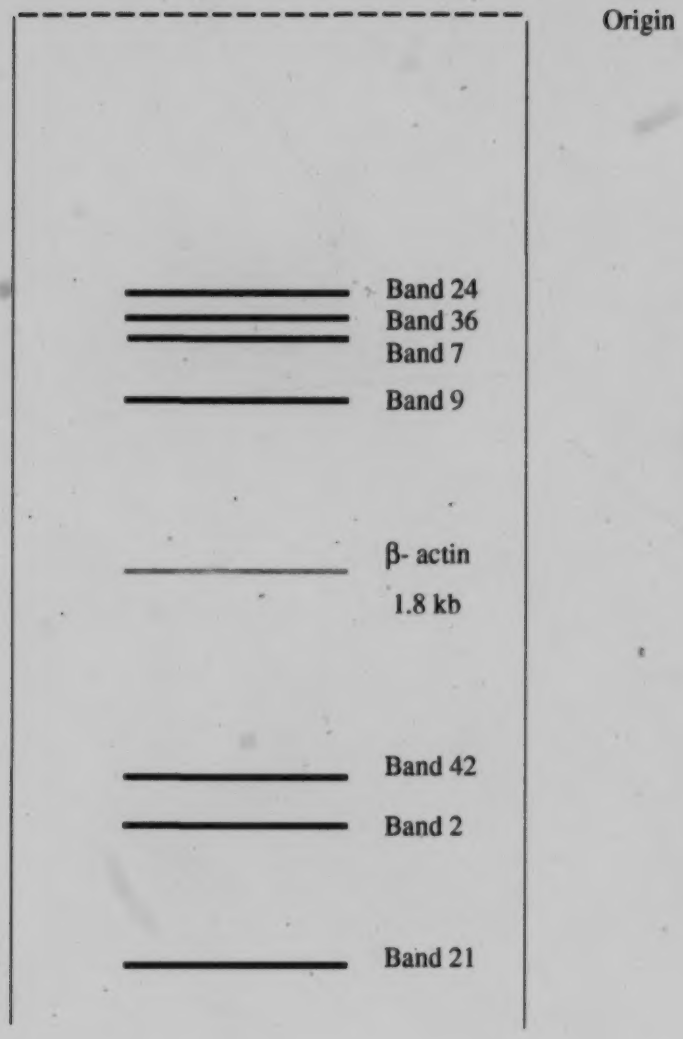

Figure 3-4. A schematic representation of the relative distances migrated by each of the mRNA species hybridized to each of the differentially expressed DD-PCR cDNA clones, as indicated by Northern blots. "Origin" indicates the wells at the top of the gel. β-actin is also included and is approximately 1.8 kb (Kost *et al.*, 1983).

Band 21 was two-fold greater in the ventral versus dorsal retina on both the original DD-PCR gel and the Northern blot (Figure 3-3A and 3-3B). Band 24 expression was two-fold greater in the ventral retina on the original DD-PCR gel but expression on the Northern blot was three to four-fold greater in the ventral retina (Figure 3-3A and 3-3B). Band 36 expression was two-fold greater in the ventral retina on both the original DD-PCR gel and the Northern blot (Figure 3-3A and 3-3B). Band 42 expression was two-fold greater in the ventral retina on the original DD-PCR gel but was approximately four to five-fold greater in the ventral retina on the Northern blot (Figure 3-3A and 3-3B).

3.3 Sequencing Results of Isolated DD-PCR cDNAs

A total of 17 of the 42 bands isolated from the DD-PCR gels were sequenced and the Genbank database searched for sequence similarity to other known sequences (BLAST search, nucleotide level) (see Table 3-1). Automated sequencing was used to sequence all DD-PCR clones. The sizes of the DD-PCR bands varied from 150 to 350 base pairs and sequences could often be generated for the entire insert. In most cases, DD-PCR inserts were used as probes for Northern blot analysis prior to being sequenced (see above for Northern blot results). Expression patterns based upon Northern blot analysis of total, dorsal and ventral retina then determined whether or not the bands would be sequenced. Bands that did not show differential expression at the RNA level were not sequenced. In a few instances the DNA inserts were sequenced prior to Northern blot analysis.

DD-PCR products are not only generated by the anchor and internal primers, but they can also be generated from two internal primers. If the region amplified by two

internal primers represents a translated region, or if the anchor primer and internal primer amplify a portion of a translated region, a BLAST search is more likely to yield a "hit," even if the chicken cDNA has not previously been cloned or entered in Genbank. This occurs because translated regions tend to be highly conserved between species relative to untranslated regions. Three of the seven differentially expressed bands yielded hits when searched against known sequences in Genbank (see Table 3-2 for a summary of sequencing results). Band 7 showed high sequence similarity (85% identity over 58 nucleotides) to *Xenopus Nopp180* cDNA (*xNopp180*), which encodes a nucleolar phosphoprotein with a possible role in ribosome biogenesis. Band 7 representing the chicken counterpart of *xNopp180* was later supported by library screening, which yielded a clone with 92% sequence identity over 39 nucleotides to *xNopp180* cDNA. Band 21 showed high sequence similarity (95% identity over 80 nucleotides) to the human, mouse and pig *Fau* cDNA, which encodes the ribosomal protein S30 fused to a ubiquitin-like protein. Band 42 showed high sequence similarity (83% identity over 242 nucleotides) to pig, mouse and human spermidine/spermine N^1-acetyltransferase (*SSAT*) cDNA, which encodes a rate-limiting enzyme involved in the degradation of polyamines.

The remaining differentially expressed clones, bands 2, 9, 24 and 36, had novel sequences (no similarity to any known sequences). Of the nondifferentially expressed DD-PCR clones, bands 6, 15, 18, 19, 27, 32, 40, and 41 also yielded hits when searched in Genbank (Table 3-2). As mentioned above, band 6, in addition to bands 15, 32 and 40, showed high sequence identity to various regions of the chicken mitochondrial genome. The sequences of bands 18 and 19 were identical to the class I (100% over 106

Table 3-2. Sequence similarities of DD-PCR clones to known sequences entered in Genbank. Searches were entered at www.ncbi.nlm.nih.gov/BLAST/.

DD-PCR BAND	SEQUENCE SIMILARITY
7	*Xenopus* Nopp180 cDNA (*xNopp180*)
21	Human, mouse and pig *Fau* cDNA
42	Pig, mouse and human spermidine/spermine N^1-acetyltransferase (*SSAT*) cDNA
2, 9, 24 and 36	Novel sequences (no similarity with any known sequences)
6, 15, 32 and 40	Various regions of the chicken mitochondrial genome
18 and 19	Class I and class II inner centromere protein (*INCENP*) cDNAs
27	Chick *TRAX* cDNA
41	Chick tyrosinase-related protein-2/DOPAchrome tautomerase (*TYRP2/DCT*) cDNA

nucleotides) and class II (100% over 200 nucleotides) chick inner centromere proteins (INCENPs) cDNAs. Band 27 sequence was identical (100% over 208 nucleotides) to the cDNA encoding chicken TRAX protein which is thought to have a role in the selective transport of Translin, a DNA binding protein. Band 41 was similar (89% identity over 73 nucleotides) to the cDNA encoding chick tyrosinase-related protein-2/DOPAchrome tautomerase (TYRP2/DCT) which encodes a protein expressed in the retinal pigment epithelium of chick embryos.

3.4 Fetal Tissue Distribution Northern Blots

All seven bands, which had previously been confirmed as differentially expressed in the retina, were used as probes for Northern blots containing polyA+ RNA from different chick fetal tissues at different stages of development (Figure 3-5A). The tissues examined included fetal retina, brain, heart, liver and kidney. Varying expression patterns were seen for the seven bands. The control probe, β-actin, showed equal loading of all lanes.

Band 2 expression was high in the retina at E5/6, lower at E7 and E10, with a slight increase by E16 (Figure 3-5A). Band 2 was moderately expressed in the E5/6 brain but then expression decreased at E7 and remained low until E15. Expression of band 2 in the heart was moderate at E6, followed by a decline in levels at E15. Expression was the highest in liver and kidney at both stages examined.

Band 7 expression showed a trend of decreasing expression with later stages of development in all tissues examined except for the kidney (Figure 3-5A). As observed

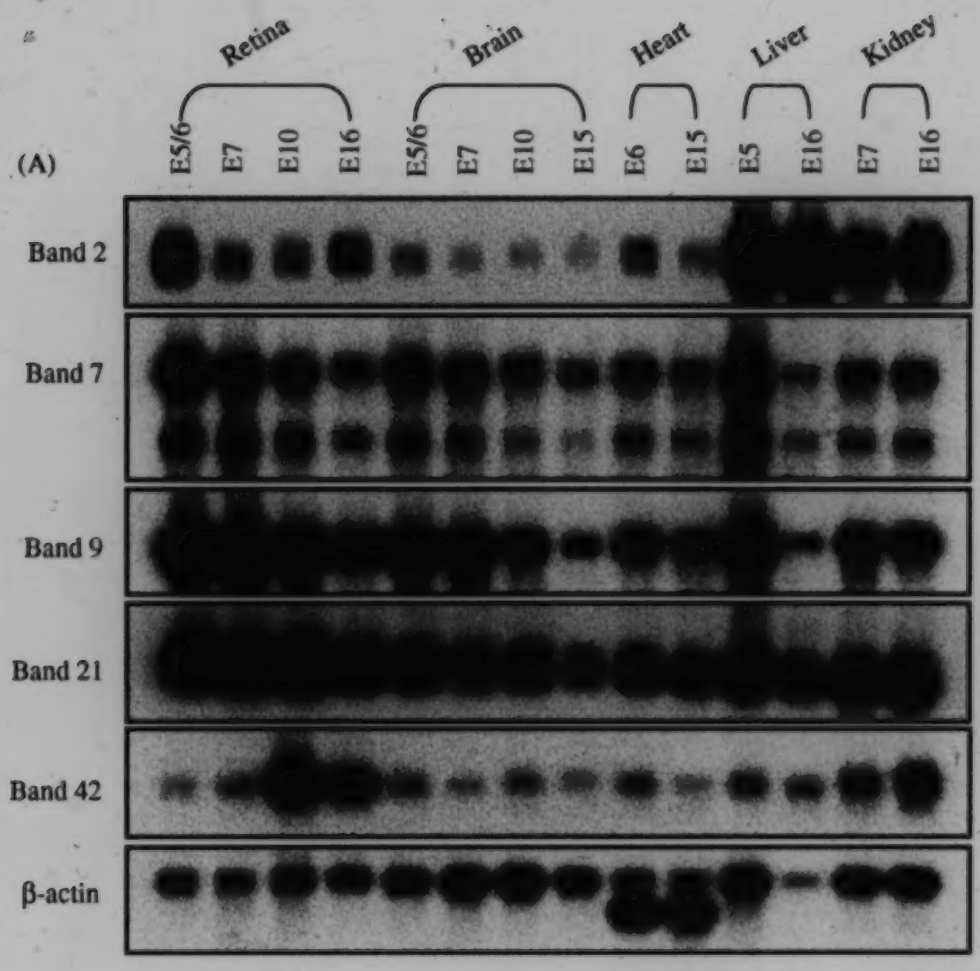

Figure 3-5. See over for figure legend.

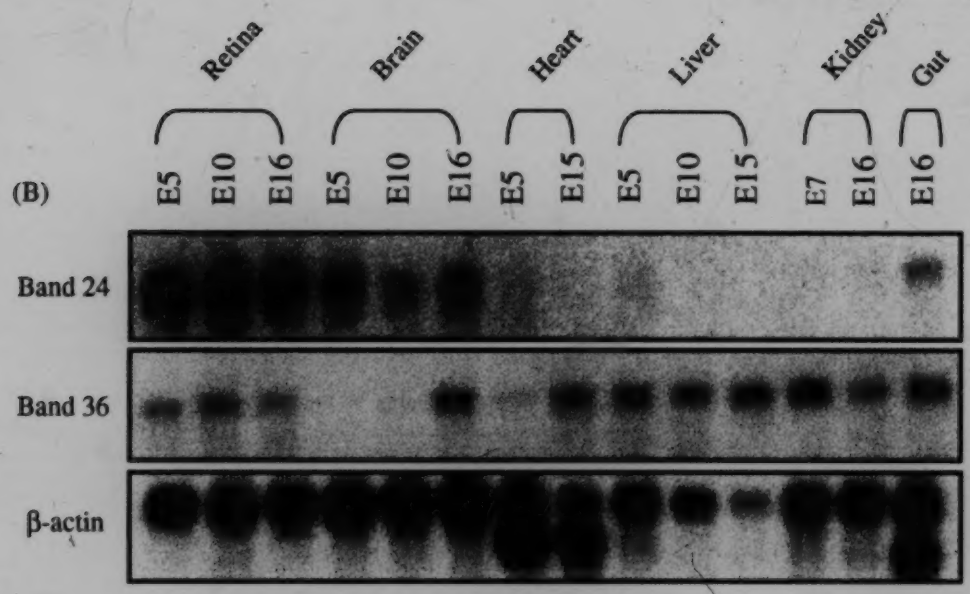

Figure 3-5. Fetal tissue distribution of differentially expressed DD-PCR bands. Two different Northern blots of fetal chick tissues were used. (A) Blot 1: Bands 2, 7, 9, 21 and 42 and β-actin. (B) Blot 2: Bands 24, 36 and β-actin . Two micrograms of poly A+ RNA were loaded per lane. DD-PCR bands (cDNAs) were labeled with α^{32}P-dCTP and used as probes. β-actin was used as a loading control.

with the Northern blot of total, dorsal and ventral retina, two transcripts of different size were again detected and both bands exhibited the same expression pattern. Expression was highest in E5/6 retina and E5 liver.

The expression pattern for band 9 was very similar to that of band 7, except that only one transcript was detected (Figure 3-5A). Expression was higher at earlier stages of development and gradually decreased. This pattern followed with the retina, brain, heart and liver. As with band 7, there was a dramatic difference in the expression levels in the liver between E5 and E16 while the expression level at E7 and E16 in the kidney was the same.

Band 21 was expressed at high levels at all stages of development for all tissues examined (Figure 3-5A). Expression in the retina showed little variation at the four different stages of development tested. Expression in the brain was constant for E5/6, E7 and E10 tissues but then decreased by approximately two-fold by E15. Expression in the liver also decreased, but only slightly, from E5 to E16.

Expression of band 24 was restricted to the brain and retina, except for low levels detected in the E16 gut (Figure 3-5B). The level of band 36 mRNA expression was constant for many of the stages examined and for the different tissues, with the exception of E5 and E10 brain, as well as E5 heart, which showed considerably reduced levels (Figure 3-5B).

Band 42 expression was highest in the retina with different levels in the retina at different stages of development (Figure 3-5A): expression was low in the retina at E5/6 and E7, high at E10 and decreased slightly by E16. Band 42 expression was low in brain, heart and liver. Expression in E7 kidney was also low, with increased expression in the E16 kidney.

Based on its differential expression in the dorsal and ventral retina, its fetal tissue distribution pattern and its identification based on sequencing, we decided to focus on band 42 (*SSAT*). We only had 241 base pairs of the *SSAT* cDNA sequence included in our original DD-PCR clone. This covered a region from 287 to 528 base pairs of the pig *SSAT*, 336 to 577 base pairs of the mouse *SSAT* and 415 to 653 base pairs of the human *SSAT*. Because the chicken *SSAT* cDNA had not been previously cloned, we screened a chick retina cDNA library to obtain the full-length cDNA. Automated and manual sequencing were used to obtain the sequence of the full-length clone. We also examined the expression pattern of *SSAT* mRNA in the chick retina by *in situ* hybridization in order to confirm the ventrodorsal gradient of expression as indicated by Northern blots.

3.5 Characterization of the Chicken *SSAT* cDNA

3.5.1 Isolating and Sequencing the Full-Length Clone

Both E7 and E16 chick retina cDNA libraries were available in our lab. Since *SSAT* mRNA is expressed at higher levels at E16 versus E7 in the retina (Figure 3-5A), the E16 library was used to isolate the full-length *SSAT* cDNA clone. In total, four attempts were made to isolate independent cDNA clones using the same cDNA library. Strong

positives were detected in all screening attempts, up to the tertiary (final) screening stage. However, despite their detection on the plaque lifts, except for one clone, positives could not be successfully recovered during the *in vivo* excision protocol, even after repeating the procedure numerous times with phage from the same plaques.

One positive clone for *SSAT* was recovered by *in vivo* excision and sequence similarity to *SSAT* was confirmed with sequencing and Southern blotting. The positive clone was approximately 900 base pairs, which was close to the original size of 1 kb predicted by Northern blot analysis (3-5A). Automated and manual sequencing of this initial clone revealed that the full-length clone had been isolated. This was shown with BLAST searches which confirmed that the 5' and 3' coding regions were present in the clone, indicated by high sequence identity to human *SSAT* cDNA. However, sequence alignments with *SSAT* cDNAs suggested that a recombination event had occurred in the internal portion of our cDNA clone. Therefore, more attempts were made to isolate additional independent clones to verify the *SSAT* cDNA sequence.

To address the possibility that the *SSAT* cDNA was undergoing rearrangement in pBluescript, we next attempted to subclone *SSAT* cDNA inserts in pBR322 directly from bacteriophage preparations rather than carry out *in vivo* excision. Inserts were isolated from the phage preparations, ligated into pBR322 and transformed into HB101. Colonies were picked onto grids and plasmids isolated using the method of lysis with boiling. These alterations proved to be successful and three additional independent clones were isolated. All independent clones were verified to be *SSAT* cDNAs by Southern blotting,

using the original DD-PCR clone as the probe. Sequencing verified that each of the clones was independent based on different 5' and 3' ends.

The entire sequence of the full-length cDNA clone was obtained by sequencing overlapping fragments of the longest clone, generated by exonuclease III and mung bean nuclease digestion. The sequences of the additional isolated independent cDNA clones were used to verify the cDNA sequence. The nucleotide and amino acid sequences of the chick *SSAT* cDNA are shown in Figure 3-6A. Sequence similarities to other known *SSAT* cDNAs are shown in Figure 3-6B. The predicted amino acid sequence of our chicken SSAT was 87% similar to the spiny mouse, human, and mouse SSAT protein and 86% similar to the golden hamster and pig SSAT.

3.5.2 Northern Blot Analysis of *SSAT* Expression throughout Retinal Development

The fetal tissue blot described earlier included E5/6, E7, E10 and E16 (Figure 3-5A). Northern blot analysis of poly A+ RNA from different stages of retinal development showed an increase in *SSAT* mRNA expression with differentiation. To extend our knowledge of *SSAT* mRNA expression in the retina, more time-points were taken and retinae were collected at additional stages of development and poly A+ RNA extracted for Northern blot analysis.

Figure 3-7 includes E7, E9, E10, E12, E14 and E16 retina. *SSAT* mRNA expression increased approximately two-fold between E7 and E9 and was found to be even higher at E12 than at E10. *SSAT* mRNA levels decreased by E14 and increased

```
1       CGT CGC CGA AGT CGG TGG GTG AGT CGT CTG CCT GCT GAA CGC CGC CGG GAC ATG CTC GCA

61      GCC TGA CTG ACC GCA GGT GGC CGC CGC GCC CGG GAC ACG AAT GAA GAA ACA GCT GCT CCT

121     CCT GTT CAC ACA CCG GGG ACT CGT CAG CCG AGG GGG CCG CAG GGG GAA ACG CCG TCG AAA

181     ATG GCT TCG TTC AGT ATC CGC GCC GCG CGT CCC GAG GAC TGC TCC GAC CTG CTG CGA CTG
          M   A   S   F   S   I   R   A   A   R   P   E   D   C   S   D   L   L   R   L     20

241     ATC AAG GAA CTA GCC AAG TAC GAG GAC ATG GAG GAT CAA GTG GTG CTA ACC GAG AAA GAG
          I   K   E   L   A   K   Y   E   D   M   E   D   Q   V   V   L   T   E   K   E     40

301     CTG CTT GAG GAC GGC TTT GGC GAG CAC CCG TTC TAC CAC TGT CTC GTT GCG GAG GTG CCG
          L   L   E   D   G   F   G   E   H   P   F   Y   H   C   L   V   A   E   V   P     60

361     AAA GAA CAG TGG TCG TCC GAA GGG CAC AGC ATT GTG GGC TTT GCT ATG TAT TAC TTC ACT
          K   E   Q   W   S   S   E   G   H   S   I   V   G   F   A   M   Y   Y   F   T     80

421     TAC GAT CCA TGG ATT GGA AAG CTG TTG TAT CTT GAA GAT TTC TAT GTG ATG GCT GAG TAC
          Y   D   P   W   I   G   K   L   L   Y   L   E   D   F   Y   V   M   A   E   Y    100

481     AGA GGA CTT GGC ATT GGA TCA GAA ATC CTG AAG AAT TTG AGT CAG GTT GCT GTC AAG TGC
          R   G   L   G   I   G   S   E   I   L   K   N   L   S   Q   V   A   V   K   C    120

541     CGC TGC AGC AGT ATG CAC TTC CTA GTT GCA GAG TGG AAT GAG CCC TCC ATC AGG TTC TAC
          R   C   S   S   M   H   F   L   V   A   E   W   N   E   P   S   I   R   F   Y    140

601     AAG AGA AGG GGT GCC TCT GAT CTG TCC ACT GAA GAG GGC TGG AGG CTC TTC AAA ATC GAC
          K   R   R   G   A   S   D   L   S   T   E   E   G   W   R   L   F   K   I   D    160

661     AAA GAG TAT CTC TTG AAG ATG GCA ACA GAA GAG TAG TGA GAG AAG GTT CCA GCG ACT AAA
          K   E   Y   L   L   K   M   A   T   E   E                                       171

721     CTC TTC AAA TGA ATA TAC ATG CTC TCT GAA TAA ACT CCT TCT TGC TTT CTG TGT TCA TAG

781     TGG AAT AAA ATA GTG TGG ATG CTA ATA CTA TGC AAC TGT GGT CAT AGA GTA ATT GGT ACT

841     GTG AGC TGG AGT GGA GGC ATC TCA AGT TGA ATA TGT GCT TGT ATC CAT CCT TTA CCA GTG

901     TGG GCT TGT AAT CTT TGT ATA TGA AAA CTT CAT TTC TTG TAA GTG TCA TTC AAA TGT GTA

961     CAA TGT ACA CAC TGG TAG GGT TTG TTT TAT TTC CTT TTA TAA GAA TAA ATA GTT TTC ACT

1021    CTA AAA AAA AAA AAA AAA AAA AAA AAA A
```

Figure 3-6A. Nucleotide and predicted amino acid sequence of the chick *SSAT* cDNA. The ATG initiation codon, the TAG stop codon and the AATAAA polyadenylation signal are in boldface.

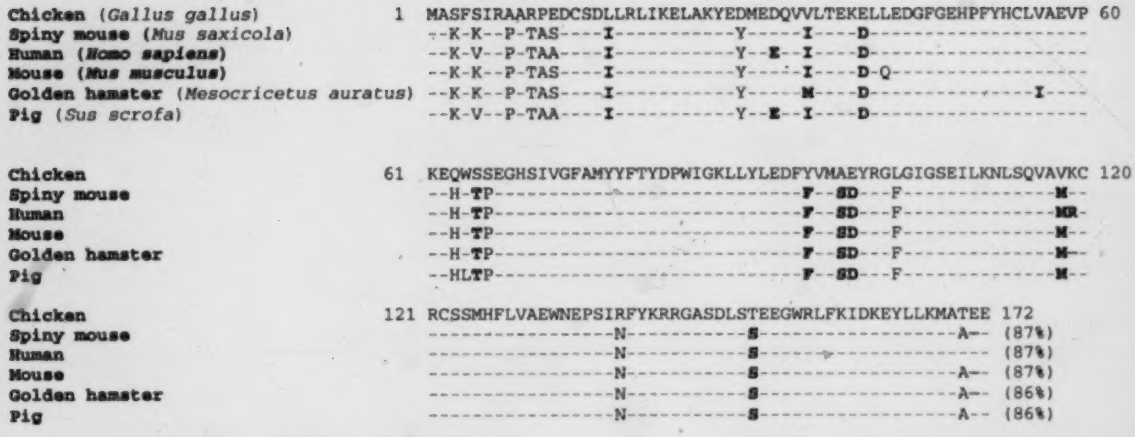

Figure 3-6B. Amino acid sequences of mammalian SSATs and chick SSAT. Identical amino acids are marked by a dash. Similar amino acids are in boldface type. The following residues were considered similar: G, A, S, T; E, D, Q, N; R, K, H; V, M, L, I; F, Y, W. Percent similarity (in brackets) are based on comparisons to chick SSAT.

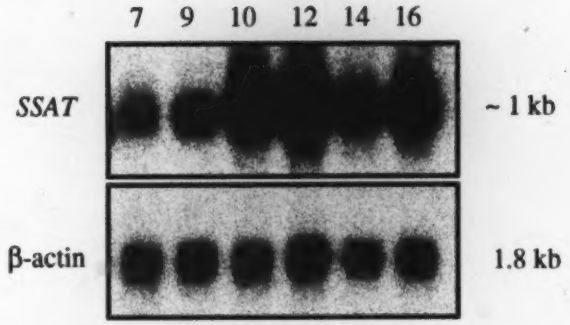

Figure 3-7. *SSAT* mRNA levels at different stages of chick retinal development. Northern blot of total chick retina from different embryonic stages (E7,E9, E10, E12, E14, E16). Poly A+ RNA was extracted from whole retinae and two micrograms were loaded per lane. *SSAT* cDNA was labeled with α^{32}P-dCTP and used as a probe. β-actin was used as a loading control (~ 1.8 kb, Kost *et al.*, 1983). Sizes are in kilobases (kb), located on the right-hand side.

again by E16. The different time-points shown in Figure 3-8 (see "total" retina lanes) indicate similar levels of *SSAT* mRNA expression at E11 and E15, compared to E10 and E16, respectively. Together, these results show that levels of *SSAT* mRNA increase significantly between E7 and E9, with a more dramatic increase between E9 and E10. Expression at E10 and E11 is relatively similar, followed by a slight increase at E12. Expression at E12 is approximately ten-fold greater than at E7. Surprisingly, there is a significant decrease in *SSAT* mRNA levels at E14, with similar levels to those observed at E9. Expression levels at E15 and E16 are similar and are elevated compared to E14 by about two to three-fold.

It should be noted that the difference in transcript levels between E10 and E16 was more dramatic in Figure 3-5A than in Figure 3-7, i.e. E16 transcript levels are greater in Figure 3-7. The difference cannot be attributed to unequal loading since β-actin was used as a loading control and did not show any loading inconsistencies. However, both blots illustrated very sudden changes in *SSAT* transcript levels throughout retinal development. This suggests that *SSAT* mRNA levels are very tightly regulated and can change very quickly, even within a certain day of development. Therefore, the difference between E10 and E16 in Figures 3-5A and 3-7 could be a reflection of a difference in the time of day when retinae were collected.

3.5.3 Northern Blot Analysis of E11 and E15 Dorsal and Ventral Retina

Next, we wanted to determine if the *SSAT* mRNA ventrodorsal pattern observed at E7 was also present at E11 and E15. Therefore, we dissected dorsal and ventral retina from

chick embryos at E11 and E15 and extracted poly A+ RNA for Northern blot analysis. The results indicated a minor ventrodorsal gradient at E11 and no gradient at E15 (Figure 3-8). β-actin was used as a loading control and verified equal loading for all lanes.

3.5.4 Differential Expression of *SSAT* – *In Situ* Hybridization

To obtain a more global picture of where *SSAT* mRNA was expressed in the retina, we carried out *in situ* hybridization of chick retina at E7 and E11. E7 and E11 chick retinae were sectioned along the dorsoventral plane. For E7 chick retina only, sections were taken serially, gradually progressing from the nasal/anterior eye to the temporal/posterior eye (see Figure 3-9 to visualize the axes of the eye). Because *ALDH1* mRNA is expressed in the dorsal retina only, *ALDH1* probe was used as a control for *in situ* hybridization to confirm that the sections were in the correct plane (Godbout *et al.*, 1996) (Figure 3-10).

SSAT mRNA Detection - *In Situ* Hybridization of E7 Retina using Serial Sections

No *SSAT* mRNA expression was detected in the first of the serial sections, which represented the nasal/anterior portion of the eye. As the sections progressed in a nasal/anterior to temporal/posterior direction, *SSAT* mRNA expression was first detected in the central retina and was very weak (Figure 3-11A-C). With further progression towards the temporal/posterior eye, *SSAT* mRNA expression remained in the central retina and was most intense at approximately halfway through the eye (Figure 3-12). As the sections progressed further towards the temporal/posterior eye, *SSAT* mRNA expression weakened but was still present in the central retina (Figures 3-13 to 3-18).

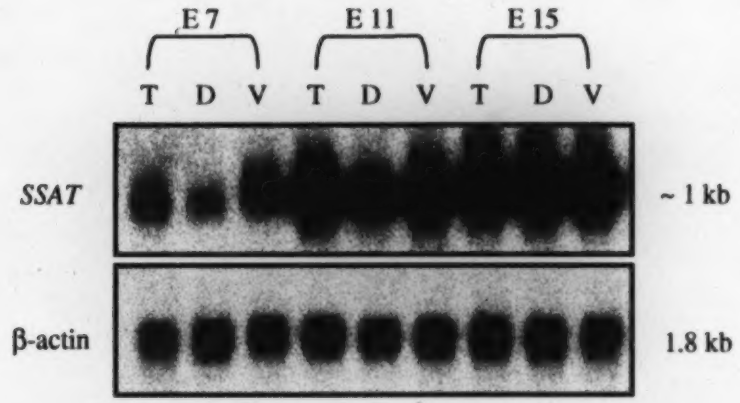

Figure 3-8. *SSAT* mRNA is differentially expressed in the developing chick retina. Northern blots of total (T), dorsal (D) and ventral (V) chick retina from different days of embryonic development (E7, E11, E15). Poly A+ RNA was extracted from retinal tissue and two micrograms were loaded per lane. *SSAT* cDNA was labeled with α^{32}P-dCTP and used as a probe. β-actin was used as a loading control(~ 1.8 kb, Kost *et al.*, 1983). Sizes are in kilobases (kb), located on the right-hand side.

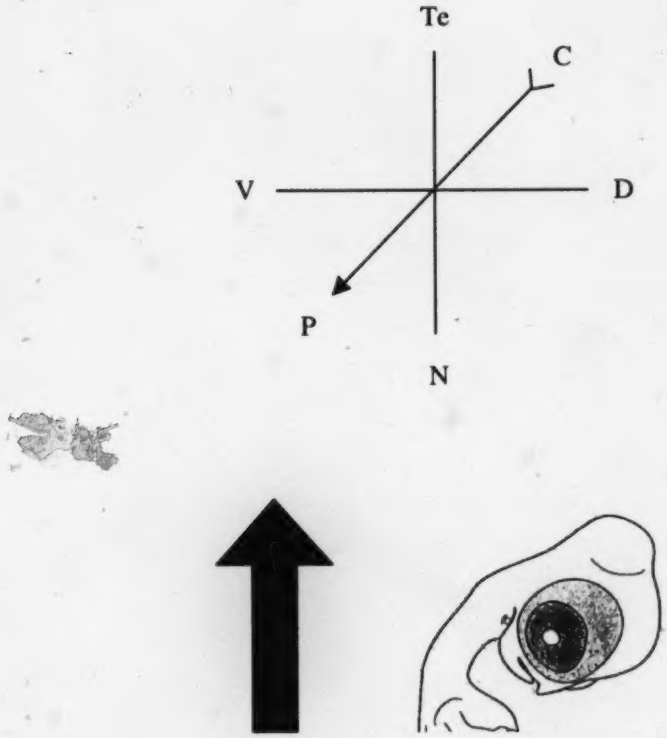

Figure 3-9. The axes of the retina. Serial sections were taken from E7 chick retina, starting nasally and progressing temporally. The tail of the arrow is towards the back of the eye. C: central; P: peripheral; N: nasal; Te: temporal; D: dorsal; V: ventral (adapted from Bellairs and Osmond, 1998).

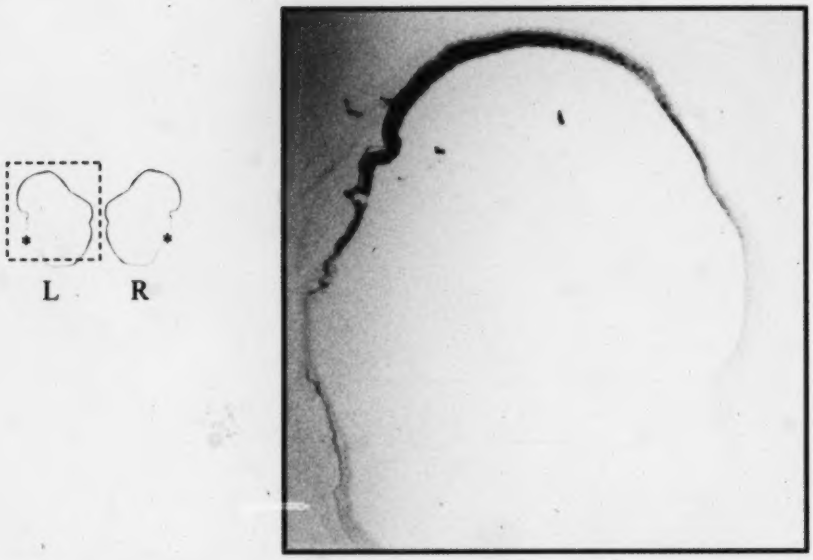

Figure 3-10. *In situ* hybridization of E7 chick retina. Serial sections were taken through the eye, starting nasally and progressing temporally, along the dorsoventral plane. *ALDH1*, expressed only in the dorsal retina, was used as a control probe to show dorsal and ventral retina. Purple color indicates positive staining for *ALDH1* mRNA. The sketch shows which eye (R: right; L: left) is represented in the section. The position of the lens is marked by *.

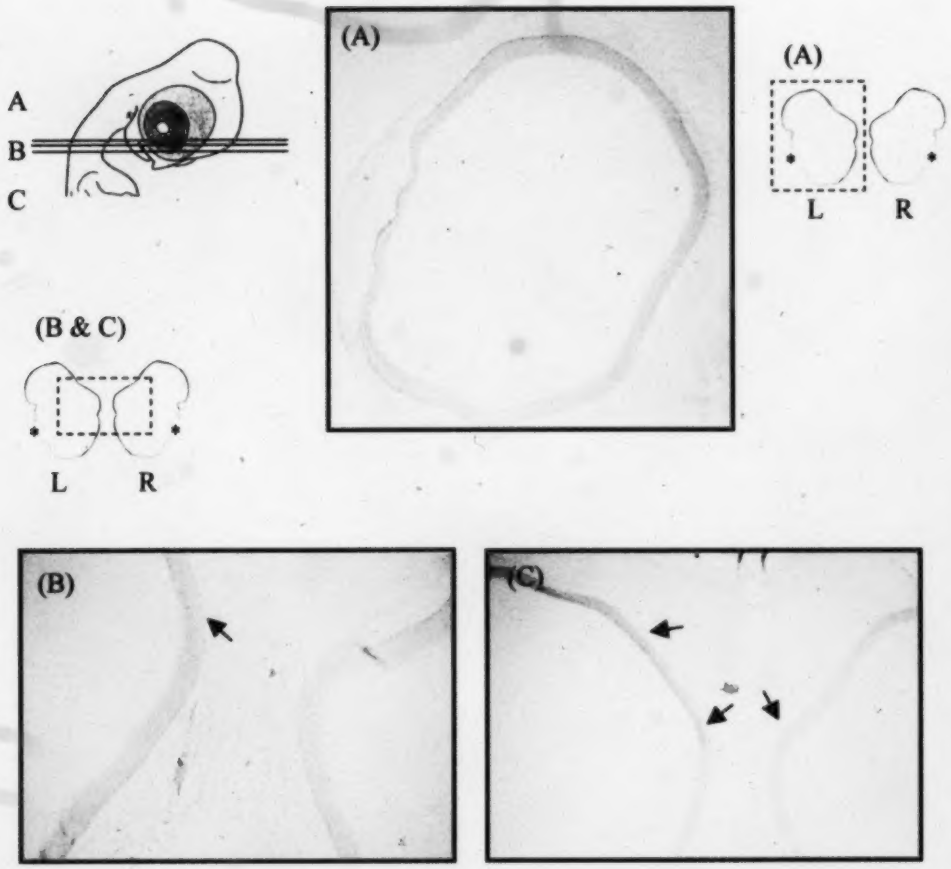

Figure 3-11. *In situ* hybridization of E7 chick retina showing *SSAT* mRNA expression. *SSAT* mRNA expression is very weak in sections representing the nasal half of the retina. (A) Section **7-1** of 31 sections. No *SSAT* mRNA is detected at this point in the retina. (B) Section **11-1** of 31 sections. *SSAT* mRNA expression is detected in the central retina but is very weak. (C) Section **13-1** of 31 sections. *SSAT* mRNA expression is still very weak and has progressed slightly from its central location in earlier sections (between the arrows). Serial sections were taken through the eye, starting nasally and progressing temporally, along the dorsoventral plane. Both eyes are shown in B and C. Purple color indicates positive staining for *SSAT* mRNA.

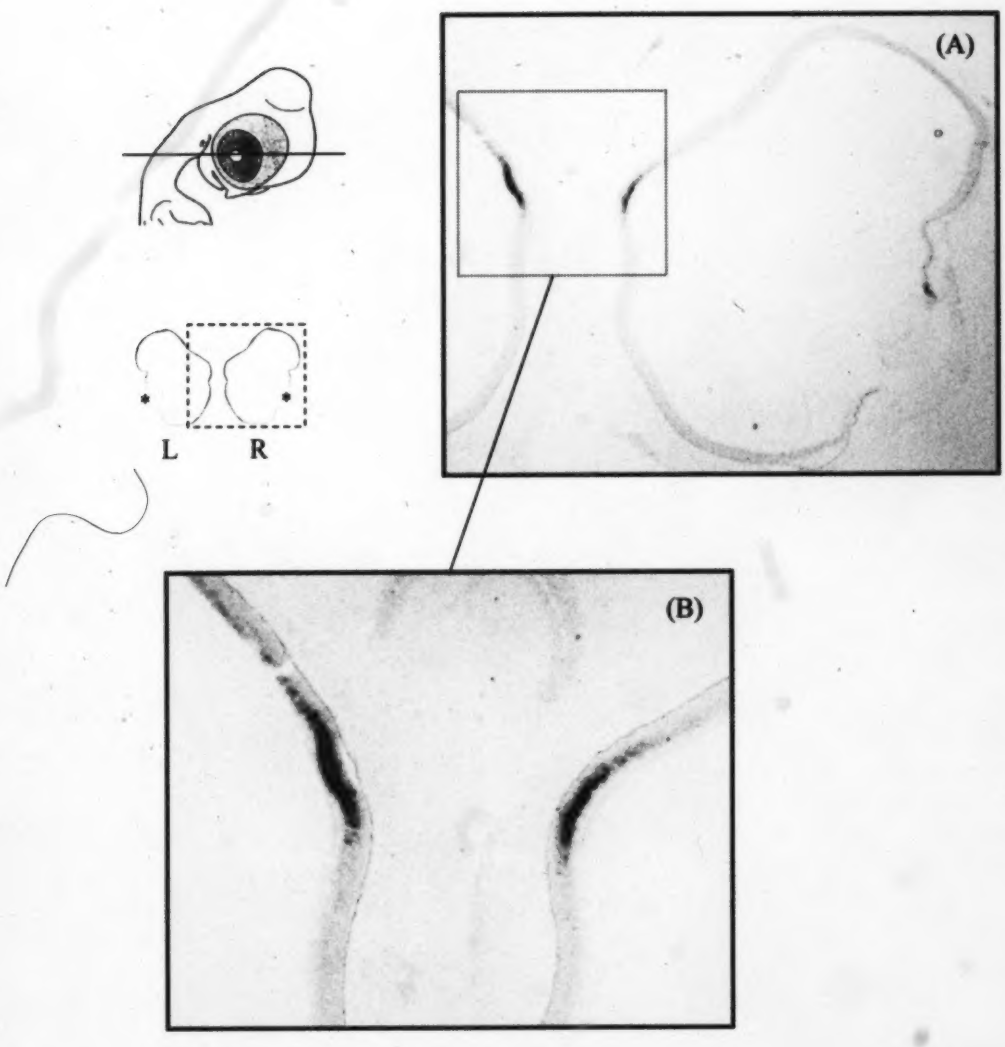

Figure 3-12. *In situ* hybridization of E7 chick retina showing *SSAT* mRNA expression. This is section **17-1** out of 31, representing the half-way point of the serial sections through the eye. (A) *SSAT* mRNA is detected early in the central retina, at approximately halfway through the eye. (B) A close-up of *SSAT* mRNA expression shown in A. Serial sections were taken throughout the eye, starting nasally and progressing temporally, along the dorsoventral plane. Both eyes are shown in A and B. Purple color indicates positive staining for *SSAT* mRNA.

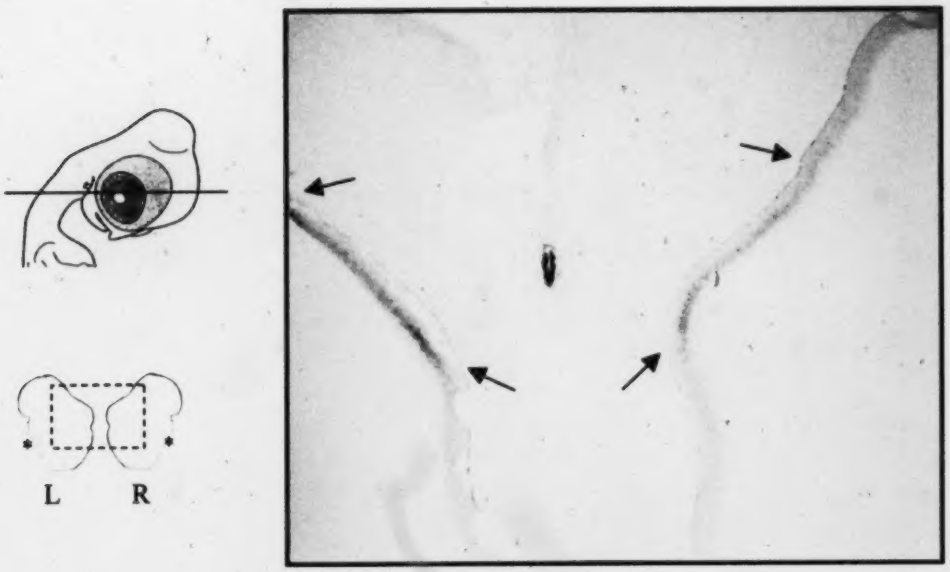

Figure 3-13. *In situ* hybridization of E7 chick retina showing *SSAT* mRNA expression. This is section **20-2** of 31 sections, past the center of the eye and towards the temporal side. The arrows mark the extent of *SSAT* mRNA expression in this section. Expression is weaker than in Figure 3-12 and has extended somewhat from its central location. Serial sections were taken through the eye, starting nasally and progressing temporally, along the dorsoventral plane. Both eyes are shown. Purple color indicates positive staining for *SSAT* mRNA (arrows).

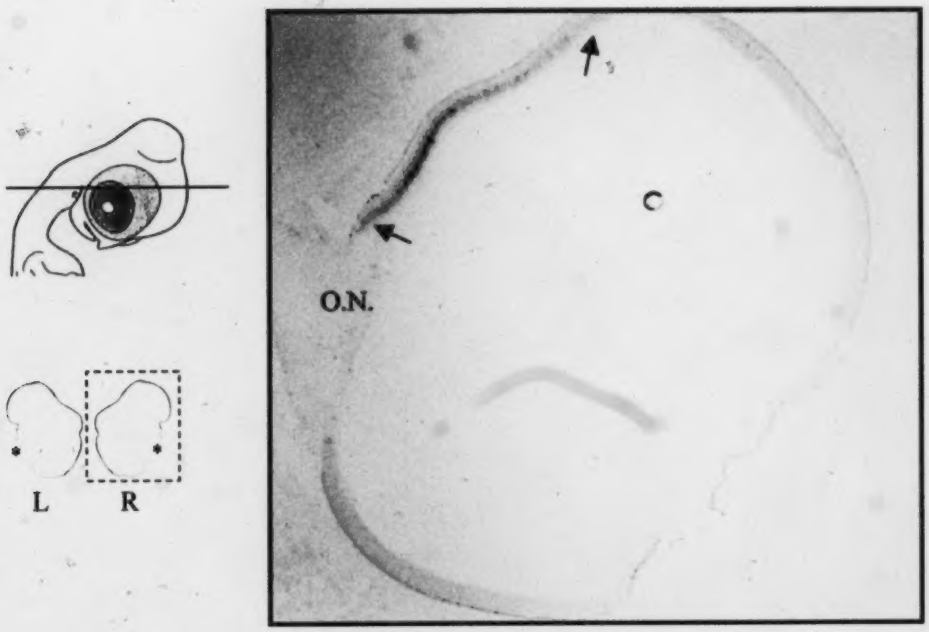

Figure 3-14. *In situ* hybridization of E7 chick retina showing *SSAT* mRNA expression. This is section **24-1** of 31 sections. The arrows mark the extent of *SSAT* mRNA expression in this section. Expression is still weaker than in Figure 3-12 and has migrated even further towards the peripheral retina. *SSAT* mRNA expression is not detected in the optic nerve (O.N). Serial sections were taken through the eye, starting nasally and progressing temporally, along the dorsoventral plane. Purple color indicates positive staining for *SSAT* mRNA (arrows).

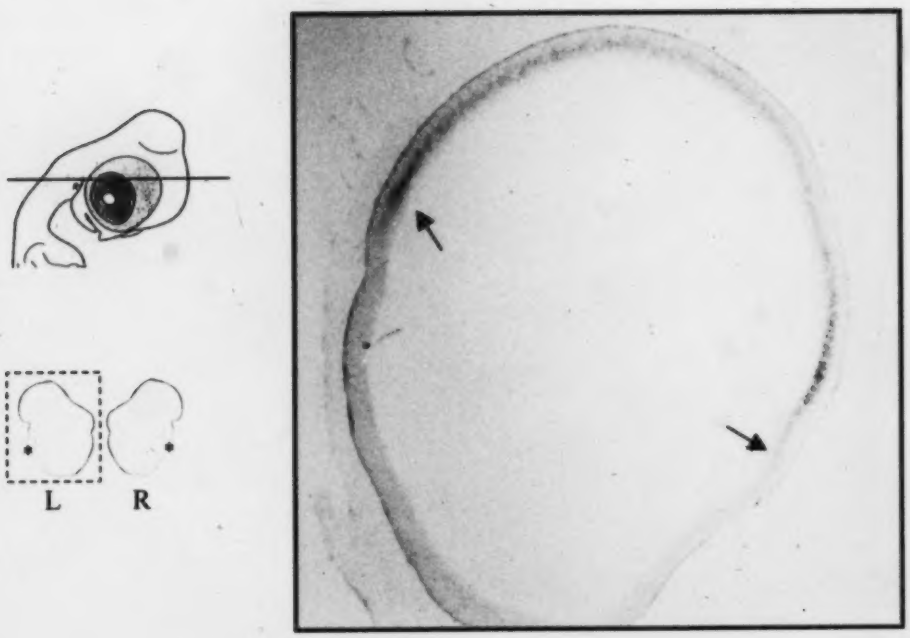

Figure 3-15. *In situ* hybridization of E7 chick retina showing *SSAT* mRNA expression. This is section **24-3** of 31 serial sections, showing a dramatic shift in *SSAT* mRNA expression towards the peripheral retina with increased progression in the temporal direction. The arrows mark the extent of *SSAT* mRNA expression in this section. Serial sections were taken through the eye, starting nasally and progressing temporally, along the dorsoventral plane. Purple color indicates positive staining for *SSAT* mRNA (arrows).

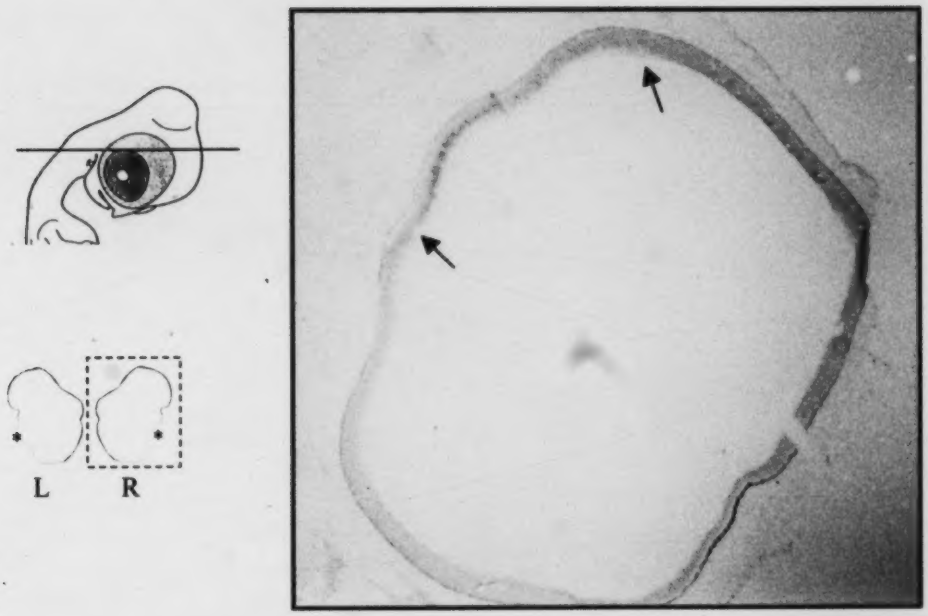

Figure 3-16. *In situ* hybridization of E7 chick retina showing *SSAT* mRNA expression. This is section **25-2** of 31 serial sections. Expression is mainly in the central retina (indicated by the arrows). Serial sections were taken through the eye, starting nasally and progressing temporally, along the dorsoventral plane. Purple color indicates positive staining for *SSAT* mRNA (arrows).

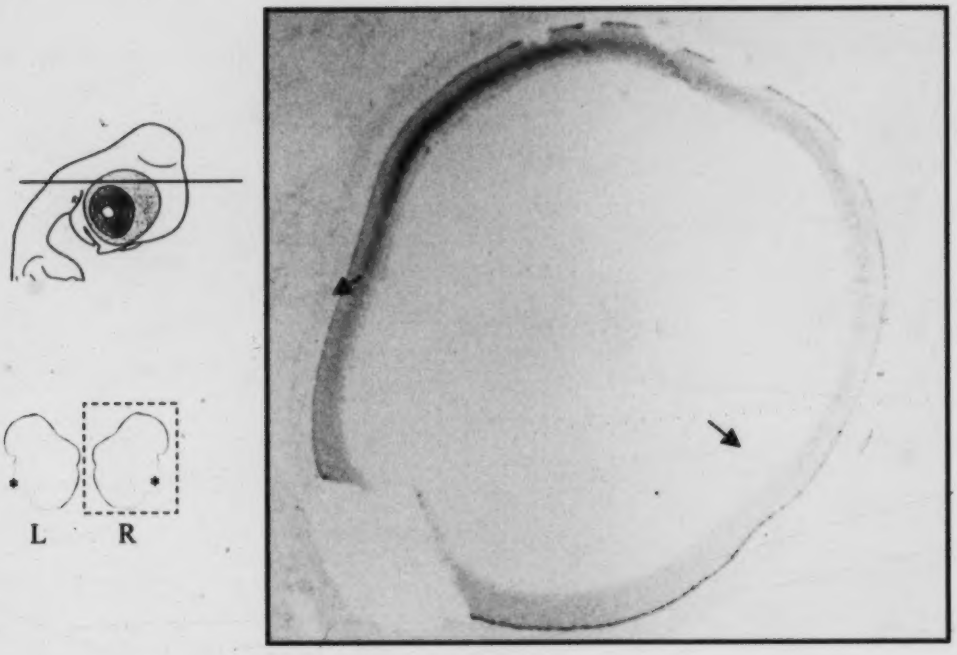

Figure 3-17. *In situ* hybridization of E7 chick retina showing *SSAT* mRNA expression. This is section **28-3** of 31 serial sections. The arrows mark the extent of *SSAT* mRNA expression in this section. *SSAT* mRNA extends from the central to the peripheral retina. Serial sections were taken through the eye, starting nasally and progressing temporally, along the dorsoventral plane. Purple color indicates positive staining for *SSAT* mRNA (arrows).

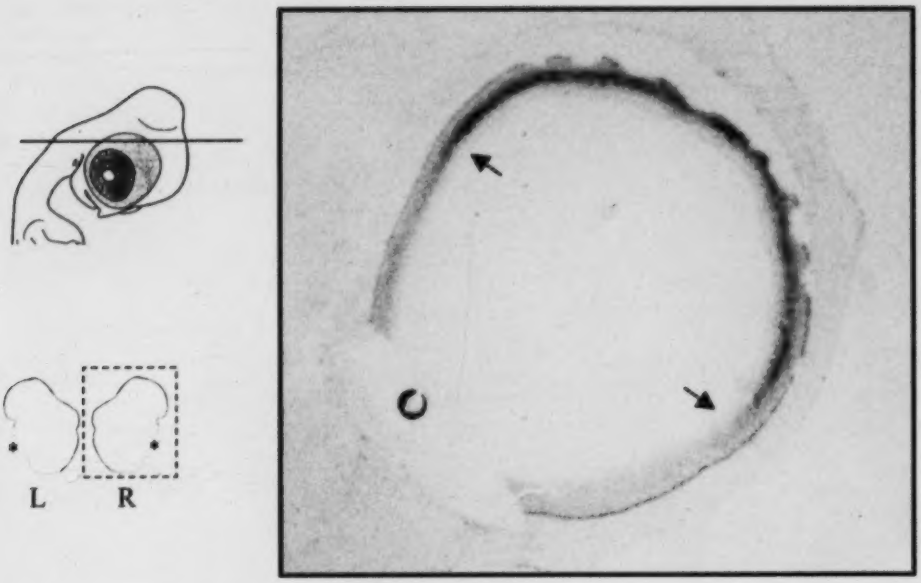

Figure 3-18. *In situ* hybridization of E7 chick retina showing *SSAT* mRNA expression. This is section **29-2** of 31 serial sections. The arrows mark the extent of *SSAT* mRNA expression in this section. Expression is similar to Figure 3-17, except that levels appear higher in this section. Serial sections were taken through the eye, starting nasally and progressing temporally, along the dorsoventral plane. Purple color indicates positive staining for *SSAT* mRNA (arrows).

SSAT mRNA expression did, however, appear to have a dorsal preference in the temporal eye (Figure 3-13 to 3-18). Based on these data, we conclude that *SSAT* mRNA appears to be expressed in an increasing nasal-temporal gradient, superimposed upon a centroperipheral gradient of expression, with a dorsal preference in the centrotemporal eye.

SSAT mRNA Detection - *In Situ* Hybridization of E11 Retina

As with E7 retinae, E11 retinae were also dissected along the dorsoventral but retinae were not serially sectioned. Instead, only one plane was examined for E11 retina. *In situ* hybridization of E11 retina revealed *SSAT* mRNA expression throughout the entire retina (Figure 3-19D). *SSAT* mRNA was detected in both the dorsal and ventral retina with similar levels of expression, although expression in the ventral retina extended further towards the peripheral retina.

CA-II mRNA Detection: Restriction of *SSAT* mRNA Expression to Müller Glia

To identify cells expressing *SSAT* mRNA, carbonic anhydrase II (*CA-II*) was used as an *in situ* hybridization probe for E7 and E11 retina sections. *CA-II* is expressed in all undifferentiated cells of the early retina and becomes restricted to Müller glial cells with differentiation (Vardimon *et al.*, 1986). Therefore, *CA-II* can be used as a marker for Müller glial cells. A comparison of *SSAT* mRNA expression with that of *CA-II* suggests that *SSAT* mRNA is expressed only in Müller glial cells (Figure 3-19B and 3-20).

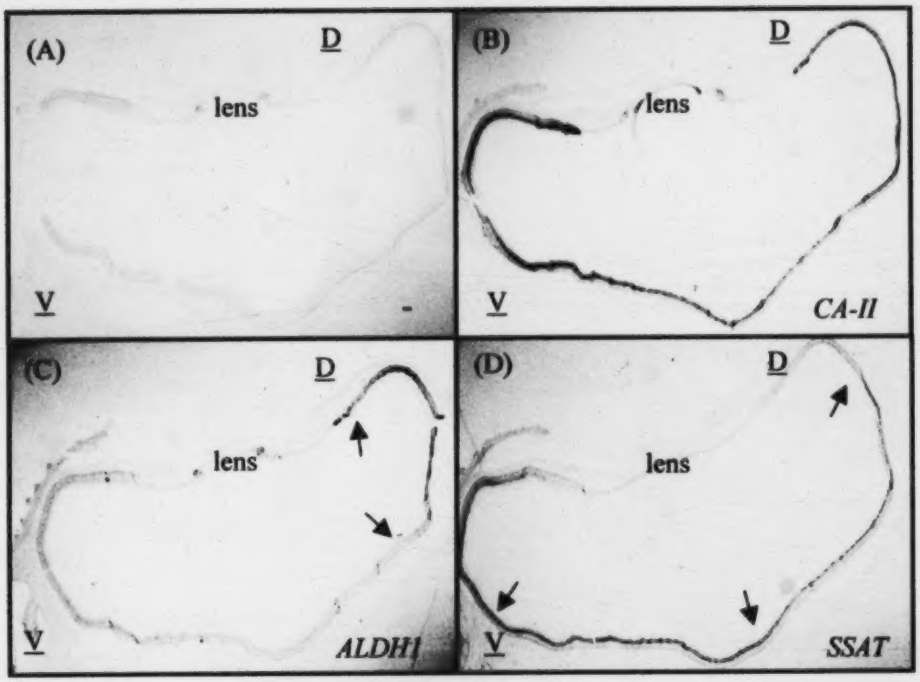

Figure 3-19: *In situ* hybridization of E11 chick retina. Purple staining is positive for *SSAT* mRNA expression. (A) Negative control. (B) *CA-II* is uniformly expressed throughout the retina. (C) *ALDH1*, expressed only in the dorsal retina, was used as a control probe to show dorsal and ventral retina. (D) *SSAT* is uniformly expressed at E11. D: Dorsal; V: Ventral. Sections were counterstained with methyl green.

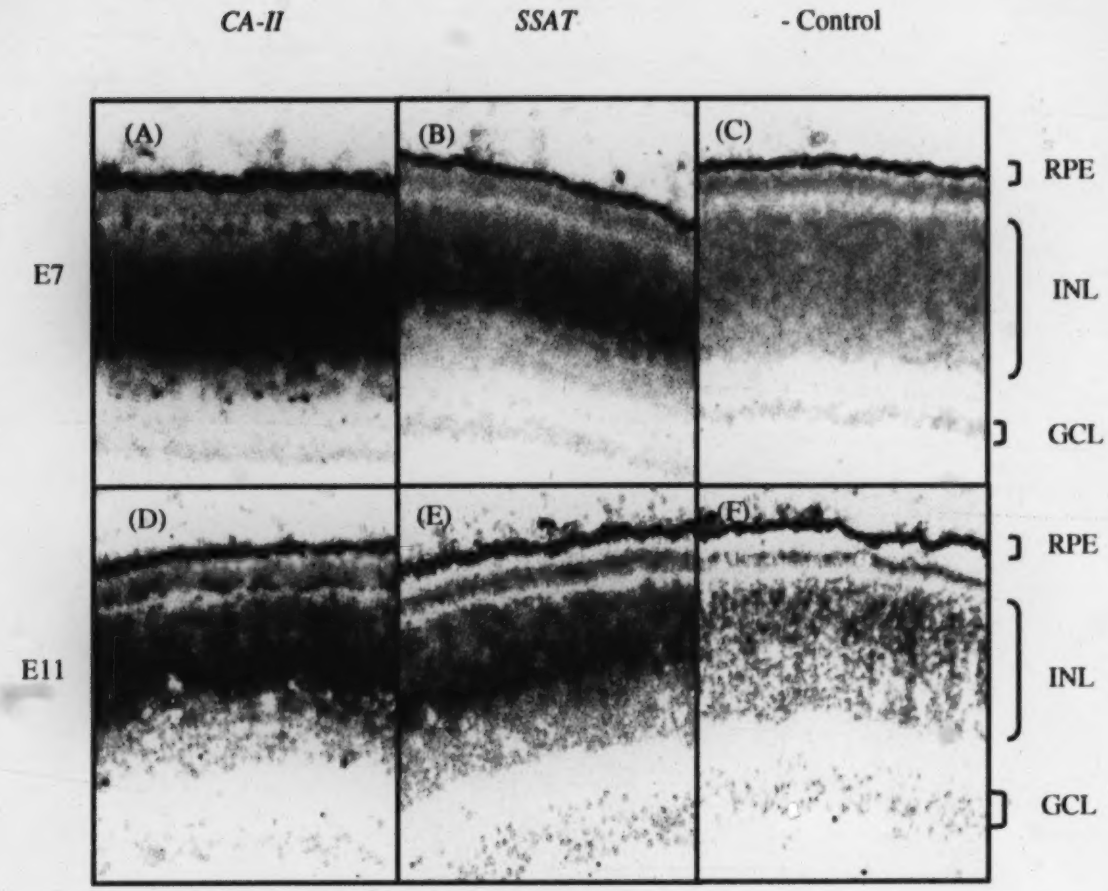

Figure 3-20. Magnified view of *in situ* hybridization of E7 and E11 chick retina showing *SSAT* expression in Müller glial cells. Purple staining is positive for mRNA expression. Sections were counterstained with methyl green. (A & D): *CA-II*, a known marker for Müller glial cells. (B & E): *SSAT*, also expressed in Müller glial cells. Expression is widespread for both *CA-II* and *SSAT* at E7 when the retina is mostly undifferentiated. At E11, the retina is almost entirely differentiated and *CA-II* and *SSAT* transcripts are confined to the Müller glial cells. (C & F): Negative controls. RPE: retinal pigmented epithelium; INL: inner nuclear layer; GCL: ganglion cell layer; E: embryonic day.

Whole Mount *In Situ* Hybridization

Attempts were made to visualize the gradient of *SSAT* mRNA expression throughout whole, intact retinae by using whole mount *in situ* hybridization. Despite repeated attempts, background staining was always too high, probably due to the probe being "trapped" in the thick retinal tissue. Therefore, the gradient could not be seen and no results are shown for this procedure.

CHAPTER 4. DISCUSSION

The identification of asymmetrically expressed genes in the developing embryo, and the factors controlling the expression of such genes, is an attractive topic for many researchers interested in developmental biology. Of great interest is the study of asymmetrically expressed genes in the central nervous system, in particular, the retina. Roger Sperry was the first to propose the existence of molecular gradients in the retina and brain which would aid in targeting the axons of retinal ganglion cells to the brain (Sperry, 1963; reviewed in Goodman and Shatz, 1993 and Meyer, 1998). Sperry proposed that molecular gradients exist along the dorsoventral, anteroposterior (nasal-temporal) and centroperipheral axes. He proposed that these gradients are expressed in a complementary fashion between the retina and the brain, such that nasal retinal axons would project to the posterior tectum, and temporal retinal axons would project to the anterior tectum. In the perpendicular axis, dorsal retinal axons would project to the ventral tectum and ventral retinal axons would project to the dorsal tectum.

Molecular gradients of the types that Sperry proposed have been documented in the retina and brain. Examples of molecules expressed in gradients are aldehyde dehydrogenase type 1 (ALDH1), expressed in the dorsal retina; chondroitin sulfate proteoglycan (CSPG) expressed in a centroperipheral gradient in the retina; the Eph-related receptors and their ligands (ephrins), expressed in complementary gradients along the anteroposterior axes in the retina and brain; and the toponymic (TOP) molecules, also expressed in complementary gradients in the retina and brain along both the dorsoventral

and anteroposterior axes. Exactly how these gradients function to guide axons along the proper path to the correct area in the brain is not well known.

Research efforts in our lab have been directed towards the identification of differentially expressed genes in the developing chick retina. The main objective of this study was to identify differentially expressed genes in the developing chick retina which, when expressed in a gradient, could possibly be involved in targeting retinal ganglion axons to the optic tectum. In particular, we were most interested in finding genes expressed in gradients along the dorsoventral axis of the retina. Earlier in our lab, *ALDH1* mRNA was found to be expressed in the dorsal retina (Godbout *et al.*, 1996). Cytosolic ALDH1 is involved in the conversion of retinaldehyde to retinoic acid (RA), an important transcriptional regulator involved in neuronal differentiation and patterning in the developing embryo (reviewed in Dräger *et al.*, 1998). Aldehyde dehydrogenase activity has also been detected in the ventral retina (McCaffery *et al.*, 1992; McCaffery *et al.*, 1993). Ventral aldehyde dehydrogenase, whose encoding gene has yet to be cloned, is more efficient than dorsal ALDH1 in the conversion of retinaldehyde to RA, resulting in higher levels of RA in the ventral retina.

It is possible that the resulting asymmetric gradient of RA, caused by the different activities of the dorsal and ventral ALDH isoforms, could result in asymmetric gene expression throughout the retina since RA is thought to have dose-dependent effects on gene expression (Durston *et al.*, 1989; Ruiz I Altaba and Jessell, 1991). Therefore, our objective was to identify ALDH-related or other genes involved in, or regulated by, this

pathway. To achieve this goal, E7 chick retinae were dissected along the dorsoventral plane, and cDNA populations from total, dorsal and ventral retinae were examined using DD-PCR. We examined E7 chick retina because this is a time when cells are actively dividing and differentiating, and contacts between the retina and brain are beginning to form. DD-PCR was the method of choice for this study for several reasons. DD-PCR has proven to be successful in many disciplines of molecular biology for the identification of differentially expressed genes, including cancer research and developmental biology. Both high and low abundance transcripts are detected by DD-PCR. Also, up and down-regulated genes can be identified simultaneously in a single DD-PCR gel. DD-PCR is a cost-effective, convenient and efficient tool for comparing gene expression between separate cell populations and has been successfully used to identify differentially expressed genes in an earlier study in our lab.

In total, approximately 7600 DD-PCR bands were generated in our analysis of E7 chick retina. Less than 1% of the 7600 DD-PCR bands visualized appeared to be differentially expressed, with 42 bands selected for further analysis. This compared to other studies which reported similar findings (Bauer *et al.*, 1993; Liang *et al.*, 1993). Seven of these 42 bands were confirmed as having differential expression in the E7 chick retina using Northern blot analysis. This meant a 17% success rate for our analysis (83% false positives), which is also comparable to other DD-PCR studies (Liang *et al.*, 1993; Gupta *et al.*, 1998). It is also interesting to note that 10 of the 42 bands (B1, B5, B10, B13, B14, B26, B29, B31, B33 and B41; 24%) used as probes for Northern blot analysis did not produce detectable signals, suggesting that these transcripts are of low abundance.

This is lower than other studies which found that 48% (Aiello *et al.*, 1994) and 40% (Liang *et al.*, 1993) of the isolated DD-PCR clones did not produce detectable signals with Northern blot analysis. Our goal of obtaining differentially expressed clones was reached using DD-PCR analysis.

Other studies have used DD-PCR as a tool to analyze differential gene expression in the eye, including the retina. For example, Godbout and Andison (1996) examined undifferentiated versus differentiated chick retina and found that cyclin D1 mRNA levels were higher in the undifferentiated chick retina. In a similar study, Cai *et al.* (1999) identified a novel gene product whose expression is altered with lens differentiation in the rat. Frog and rat retina have been examined using DD-PCR to find genes which are altered according to the circadian clock (Green and Besharse, 1996; Gauer *et al.*, 1995). Both of these studies were successful and revealed mRNAs which appear to vary with the circadian rhythm. Sequencing analysis revealed high sequence identity for one of the mRNAs to F3, a known cell adhesion protein (Gauer *et al.*, 1995). Aiello and colleagues (1994) used DD-PCR to identify glucose-regulated genes which may be involved in the loss of retinal capillary pericytes. This cellular loss is a common finding in patients with diabetic retinopathy and is associated with hyperglycemia. To find glucose-regulated genes, retinal pericytes were exposed to physiologic and pathologic glucose concentrations and examined using DD-PCR. Ten genes, [encoding fibronectin, caldesmon, Rieske FeS reductase, two ribosomal proteins (28S and 27S), molecules with sequence homology to human 75-kDa autoantigen and human papillary thyroid carcinoma protooncogene tyrosine kinases and three novel sequences], were identified

which appear to be glucose-regulated. To our knowledge, no studies have been performed using DD-PCR to compare gene expression in the dorsal and ventral retina, with the goal of identifying genes involved in the formation of the retinotectal map. However, a study which compared nasal and temporal chick retina using DD-PCR has previously been performed, leading to the identification of a cDNA fragment which appeared to be specific for the nasal versus the temporal retina (Hong *et al.*, 1998). Neither Northern blotting nor *in situ* hybridization analysis was performed to confirm differential expression for this clone and the cDNA was not sequenced.

For our study, four anchor primers were paired with each of the 19 internal primers used. Each anchor primer generated a different number of bands displayed on the DD-PCR gels, ranging from 100 to 150 bands per lane for $T_{11}MG$, $T_{11}MC$ and $T_{11}MA$, and 40 bands for $T_{11}MT$. The average number of bands per lane is similar to that found in other DD-PCR studies (Bauer *et al.*, 1993; Liang *et al.*, 1993; Guimaraes *et al.*, 1995; Carter *et al.*, 1999). Of the four anchor primers, $T_{11}MG$ and $T_{11}MA$ consistently gave better results than $T_{11}MC$, generating a greater number of differentially expressed bands (see Chapter 3). Consistent with the literature, we found $T_{11}MG$ and $T_{11}MC$ to be efficient primers, generating many bands per lane (Mou *et al.*, 1994; Malhotra *et al.*, 1998). However, in contrast to the literature, which states that $T_{11}MA$ and $T_{11}MT$ are less efficient that $T_{11}MG$ and $T_{11}MC$ (Mou *et al.*, 1994; Malhotra *et al.*, 1998), we found $T_{11}MA$ to be an efficient primer, generating the same number of bands per lane as $T_{11}MG$ and $T_{11}MC$. In fact, $T_{11}MA$ generated a greater number of differentially expressed bands than $T_{11}MC$. We often observed sets of two or three closely spaced bands of the same

intensity on the DD-PCR gels. Such sets of bands have often been described in other studies using DD-PCR and are now known to represent the same cDNA. One study examined each band in such groups and found the difference in size was due to the presence or absence or an additional 'A,' known to be added by *Taq* polymerase to the 3' ends of PCR products (Bauer *et al.*, 1993).

The number of transcripts per cell has been estimated to be approximately 10,000, representing 10 to 20% of the genes found in the chicken genome (Liang *et al.*, 1993; Zhang *et al.*, 1998). We estimate that 7600 bands were visualized in our DD-PCR analysis, meaning that we examined a maximum of 76% of all transcripts expressed in a cell. Based on this estimate, we would have expected to find abundant clones such as *ALDH1*. *ALDH1* is a very abundant transcript at E7 and is expressed only in the dorsal half of the developing chick retina. Of the 42 bands isolated based on their differential expression pattern on the original DD-PCR gel, none were identified as *ALDH1* when sequenced.

There are numerous explanations for why *ALDH1*, and other differentially expressed clones, were not detected in our analysis. Theoretically, each band visualized on a DD-PCR gel represents a different cDNA. However, it is quite possible that there are multiple cDNAs represented by a single DD-PCR band, each co-migrating the same distance because they are the same size. Of the multiple cDNAs in a single band, only one may be differentially expressed and only one of these cDNAs may be isolated after subcloning. If the non-differentially expressed transcript is isolated, the differentially

expressed transcript will not be detected and the original DD-PCR band will be considered to be a false-positive. It could also be the case that in a single band containing multiple cDNAs, each cDNA may be differentially expressed but in a different pattern than the other cDNAs in that band. Therefore, if a cDNA with dorsoventral expression was in the same band as a cDNA with ventrodorsal expression, the band may not appear to be differentially expressed because the signals would cancel out. Also, a single cDNA may be represented more than once during DD-PCR analysis by different DD-PCR bands. For example, if the same cDNA is amplified by different primer sets, bands of different sizes will be generated, with each band considered to represent a separate cDNA. Taking the above illustrations into account, it is likely that we detected fewer transcripts than estimated based on the number of DD-PCR bands visualized. Furthermore, the estimated number of 10,000 transcripts per cell may not accurately reflect the number of transcripts in the cells of the developing retina, which is a highly specialized tissue of the central nervous system requiring the cooperation of many genes. These possibilities may account for why *ALDH1*, and other differentially expressed transcripts, were not detected. Nonetheless, our search was successful, resulting in the identification of seven differentially expressed transcripts in the developing chick retina.

Out of the 17 DD-PCR clones sequenced, six produced novel sequences when compared to other references in the Genbank database while all others showed sequence similarity to various known sequences (Table 3-1). Because of the nature of DD-PCR, it was not surprising that BLAST searches with some DD-PCR clones yielded novel

sequences. DD-PCR is highly selective for the 3' ends of cDNAs because it uses a poly T anchor primer. The 3' untranslated regions of cDNAs are not highly conserved between species. The fact that our lab works with chicken made 3' untranslated sequence matches unlikely since many of the chicken genes have not yet been cloned and sequenced. Most often, it is only when comparing translated regions of genes that matches are found between chicken and other species. These reasons do not account for why we did not detect *ALDH1* in our analysis, as chicken *ALDH1* cDNA has been cloned almost in its entirety by our lab. As well, because we already knew the pattern of expression for *ALDH1* on a Northern blot of total, dorsal and ventral poly A+ RNA, it is unlikely that *ALDH1* was isolated since we did not see a similar pattern of expression on Northern blot analysis for any of the DD-PCR bands isolated.

Of those clones that showed high sequence identity to known sequences in Genbank, band 42 was the most interesting. This clone was 83% identical over 242 nucleotides to pig, mouse and human spermidine/spermine N^1-acetyltransferase (*SSAT*) cDNA. SSAT is the rate-limiting enzyme involved in the metabolism of the polyamines spermidine and spermine to putrescine. In this study, Northern blots showing the expression pattern of this clone revealed a ventrodorsal pattern of expression in the retina and low levels of expression in all fetal tissues examined, except for the retina.

The ventrodorsal pattern of expression detected by Northern analysis of total, dorsal and ventral poly A+ RNA was later shown by *in situ* hybridization to be a temporal-nasal gradient, with a minor preference towards the dorsal retina. The

explanation for the discrepancy between the Northern and *in situ* hybridization analyses can be addressed using both dissecting technique and the *in situ* hybridization results. Retinae were dissected through the center of the eye, along the dorsoventral plane, using a scalpel. There are no external markers, however, to indicate the demarcation between the dorsal and ventral eye and we had to estimate where to dissect. The results of the *in situ* hybridization analyses revealed that *SSAT* mRNA expression was very intense in the central retina (discussed below). It is highly possible that we unintentionally included the intense central region of *SSAT* mRNA expression in our collection of ventral retina. As a result, DD-PCR and Northern analysis using the poly A+ RNA extracted from dorsal and ventral retinae artificially indicated higher levels of *SSAT* mRNA in the ventral retina and suggested a ventrodorsal gradient of expression.

We found that *SSAT* mRNA expression was weak early in retinal development (E5/6, E7), started to increase at E9 and peaked at E12, then decreased slightly at E14 and increased again by E16. This pattern of expression (low levels in undifferentiated retina followed by an increase in RNA levels with differentiation) suggests that SSAT may be important in the maturation of the developing retina, since differentiation of the retina occurs from approximately E11 to hatching. A study by Grillo *et al.* (1984) showed a similar pattern for SSAT enzyme activity in the chick retina. They found that SSAT activity was low early in embryonic development, increased dramatically at E14 and then decreased gradually until hatching and remained low after hatching. Our results are somewhat different since we showed that transcript levels peaked at E12, contradicting the increase in enzyme activity detected by Grillo and colleagues (1984) at E14.

However, these results could be explained by a delay in protein production in relation to mRNA expression.

Grillo *et al.* (1983) demonstrated in an earlier paper that activity levels of the polyamine biosynthetic enzyme ornithine decarboxylase (ODC) were the highest at E7 in the chick embryonic retina and decreased rapidly, with very low activity detected between E12 and E14. This pattern of ODC activity is opposite to the pattern of SSAT activity and *SSAT* mRNA expression in the chick retina. Furthermore, it is interesting to note that levels of the polyamine putrescine, the end product of both ODC and SSAT, follow a pattern consistent with the production of both ODC and SSAT in the developing retina. Putrescine levels are very high at E6 through E8 but decrease sharply by E10 (although they remain relatively high) and continue to decrease slowly until E16, followed by a slow increase in levels until E19 (Taibi *et al.*, 1994). Levels of the polyamines spermidine and spermine follow a pattern similar to that of putrescine. This would suggest that SSAT activity, highest at E14, may contribute to putrescine synthesis via the metabolism of spermidine and spermine when ODC activity has diminished.

It has been suggested that putrescine present in the developing retina serves as a precursor for GABA synthesis (Hokoç *et al.*, 1990; Taibi *et al.*, 1994; Eliasson *et al.*, 1997; Yamasaki *et al.*, 1999). GABA is a major inhibitory neurotransmitter in the central nervous system, including the vertebrate retina, and there are two known pathways of GABA synthesis. The first pathway, regarded as the classical pathway, uses glutamic acid decarboxylase (GAD) as the rate-limiting enzyme for the synthesis of GABA from

L-glutamate. GAD is responsible for the majority of GABA synthesis in the mature central nervous system, including the retina. The second pathway is an alternative pathway which does not require GAD activity, and uses putrescine as the precursor for GABA synthesis. GAD levels are very low in the early stages of the developing chick retina (prior to E15, Gonzalez *et al.*, 1990), whereas GABA is detected as early as E6 (Hokoç *et al.*, 1990; Taibi *et al.*, 1994). Taibi *et al.* (1994) examined the levels of GABA throughout chick retinal development and interestingly, their results parallel the levels of *SSAT* mRNA expression detected in our study. They found that GABA levels are low at E6 and increase two-fold and four-fold by E8 and E10, respectively. This is followed by a slight decrease in levels at E12 and E14, after which GABA levels increase again until hatching. Therefore, the synthesis of putrescine by SSAT could account for the pattern of GABA expression detected during retinal development, at least in the early embryonic days prior to GAD expression at E15. A portion of the putrescine synthesized by ODC may also serve as a substrate for GABA synthesis (Eliasson *et al.*, 1997; Yamasaki *et al.*, 1999), although the expression patterns of GABA and SSAT are more closely related. It would be interesting to examine whether a direct correlation exists between GABA and SSAT at the protein level, using anti-GABA and anti-SSAT antibodies for immunofluorescence studies with retinal sections from different stages of development.

There is little information in the literature regarding *SSAT* mRNA expression in the vertebrate central nervous system. The distribution of *SSAT* mRNA in the rat brain has been previously examined by *in situ* hybridization (Zoli *et al.*, 1996). *SSAT* mRNA was detected in both neuronal and non-neuronal (glial) cells of the brain, but the degree

of labelling varied between the different regions examined, with some regions showing higher levels of *SSAT* mRNA expression than others. Labelling also varied within the brain regions expressing *SSAT* mRNA. For example, *SSAT* mRNA expression was not uniform throughout a group of neuronal cells, such that some neurons were more intensely labelled than neighboring neurons, and similarly for non-neuronal cells. Such heterogeneous expression for *SSAT* mRNA corresponds to our observations with *in situ* hybridization of chick retinal sections which also included the chick brain. Highly specific regions of intense *SSAT* mRNA labelling were detected in our sections, especially in the cerebral vesicles, and the degree of labelling within these regions varied between cells (results not shown). In future experiments, we would like to examine in detail *SSAT* mRNA expression in the brain, with the assistance of Dr. Sara Zalik at the University of Alberta for the identification of brain structures.

Our study is the first that we know of reporting the cloning of the chick *SSAT* cDNA and analysis of *SSAT* mRNA expression in the chick retina by *in situ* hybridization. *In situ* hybridization of *SSAT* mRNA in the chick retina at E7 and E11 showed staining predominately in the Müller glial cells. However, even in regions of the retina where staining was most intense, not all Müller cells appeared to express *SSAT* mRNA. This finding is in agreement with Zoli *et al.* (1996) who reported variable *SSAT* mRNA expression in the cells found within a positive region of staining. It would be interesting to further analyze the expression pattern of SSAT protein in Müller glial cells using confocal microscopy with anti-SSAT antibody. Co-localization studies with CA-II,

a known marker for Müller glial cells, would provide an accurate assessment of SSAT expression, and help determine the proportion of Müller glial cells expressing SSAT.

As previously mentioned, the goal of this project was to identify differentially expressed transcripts in the chick retina which could possibly be involved in targeting retinal ganglion axons to the optic tectum. Using *in situ* hybridization, we found that *SSAT* mRNA was expressed in a temporal-nasal (posterior-anterior) gradient in the E7 chick retina. Gradients of this type have been implicated in retinotectal mapping and include the Eph-related receptors and the ephrins, as well as TOP_{AP} molecules. Therefore, it is possible that a gradient of SSAT expression may also be involved in establishing the connections between the retina and the optic tectum. Since *SSAT* mRNA is expressed in Müller glial cells and not in ganglion cells (our results), it is possible that SSAT is involved in the creation of a secondary gradient which would serve to guide ganglion axons through the retina to the optic nerve. Müller glial cells are known to be of structural importance in the retina by providing an orientation scaffold which can serve as a guide for migrating neurons (reviewed in Willbold and Layer, 1998). Therefore, SSAT may be involved in this guidance role of Müller glial cells. Furthermore, retinal ganglion axons are the first neurons to differentiate in the retina and they begin to contact the optic tectum as early as E6 (Thanos and Bonhoeffer, 1987). The temporal-nasal gradient of *SSAT* mRNA expression was predominant at E7. It is possible that the gradient of *SSAT* expression at E7 is important for the establishment of initial contacts between retinal ganglion cells and the optic tectum. Further studies will involve *in situ* hybridization of serial sections taken along the nasotemporal plane of chick retinae at later stages of

development, including E11 and E16. If we find that the gradient of *SSAT* mRNA expression is retained at later developmental stages, this will suggest a role for SSAT in the establishment of initial contacts, as well as the maintenance of correct contacts at later stages. It is difficult to say exactly how SSAT would perform such a guiding function for retinal ganglion axons, but it would likely be through its regulation of polyamine levels and the subsequent effects on a variety of cellular processes involving polyamines, including cell growth and differentiation (reviewed in Heby and Persson, 1990; Seiler, 1990 and Casero and Pegg, 1993).

A gradient of SSAT expression may also serve to alter neuronal activity in the developing retina. Spontaneous neuronal activity occurs in the developing retina before the onset of vision and is important for the refinement of retinotopic maps (Nakamura and O'Leary, 1989; Catsicas *et al.*, 1998; Wong *et al.*, 1998; Ichijo, 1999). Neurotransmission has been shown to affect the bursting activity of ganglion cells in the developing chick retina and has been detected as early as E7 (Catsicas *et al.*, 1998; Wong *et al.*, 1998). Interestingly, it has been suggested that target cells in the brain may be able to distinguish between intraretinal differences in bursting activity caused by waves of activity which propagate across the retina at varying speeds (Wong *et al.*, 1998). It has been demonstrated that GABAergic neurotransmission is involved in modulating bursting activity by suppressing it (Wong *et al.*, 1998). Therefore, it is possible that SSAT through its production of putrescine, a precursor of GABA (discussed above), may be indirectly involved in regulating the spontaneous neuronal activity detected in the embryonic chick retina. Putrescine is easily excreted from cells (Sakata *et al.*, 2000) and

could be transported from the Müller glial cells to the amacrine and horizontal cells for GABA synthesis (Brandon, 1985). Specifically, the gradient of *SSAT* mRNA expression at E7 (our results) may serve to vary the bursting patterns and help the target cells in the optic tectum to distinguish between the temporal and nasal retina. SSAT expression at E11 and later stages of development, whether uniform or in a gradient, may also be involved in the modulation of neuronal activity via GABA synthesis, at least until GAD levels increase (E15) and account for the majority of GABA synthesis.

The above describes a role for SSAT in the synthesis of GABA subsequent to the production of putrescine. It is unlikely that SSAT would play such a role at later stages of development and post-hatching because of the presence of GAD. So what could be the role of SSAT in Müller glial cells later in development and in the mature chick retina? First, *in situ* hybridization and confocal microscopy experiments would have to be done using late stage embryonic and adult retinal sections to show that SSAT continues to be expressed in the Müller glia. Assuming that SSAT continues to be expressed in the Müller glial cells, it may be involved in regulating K^+ ion uptake from the extracellular space in the mature chick retina. Intracellular polyamines have been shown to regulate the uptake of K^+ ions via their interaction with K_{ir} channels, a marker for differentiated Müller glial cells, in a process termed K^+ siphoning (Chapter 1) (Frishmann *et al.*, 1992; Johnson, 1996; Nichols and Lopatin, 1997; Williams, 1997a and b). This is a fundamental homeostatic process of the mature Müller glial cell and without it, neurotransmission could be adversely affected by a build-up of K^+ ions in the extracellular space (Reichenbach *et al.*, 1993; Newman and Reichenback, 1996). SSAT,

through its regulation of polyamine levels, could have an important role in regulating K^+ siphoning in the mature retina.

Our results, which show *SSAT* mRNA expressed in a temporal-nasal gradient in the embryonic chick retina, suggest an important role for SSAT in development. Exactly how SSAT is involved in the developmental process is unknown and we can only speculate on its role. More studies will be performed in the future to further characterize the expression of *SSAT* mRNA and protein in the developing chick retina, including later stages of development. Functional analyses will also be carried out in order to define a role for SSAT in the developing retina.

CHAPTER 5. FUTURE OBJECTIVES

Objective 1. To Further Characterize the Remaining Differentially Expressed DD-PCR clones

We identified seven differentially expressed clones using DD-PCR analysis to compare mRNA populations of dorsal and ventral E7 chick retina. Band 42, the *SSAT* cDNA clone, was chosen for further analysis. However, we still need to examine the remaining six cDNA clones: B2, B7, B9, B21, B24 and B36. To do this, library screening will be used to isolate the full-length cDNAs. Band 7 has already been used to screen an E7 chick retina cDNA library but the full-length clone has not yet been isolated. None of the other differentially expressed clones have been used to screen libraries. Searches of the Genbank database, using sequences generated from B2, B7, B9, B21, B24 and B36, yielded high sequence similarities to *Xenopus Nopp180* and human, mouse and pig *Fau* cDNAs for B7 and B21, respectively. Novel sequences were revealed for B2, B9, B24 and B36. Library screening will generate larger cDNA clones for each of these bands, which may then reveal sequence similarities to known sequences. *In situ* hybridization, using probes generated from B2, B7, B9, B21, B24 and B36, will also be performed to confirm asymmetrical expression in the retina.

As mentioned in Chapter 3, the differential expression patterns of ten clones (B1, B5, B10, B13, B14, B26, B29, B31, B33 and B41) could not be ascertained because they did not produce a detectable signal when analyzed by Northern blotting. We would like to determine the expression patterns for these clones by using Northern blots with more poly A+ RNA loaded per lane or by using quantitative RT-PCR.

Objective 2. To Further Characterize SSAT Expression in the Developing CNS

Future studies in our lab will focus on expanding our knowledge and understanding of SSAT in the central nervous system. In particular, our lab will examine SSAT expression, at both the protein and mRNA level, in the brain and retina of the developing chick. We have already found *SSAT* mRNA to be expressed in a temporal-nasal gradient in the E7 chick retina. This gradient was detected using sections taken along the dorsoventral plane. Next, we would like to section chick retinae from E7 and later developmental stages along the nasotemporal plane for *in situ* hybridization analyses. This would allow for a better understanding of the pattern of *SSAT* expression throughout development. We would also like to use these sections to perform immunohistochemical studies using anti-SSAT antibody. This would reveal whether the pattern of protein expression follows that of the mRNA.

As mentioned in Chapter 4, SSAT, through its production of putrescine, may be indirectly involved in the synthesis of the inhibitory neurotransmitter GABA. Therefore, it is possible that the pattern of GABA expression may be similar to the gradient of *SSAT* mRNA expression detected by *in situ* hybridization. Immunohistochemical studies using anti-GABA and anti-SSAT antibodies at different stages of development would determine whether or not they share a similar pattern of expression. If a similar expression pattern exists, this would link SSAT activity to GABA synthesis, helping to further define a role for SSAT in the embryonic retina. Also, it would be interesting to use anti-GAD antibody for immunohistochemical studies in order to determine whether

its expression at later stages of development coincides with a change in the expression pattern of GABA compared to SSAT.

Others have described how complementary gradients function to guide retinal ganglion axons to their target areas in the optic tectum. We would like to determine whether the temporal-nasal gradient of *SSAT* mRNA expression detected at E7 is somehow involved in guiding retinal ganglion axons. To do this, we would like to perform *in situ* hybridization on chick optic tectum at E7, and at later stages of development, to determine whether *SSAT* mRNA is expressed in a complementary gradient in the optic tectum. The existence of such a gradient would support a role for SSAT in the formation of the retinotectal map. Immunohistochemical studies of sections through chick optic tectum using anti-SSAT antibody will also be performed.

Also, we would like to measure the protein levels of SSAT, as well as the levels of spermine, spermidine and putrescine in the chick retina in both nasal and temporal halves, at different stages of development. As well, other enzymes involved in polyamine biosynthesis/catabolism (ie. ODC) will also be assayed to determine whether they are asymmetrically expressed in the retina. It would also be interesting to misexpress SSAT in the nasal chick retina at E7, using retroviral infection, in order to determine the consequences of SSAT over-expression on retinal development and retinal patterning.

CHAPTER 6. BIBLIOGRAPHY

Aiello, L. P., Robinson, G. S., Lin, Y-W., Nishio, Y. and King, G. L. (1994) Identification of multiple genes in bovine retinal pericytes altered by exposure to elevated levels of glucose by using mRNA differential display. Proc. Natl. Acad. Sci. USA 91: 6231-6235.

Altshuler, D., Turner, D. and Cepko, C. (1991) *Development of the Visual System*, Proceedings of the Retina Research Foundation Symposia (Massachusetts Inst. Technology, Cambridge, MA), 37-58.

Altshuler, D., LoTurco, J. J., Rush, J. and Cepko, C. L. (1993) Taurine promotes the differentiation of a vertebrate retinal cell type in vitro. Development 119: 1317-1328.

Amédée, T., Robert, A. and Coles, J. A. (1997) Potassium homeostasis and glial energy metabolism. Glia 21: 46-55.

Anderson, R. B., Walz, A., Holt, C. E. and Key, B. (1998) Chondroitin sulfates modulate axon guidance in embryonic *Xenopus* brain. Dev Biol 202: 235-243.

Antony, T., Thomas, T., Shirahata, A. and Thomas, T. J. (1999) Selectivity of polyamines on the stability of RNA-DNA hybrids containing phosphodiester and phosphorothioate oligodeoxyribonucleotides. Biochemistry 38: 10775-10784.

Ashcroft, F. M. Ion Channels and Disease: Channelopathies. Academic Press. San Diego, California. (2000).

Ausubel, F. M. Current Protocols in Molecular Biology. John Wiley and Sons, Inc. USA. pp. 15.7.1, Supplement 32, 1995.

Barbieri, A. M., Lupo, G., Bulfone, A., Andreazzoli, M., Mariani, M., Fougerousse, F., Consalez, G. G., Borsani, G., Beckmann, J. S., Barsacchi, G., Ballabio, A. and Banfi, S. (1999) A homeobox gene, vax2, controls the patterning of the eye dorsoventral axis. Proc Natl Acad Sci USA 96: 10729-10734.

Bauer, D., Müller, H., Reich, J., Riedel, H., Ahrenkeil, V., Warthoe, P. and Strauss, M. (1993) Identification of differentially display expressed mRNA species by an improved display technique (DDRT-PCR) Nucleic Acids Res. 21: 4272-4280.

Belecky-Adams, T., Tomarev, S., Li, H.-S., Ploder, L., McInnes, R. R., Sundin, O. and Adler, R. (1997) Pax-6, Prox 1, and Chx10 homeobox gene expression correlates with phenotypic fate of retinal precursor cells. Invest Ophthalmol Vis Sci 38: 1293-1303.

Bellairs, R. and Osmond, M. The Atlas of Chick Development. Academic Press. San Diego, California. (1998).

Bertoli, D. J., Schlichter, U. H. A., Adams, M. J., Burrows, P. R., Steinbiß, H. –H. and Antoniw, J. F. (1995) An analysis of differential display shows a strong bias towards high copy number mRNAs. Nucleic Acids Res 23: 4520-4523.

Bettuzzi, S., Davalli, P., Astancolle, S., Pinna, C., Roncaglia, R., Boraldi, F., Tiozzo, R., Sharrard, M. and Corti, A. (1999) Coordinate changes of polyamine metabolism regulatory proteins during the cell cycle of normal human dermal fibroblasts. FEBS Letters 446: 18-22.

Biedermann, B., Skatchkov, S. N., Brunk, I., Bringmann, A., Pannicke, T., Bernstein, H-G., Faude, F., Germer, A., Veh, R. and Reichenback, A. (1998) Spermine/spermidine is expressed by retinal glial (Müller) cells and controls distinct K^+ channels of their membrane. Glia 23: 209-220.

Bovolenta, P., Mallamaci, A., Briata, P., Corte, G. and Boncinelli, E. (1997) Implication of OTX2 in pigment epithelium determination and neural retina differentiation. J Neurosci 17: 4243-4252.

Brandon, C. (1985) Retinal GABA neurons: localization in vertebrate species using an antiserum to rabbit brain glutamate decarboxylase. Brain Res 344: 286-295.

Brittis, P.A., Canning, D.R. and Silver, J. (1992) Chondroitin sulfate as a regulator of neuronal patterning in the retina. Science 255: 733-736.

Cai, J., Howells, R. D. and Wagner, B. J. (1999) Identification of a novel gene product preferentially expressed in rat lens epithelial cells. Mol Vis 5: 3-6.

Calderon, F., Pichardo, I., Lopez, E. and Lopez-Colome, A. M. (1999) [^{3}H] Spermine binding to synaptosomal membranes from the chick retina. Brain Res 844: 150-156.

Callard, D., Lescure, B. and Mazzolini, L. (1994) A method for the elimination of false positives generated by the mRNA differential display technique. BioTechniques 16: 1096-1103.

Carter, D., Goepel, J. R., Winship, P. R. and Goyns, M. H. (1999) Identification of different gene expression patterns in low and high grade non-Hodgkin's lymphomas by differential display. Leuk Lymphoma 33: 343-350.

Casero, R. A. and Pegg, A. E. (1993) Spermidine/spermine N^1-acetyltransferase – the turning point in polyamine metabolism. FASEB Journal 7:653-661.

Casero, R. A. Jr., Gabrielson, E. W. and Pegg, A. E. (1994) Immunohistochemical staining of human spermidine/spermine N^1-acetyltransferase superinduced in response to treatment with antitumor polyamine analogues. Cancer Res 54: 3955-3958.

Catsicas, M., Bonness, B., Becker, D. and Mobbs, P. (1998) Spontaneous Ca^{2+} transients and their transmission in the developing chick retina. Current Biology 8: 283-286.

Cepko, C. L., Austin, C. P., Yang, X., Alexiades, M. and Ezzeddine, D. (1996) Cell fate determination in the developing retina. Proc Natl Acad Sci USA 93: 589-595.

Cheng, H-J., Nakamoto, M., Bergemann, A. D. and Flanagan, J. G. (1995) Complementary gradients in expression and binding of ELF-1 and Mek4 in development of the topographic retinotectal projection map. Cell 82: 371-381.

Chung, K. Y., Shum, D. K. and Chan S. O. (2000) Expression of chondroitin sulfate proteoglycans in the chiasm of mouse embryos. J Comp Neurol 417: 152-163.

Clark, J. M. (1988) Novel non-templated nucleotide addition reactions catalyzed by procaryotic and eucaryotic DNA polymerases. Nucleic Acids Res 16: 9677-9686.

Cullis, P. M., Green, R. E., Merson-Davies, L. and Travis, N. (1999) Probing the mechanism of transport and compartmentalization of polyamines in mammalian cells. Chem Biol 6: 717-729.

Davis, J. A. and Reed, R. R. (1996) Role of Olf-1 and Pax-6 transcription factors in neurodevelopment. J Neurosci 16: 5082-5094.

Denovan-Wright, E. M., Howlett, S. E. and Robertson, H. A. (1999) Direct cloning of differential display products eluted from Northern blots. BioTechniques 26: 1046-1050.

Dowling, J. E. The Retina: An Approachable Part of the Brain. The Belknap Press of Harvard University Press. Cambridge, Massachusetts and London, England. (1987).

Dräger, U.C., Wagner, E. and McCaffery, P. (1998) Aldehyde dehydrogenase in the generation of retinoic acid in the developing vertebrate: A central role of the eye. J Nutr 128: 463S-466S.

Drescher, U., Kremoser, C., Handwerker, C., Loschinger, J., Noda, M. and Bonhoeffer, F. (1995) In vitro guidance of retinal ganglion cell axons by RAGS, a 25 kDa tectal protein related to ligands for Eph receptor tyrosine kinases. Cell 82: 359-370.

Drescher, U., Bonhoeffer, F. and Muller, B. K. (1997) The Eph family in retinal axon guidance. Curr Opin Neurobiol 7: 75-80.

Durston, A. J., Timmermans, J. P. M., Hage, W. J., Hendriks, H. F. J., de Vries, N. J., Heideveld, M. and Nieuwkoop, P. D. (1989) Retinoic acid causes an anteroposterior transformation in the developing central nervous system. Nature 340: 140-144.

Edlund, T. and Jessell, T. M. (1999) Progression from extrinsic to intrinsic signaling in cell fate specification: A view from the nervous system. Cell 96: 211-224.

Eliasson, M. J. L., McCaffery, P., Baughman, R. W. and Dräger, U. C. (1997) A ventrodorsal GABA gradient in the embryonic retina prior to expression of glutamate decarboxylase. Neuroscience 79: 863-869.

Erskine, L. and McCaig, C. D. (1997) Integrated interactions between chondroitin sulphate proteoglycans and weak dc electric fields regulate nerve growth cone guidance in vitro. J Cell Sci 110: 1957-1965.

Fekete, D. M., Perez-Miguelsanz, J., Ryder, E. and Cepko, C. L. (1994) Clonal analysis in the chicken retina reveals tangential dispersion of clonally related cells. Dev Biol 166: 666-682.

Ficker, E., Taglialatela, M., Wible, B. A., Henley, C. M. and Brown, A. M. (1994) Spermine and spermidine as gating molecules for inward rectifier K^+ channels. Science 266: 1068-1072.

Fogel-Petrovic, M., Vujcic, S., Brown, P. J., Haddox, M.K. and Porter, C. W. (1996) Effects of polyamines, polyamine analogs, and inhibitors of protein synthesis on spermidine-spermine N^1-acetyltransferase gene expression. Biochemistry 35: 14436-14444.

Fogel-Petrovic, M., Kramer, D. L., Vujcic, S., Miller, J., Mcmanis, J. S., Bergeron, R. J. and Porter, C. W. (1997) Structural basis for differential induction of spermidine/spermine N^1-acetyltransferase activity by novel spermine analogs. Mol Pharmacol 52: 69-74.

Gauer, F., Kedzierski, W. and Craft, C. M. (1995) Identification of circadian gene expression in the rat pineal gland and retina by mRNA differential display. Neurosci Lett 187: 69-73.

Godbout, R. and Andison, R. (1996) Elevated levels of cyclin D1 mRNA in the undifferentiated chick retina. Gene 182: 111-115.

Godbout, R., Packer, M., Poppema, S. and Dabbagh, L. (1996) Localization of cytosolic aldehyde dehydrogenase in the developing chick retina: *in situ* hybridization and immunohistochemical analyses. Dev Dyn 205: 319-31.

Gonzalez, N. N., Alfie, J. and de Plazas, S. F. (1990) Glutamic acid decarboxylase in different areas of the developing chick central nervous system. Neurochemical Research 9: 917-921.

Goodhill, G. J. (1998) Mathematical guidance for axons. Trends Neurosci 21: 226-231.

Goodman, C. S. and Shatz, C. J. (1993) Developmental mechanisms that generate precise patterns of neuronal connectivity. Cell 72/Neuron 10 (Suppl.): 77-98.

Green, C. B. and Besharse, J. C. (1996) Use of a high stringency differential display screen for identification of retinal mRNAs that are regulated by a circadian clock. Brain Res Mol Brain Res 37: 157-165.

Grillo, M. A., Fossa, T. and Dianzani, U. (1983) Arginase, ornithine decarboxylase and S-adenosylmethionine decarboxylase in the chicken brain and retina. Int. J. Biochem. 15: 1081-1084.

Grillo, M. A., Dianzani, U. and Pezzali, D. C. (1984) Acetylation of polyamines in chicken brain and retina. Int. J. Biochem. 16: 1349-1352.

Guimaraes, M. J., Lee, F., Zlotnik, A. and McClanahan, T. (1995) Differential display by PCR: novel findings and applications. Nucleic Acids Res 23: 1832-1833.

Gupta, R., Thomas, P., Beddington, R. S. P. and Rigby, P. W. J. (1998) Isolation of developmentally regulated genes by differential display screening of cDNA libraries. 26: 4538-4539.

Ha, H. C., Woster, P. M., Yater, J. D. and Casero, R. A. (1997) The role of polyamine catabolism in polyamine analogue-induced programmed cell death. Proc Natl Acad Sci 94: 11557-11562.

Hamburger, V. and Hamilton, H. L. (1951) A series of normal stages in the development of the chick embryo. J. Morphol 88: 49-92.

Heby, O. and Persson, L. (1990) Molecular genetics of polyamine synthesis in eukaryotic cells. Trends Biochem Sci 15: 153-158.

Henikoff, S. (1987) Unidirectional digestion with exonuclease III in DNA sequence analysis. Methods Enzymol.155:156-65.

Henrique, D., Adam, J., Myat, A., Chitnis, A., Lewis, J., and Ish-Horowicz, D. (1995) Expression of a Delta homologue in prospective neurons in the chick. Nature 375: 787-790.

Hokoç J. N., Ventura, A. L. M., Gardino, P. F., and De Mello, F. G. (1990) Developmental immunoreactivity for GABA and GAD in the avian retina: possible alternative pathway for GABA synthesis. Brain Research 532: 197-202.

Holm, I., Persson, L., Stjernborg, L., Thorsson, L. and Heby, O. (1989) Feedback control of ornithine decarboxylase expression by polyamines. Biochem J 258: 343-350.

Holt, C.E., Bertsch, T.W., Ellis, H.M. and Harris, W.A. (1988) Cellular determination in the *Xenopus* retina is independent of lineage and birth date. Neuron 1:15-16.

Hong, Y. M., von Kannen, S. and Thanos, S. (1998) Asymmetric mRNA expression in the retina neuroepithelium of chick embryo assessed by differential display polymerase chain reaction. Neuroreport 9: 2405-2408.

Ikonomov, O. C. and Jacob, M. H. (1996) Differential display protocol with selected primers that preferentially isolates mRNAs of moderate to low abundance in a microscopic system. BioTechniques 20: 1030-1042.

Hyatt, G. A., Schmitt, E. A., Marsh-Armstrong, N., McCaffery, P., Dräger, U. C. and Dowling, J. E. (1996) Retinoic acid establishes ventral retinal characteristics. Development 122: 195-204.

Ichijo, H. (1999) Differentiation of the chick retinotectal topographic map by remodeling in specificity and refinement in accuracy. Developmental Brain Res 117: 199-211.

Jean, D., Ewan, K. and Gruss, P. (1998) Molecular regulators involved in vertebrate eye development. Mech Dev 76: 3-18.

Jo, J., Zhang, J., Zhang, R. and Liang, P. (1998) Cloning oncogenic Ras-regulated genes by differential display. Methods 16: 365-372.

Johnson, D. T. (1996) Modulation of channel function by polyamines. Trends Pharmacol Sci 17: 22-27.

Kociok, N., Unfried, K., Esser, P., Krott, R., Schraermeyer, U. and Heimann, K. (1998) The nonradioisotopic representation of differentially expressed mRNA by a combination of RNA fingerprinting and differential display. Mol Biotechnol 9: 25-33.

Koshiba-Takeuchi, K., Takeuchi, J. K., Matsumoto, K., Momose, T., Uno, K., Hoepker, V., Ogura, K., Takahashi, N., Nakamura, H., Yasuda, K. and Ogura, T. (2000) Tbx5 and the retinotectum projection. Science 287: 134-137.

Kost, T. A., Theodorakis, N. and Hughes, S. H. (1983) The nucleotide sequences of the chick cytoplamsic β-actin gene. Nucleic Acids Res 11: 8287-8301.

Ledakis, P., Tanimura, H. and Fojo, T. (1998) Limitations of differential display. Biochem Biophys Res Commun 251: 653-656.

Ledig, M. M., McKinnell, I. W., Mrsic-Flogel, T., Wang, J., Alvares, C., Mason, I., Bixby, J. L., Mueller, B. K. and Stoker, A.W. (1999) Expression of receptor tyrosine phosphatases during development of the retinotectal projection of the chick. J Neurobiol. 39: 81-96.

Leimeister, C., Bach, A., Woolf, A. S. and Gessler, M. (1999) Screen for genes regulated during early kidney morphogenesis. Dev Genet 24: 273-283.

Liang, P. and Pardee, A. B. (1992) Differential display of eukaryotic messenger RNA by means of the polymerase chain reaction. Science 257: 967-971.

Liang, P., Averboukh, L. and Pardee, A. B. (1993) Distribution and cloning of eukaryotic mRNAs by means of differential display: refinements and optimization. Nucleic Acids Res 21: 3269-3275.

Liang, P., Zhu, W., Zhang, X., Guo, Z., O'Connell, R. P., Averboukh, L., Wang, F. and Pardee, A. B. (1994) Differential display using one-base anchored oligo-dT primers. Nucleic Acids Res 22: 5763-5764.

Linskens, M. H. K., Feng, J., Andrews, W. H., Enlow, B. E., Saati, S. M., Tonkin, L. A., Funk, W. D. and Villeponteau, B. (1995) Cataloging altered gene expression in young and senescent cells using enhanced differential display. Nucleic Acids Res 23: 3244-3251.

Liu, I. S. C., Chen, J.-de., Ploder, L., Vidgen, D., van der Kooy, D., Kalnins, V. I. and McInnes, R. R. (1994) Developmental expression of a novel murine homeobox gene (*Chx10*): Evidence for roles in determination of the neuroretina and inner nuclear layer. Neuron 13: 377-393.

Lopatin, A. N., Makhina, E. N. and Nichols, C. G. (1994) Potassium channel block by cytoplasmic polyamines as the mechanism of intrinsic rectification. Nature 372: 366-369.

Makita, N. and Yoshikawa, K. (1999) ATP/ADP switches the higher-order structure of DNA in the presence of spermidine. FEBS Letters. 460: 333-337.

Malhotra, K., Foltz, L., Mahoney, W. C. and Schueler, P. A. (1998) Interaction and effect of annealing temperature on primers used in differential display RT-PCR. Nucleic Acids Res 26: 854-856.

Mann, I. The Development of the Human Eye. Third Edition. New York, Grune & Stratton. (1964).

Marsh-Armstrong, N., McCaffery, P., Gilbert, W., Dowling, J. E. and Dräger, U. C. (1994) Retinoic acid is necessary for development of the ventral retina in zebrafish. Proc Natl Acad Sci USA 91: 7286-7290.

Martin, K. J., Kwan, C. –P., O'Hare, M. J., Pardee, A. B. and Sager, R. (1998) Identification and verification of differential display cDNAs using gene-specific primers and hybridization arrays. BioTechniques 24: 1018-1026.

McCaffery, P., Tempst, P., Gustavo, L. and Dräger, U. C. (1991) Aldehyde dehydrogenase is a positional marker in the retina. Development 112: 693-702.

McCaffery, P., L, M-O., Wagner, M.A., Sladek, N.E. and Dräger, U.C. (1992) Asymmetrical retinoic acid synthesis in the dorsoventral axis of the retina. Development 115: 371-382.

McCaffery, P., Posch, K. C., Napoli, J.L., Gudas, L. and Dräger, U.C. (1993) Changing patterns of the retinoic acid system in the developing retina. Dev Biol 158: 390-399.

McClelland, M., Mathieu-Daude, F. and Welsh, J. (1995) RNA fingerprinting and differential display using arbitrarily primed PCR. Trends Genet 11: 242-246.

Meister, M., Wong, R. O. L., Baylor, D. A. and Shatz, C. J. (1991) Synchronous bursts of action potentials in ganglion cells of the developing mammalian retina. Science 252: 939-943.

Meyer, R. L. (1998) Roger Sperry and his chemoaffinity hypothesis. Neuropsychologia 36(10): 957-980.

Miele, G., MacRae, L., McBride, D., Manson, J. and Clinton, J. (1998) Elimination of false positives generated through PCR re-amplification of differential display cDNA. BioTechniques 25:138-144.

Mierendorf, R. C. and Pfeffer, D. (1987) Direct sequencing of denatured plasmid DNA. Methods Enzymol 152: 556-562.

Miller, H. (1987) Practical aspects of preparing phage and plasmid DNA: Growth, maintenance, and storage of bacteria and bacteriophage. Methods Enzymol 152: 158-162.

Monschau, B., Kremoser, C., Ohta, K., Tanaka, H., Kaneko, T., Yamada, T., Handwerker, C., Hornberger, M. R., Loschinger, J., Pasquale, E. B., Siever, D. A., Verderame, M. F., Muller, B. K., Bonhoeffer, F. and Drescher, U. (1997) Shared and distinct functions of RAGS and ELF-1 in guiding retinal axons. EMBO 16: 1258-1267.

Morgan, D. M. L. (1999) Polyamines. An overview. Mol Biotechnol 11: 229-250.

Mou, L., Miller, H., Li, J., Wang, E. and Chalifour, L. (1994) Improvements to the differential display method for gene analysis. Biochem Biophys Res Commun 199(2): 564-569.

Mueller, B. K. (1999) Growth cone guidance: First steps towards a deeper understanding. Annu Rev Neurosci 22: 351-388.

Murakami, Y., Matsufuji, S., Miyazaki, Y. and Shin-ichi, H. (1994) Forced expression of antizyme abolishes ornithine decarboxylase activity, suppresses cellular levels of polyamines and inhibits cell growth. Biochem J 304: 183-187.

Nakamura, H. and O'Leary, D. D. M. (1989) Inaccuracies in initial growth and arborization of chick retinotectal axons followed by course corrections and axon remodeling to develop topographic order. J Neurosci 9: 3776-3795.

Newman, E. A., Framback, D. A. and Odette, L. L. (1984) Control of extracellular potassium levels by retinal glial cell K^+ siphoning. Science 225: 1174-1175.

Newman, E. A. (1986) Regulation of potassium levels by Müller cells in the vertebrate retina. Can J Physiol Pharmacol 65: 1028-1034.

Newman, E. A. (1993) Inward-rectifying potassium channels in retinal glial (Müller) cells. J Neurosci 13: 3333-3345.

Newman, E. A. and Reichenback, A. (1996) The Müller cell: a functional element of the retina. Trends Neurosci 19: 307-312.

Nichols, C. G. and Lopatin, A. N. (1997) Inward rectifier potassium channels. Annu Rev Physiol 59: 171-191.

Nolte, J. The Human Brain. An Introduction to its Functional Anatomy. Second Edition. The C.V. Mosby Company, St. Louis (1988).

Nonradioactive *in situ* hybridization application manual. Second Edition. (1996) Boehringer Mannheim GmbH, Biochemica.

Ogden, T. E. Retina. Basic Science and Inherited Retinal Diseases. The C.V. Mosby Company, St. Louis (1987).

O'Leary, D. D. M., Yates, P. A and McLaughlin, T. (1999) Molecular development of sensory maps: Representing sights and smells in the brain. Cell 96: 255-269.

Pasquale, E. B. (1997) The Eph family of receptors. Curr Opin Cell Biol 9: 608-615.

Pegg, A. E. (1988) Polyamine metabolism and its importance in neoplastic growth and a target for chemotheraphy. Cancer Res 48: 759-774.

Poirier, G. M.-C. and Erlander, M. G. (1998) Postdifferential display: Parallel processing of candidates using small amounts of RNA. Methods 16: 444-452.

Prada, C., Puga, J., Mendez-P., L., Lopez, R. and Ramirez, G. (1991) Spatial and temporal patterns of neurogenesis in the chick retina. Eur J Neurosci 3: 559-569.

Reichenback, A., Stolzenburg, J.-U., Eberhardt, W., Chao, T. I., Dettmer, D. and Hertz, L. (1993) What do retinal Müller (glial) cells do for their neuronal 'small siblings'? J Chem Neuroanat 6: 201-213.

Rock, D. M. and Macdonald, R. L. (1995) Polyamine regulation of N-methyl-D-aspartate receptor channels. Annu Rev Pharmacol Toxicol 35: 463-482.

Rohde, M., Hummel, R., Pallisgaard, N., Podstufka, T., Riedel, H., Leffers, H. and Strauss, M. (1997) Identification and cloning of differentially expressed genes by DDRT-PCR. Methods Mol Biol 67: 419-430.

Ruiz I Altaba, A. and Jessell, T. (1991) Retinoic acid modifies mesodermal patterning in the early *Xenopus* embryo. Genes Dev 5: 175-187.

Sakata, K., Kashiwagi, K. and Igarashi, K. (2000) Properties of a polyamine transporter regulated by antizyme. Biochem J 347: 297-303.

Sambrook, J., Fritsch, E. F., Maniatis, T. Molecular cloning. A laboratory manual. Second edition. Cold Spring Harbor Laboratory Press, New York (1989).

Sanger, F., Nicklen, S., Coulson, A. R. (1977) DNA sequencing with chain-terminating inhibitors. Proc Natl Acad Sci USA 74: 5463-5467.

Satriano, J., Ishizuka, S., Archer, D. C., Blantz, R. C. and Kelly, C. J. (1999) Regulation of intracellular polyamine biosynthesis and transport by NO and cytokines TNF-α and IFN-γ. Am J Physiol 276: C892-C899.

Savitt, J. M., Trisler, D. and Hilt, D. C. (1995) Molecular cloning of TOP_{AP}: A topographically graded protein in the developing chick visual system. Neuron 14: 253-261.

Schulte, D., Furukawa, T., Peters, M. A., Kozak, C. A. and Cepko, C. L. (1999) Misexpression of the Emx-related homeobox genes *cVax* and *mVax2* ventralizes the retina and perturbs the retinotectal map. Neuron 24: 541-553.

Seiler, N. (1990) Polyamine metabolism. Digestion 46(Suppl.2): 319-330.

Seiler, N., Atanassov, C. L. and Raul, F. (1998) Polyamine metabolism as target for cancer chemoprevention (Review). Int J of Oncol 13: 993-1006.

Skatchkov, S. N., Vyklicky, L. and Orkan, R. K. (1995) Potassium currents in the endfeet of isolated Müller cells from the frog retina. Glia 15: 54-64.

Smith, N. R., Li, A., Aldersley, M., High, A. S., Markham, A. F. and Robinson, P. A. (1997) Rapid determination of the complexity of cDNA bands extracted from DDRT-PCR polyacrylamide gels. Nucleic Acids Res 25: 3552-3554.

Snow, D. M., Lemmon, V., Carrino, D. A., Caplan, A. I. and Silver, J. (1990) Sulfated proteoglycans in astroglial barriers inhibit neurite outgrowth in vitro. Exp Neurol 109: 111-130.

Snow, D. M., Watanabe, M., Letourneau, P. C. and Silver, J. (1991) A chondroitin sulfate proteoglycan may influence the direction of retinal ganglion cell outgrowth. Development 113: 1473-1485.

Solessio, E., Linn, D. M., Perlman, I. and Lasater, E. M. (2000) Characterization with barium of potassium currents in turtle retinal Müller cells. J Neurophysiol 83: 418-430.

Sompayrac, L, Jane, S., Burn, T. C., Tenen, D. G. and Dann, K. J. (1995) Overcoming limitations of the mRNA differential display technique. Nucleic Acids Res 23: 4738-4739.

Spencer, W. E. and Christensen, M. J. (1999) Multiplex relative RT-PCR method for verification of differential gene expression. BioTechniques 27: 1044-1052.

Sperry, R. W. (1963) Chemoaffinity in the orderly growth of nerve fiber patterns and connections. Proc Natl Acad Sci USA. 50: 703-710.

Stevens, C. F. (1998) Neuronal diversity: too many cell types for comfort? Curr Biol 8: 708-710.

Taibi, G., Schiavo, M. R., Calvaruso, G. and Tesoriere, G. (1994) Pattern of polyamines and related monoacetyl derivatives in chick embryo retina during development. Int. J. Devl. Neuroscience 12: 423-429.

Thanos S. and Bonhoeffer F. (1987) Axonal arborization in the developing chick retinotectal system. J Comp Neurol 261: 155-64.

Trisler, D. (1991) Cell recognition and pattern formation in the developing nervous system. J Exp Biol 153: 11-28.

Trisler, G. D., Schneider, M. D. and Nirenberg, M. (1981) A topographic gradient of molecules in retina can be used to identify neuron position. Proc Natl Acad Sci USA 78: 2145-2149.

Turner, D. L. and Cepko, C. L. (1987) A common progenitor for neurons and glia persists in rat retina late in development. Nature 328: 131-136.

Turner, D. L., Snyder, E. Y. and Cepko, C. L. (1990) Lineage-independent determination of cell type in the embryonic mouse retina. Neuron 4: 833-845.

Van Groningen, J. J. M., Bloemers, H. P. J. and Swart, G. W. M. (1995) Identification of melanoma inhibitory activity and other differentially expressed messenger RNAs in human melanoma cell lines with different metastatic capacity by messenger RNA differential display. Cancer Res 55: 6237-6243.

Vardimon, L., Fox, L. E. and Moscona, A. A. (1986) Developmental regulation of glutamine synthetase and carbonic anhydrase II in neural retina. Proc Natl Acad Sci USA 83: 9060-9064.

Wang, Y., Xiao, L., Thiagalingam, A., Nelkin, B. D. and Casero, R. A. (1998) The identification of a cis-element and a trans-acting factor involved in the response to polyamines and polyamine analogues in the regulation of the human spermidine/spermine N^1-acetyltransferase gene transcription. J Biol Chem 273: 34623-34630.

Wetts, R. and Fraser, S. E. (1988) Multipotent precursors can give rise to all major cell types of the frog retina. Science 239: 1142-1145.

Wetts, R., Serbedzija, G. N. and Fraser, S. E. (1989) Cell lineage analysis reveals multipotent precursors in the ciliary margin of the frog retina. Dev Biol 136: 254-263.

Willbold, E. and P. G. Layer (1998) Müller glia cells and their possible roles during retina differentiation in vivo and in vitro. Histol Histopathol 13: 531-552.

Williams, K. (1997a) Interactions of polyamines with ion channels. Biochem J 325: 289-297.

Williams, K. (1997b) Modulation and block of ion channels: A new biology of polyamines. Cell Signal 9: 1-13.

Wong, R. O. L., Meister, M. and Shatz, C. J. (1993) Transient period of correlated bursting activity during development of the mammalian retina. Neuron 11: 923-938.

Wong, W. T., Sanes, J. R. and Wong, R. O. L. (1998) Developmentally regulated spontaneous activity in the embryonic chick retina. J Neurosci 189: 8839-8852.

Xiao, L. and Casero, R. A. (1996) Differential transcription of the human spermidine/spermine N^1-acetyltransferase (*SSAT*) gene in human lung carcinoma cells. Biochem J 313: 691-696.

Yamakura, T. and Shimoji, K. (1999) Subunit- and site-specific pharmacology of the NMDA receptor channel. Prog Neurobiol 59: 279-298.

Yamasaki, E. N., Barbosa, V. D., De Mello, F. G. and Hokoç J. N. (1999) GABAergic system in the developing mammalian retina: dual sources of GABA at early stages of postnatal development. Int. J. Devl. Neuroscience 17: 201-213.

Zhang, H., Zhang, R. and Liang, P. (1996) Differential screening of gene expression difference enriched by differential display. BioTechniques 24: 2454-2455.

Zhang, J. S., Duncan, E. L., Chang, A. C.-M. and Reddel, R. R. (1998) Differential display of mRNA. Mol Biotechnol 10: 155-165.

Zhang, L. I., Huizhong, W. T, Holt, C. E., Harris, W. A. and Poo, M-M. (1998) A critical window for cooperation and competition among developing retinotectal synapses. Nature 395: 37-44.

Zhu, C., Lang, D. W., Coffino, P. (1999) Antizyme2 is a negative regulator of ornithine decarboxylase and polyamine transport. J Biol Chem 274: 26425-26430.

Zhu, W. and Liang, P. (1997) Detection and isolation of differentially expressed genes by differential display. Methods Mol Biol 68: 211-220.

Zoli, M., Pedrazzi, P. and Agnati, L. F. (1996) Regional and cellular distribution of spermidine/spermine N^1-acetyltransferase (SSAT) mRNA in the rat central nervous system. Neuroscience Letters 207: 13-16.

Zuo, J., Neubauer, D., Dyess, K., Ferguson, T.A. and Muir, D. (1998) Degradation of chondroitin sulfate proteoglycan enhances the neurite-promoting potential of spinal cord tissue. Exp Neurol 154: 654-662.